

Wideband Man-Made Radio Noise Measurements in the VHF and Low UHF Bands

Jeffery A. Wepman
Geoffrey A. Sanders



report series

Wideband Man-Made Radio Noise Measurements in the VHF and Low UHF Bands

Jeffery A. Wepman
Geoffrey A. Sanders



U.S. DEPARTMENT OF COMMERCE

July 2011

DISCLAIMER

Certain commercial equipment and materials are identified in this report to specify adequately the technical aspects of the reported results. In no case does such identification imply recommendation or endorsement by the National Telecommunications and Information Administration, nor does it imply that the material or equipment identified is the best available for this purpose.

CONTENTS

	Page
FIGURES	vi
TABLES	xiv
1 INTRODUCTION.....	1
2 BACKGROUND	3
2.1 Description of Noise Parameters	3
2.2 Man-Made Noise Models.....	5
2.3 Previous Noise Measurements	6
3 NOISE MEASUREMENT LOCATION SELECTION.....	8
4 NOISE MEASUREMENT FREQUENCY AND BANDWIDTH SELECTION	14
4.1 Noise Measurement Bandwidth Selection	14
4.2 Noise Measurement Frequency Selection	14
5 NOISE MEASUREMENTS	19
5.1 Noise Measurement System	19
5.2 Noise Measurement System Optimization and Verification	22
5.3 Noise Measurement Procedure.....	23
6 DATA ANALYSIS	26
6.1 Time Domain Characteristics and APDs of Individual Noise Data Records.....	26
6.2 Median, Mean, and Peak Noise Power Analysis.....	30
6.3 Complementary Cumulative Distributions of Hourly Median Noise Power	37
6.4 Statistics of the Hourly Medians of Mean Noise Power	37
6.5 Comparison of Measured Results with Models.....	41
7 SUMMARY AND CONCLUSIONS.....	46
8 ACKNOWLEDGEMENTS.....	48
9 REFERENCES	49
APPENDIX: SPECTRUM SURVEY MEASUREMENTS	51
A.1 Spectrum Survey Measurement System.....	51
A.2 Spectrum Survey Measurement Procedure	52
A.3 Spectrum Survey Measurement Results.....	54

FIGURES

		Page
Figure 1.	Model of an RF receiving system.	3
Figure 2.	Predicted F_{am} values versus frequency for both the ITU and Hagn models.....	6
Figure 3.	Photograph of the RSMS-4G measurement vehicle.	8
Figure 4.	Aerial photograph of residential measurement location in Boulder (courtesy of the U.S. Geological Survey). The marker near the bottom of the photograph shows the location of the residential Boulder spectrum survey measurements discussed in Section 4 and described in the Appendix.	10
Figure 5.	Aerial photograph of business measurement location in Boulder (courtesy of the U.S. Geological Survey).	11
Figure 6.	Aerial photograph of residential measurement location in Denver (courtesy of the U.S. Geological Survey).	12
Figure 7.	Aerial photograph of business measurement location in Denver (courtesy of the U.S. Geological Survey).	13
Figure 8.	Maximum, mean, and median received signal power at all measurement locations for 110–115 MHz (RBW = 10 kHz, 100 sweeps, sweep time = 300 ms).	16
Figure 9.	Maximum, mean, and median received signal power at all measurement locations for 219–224 MHz (RBW = 3 kHz, 60 sweeps, sweep time = 900 ms).	17
Figure 10.	Maximum, mean, and median received signal power at all measurement locations for 400–404 MHz (RBW = 3 kHz, 60 sweeps, sweep time = 900 ms).	18
Figure 11.	Block diagram of the noise measurement system installed in the RSMS-4G measurement vehicle.	19
Figure 12.	VSWR versus normalized frequency for the quarter-wave monopole antennas.	20
Figure 13.	Photograph of the noise measurement system installed in the RSMS-4G measurement vehicle.	22
Figure 14.	Example time domain plot showing 60 ms of a noise data record from the residential Boulder location at 0349 on September 1, 2009 with a 112.5-MHz center frequency and 1.16-MHz span.....	27

Figure 15.	Example APD from the residential Boulder location at 0349 on September 1, 2009 with a 112.5-MHz center frequency and 1.16-MHz span.....	28
Figure 16.	Example APD from the Denver business location at 0723 on August 19, 2009 with a 221.5-MHz center frequency and 1.16-MHz span.....	28
Figure 17.	Example APD from the Boulder business location at 1211 on July 22, 2009 with a 401-MHz center frequency and 1.16-MHz span.	29
Figure 18.	Example APD from the Denver residential location at 2319 on July 29, 2009 with a 112.5-MHz center frequency and 1.16-MHz span.....	29
Figure 19.	Median, mean, and peak measured noise power in a 1-MHz bandwidth at a center frequency of 112.5 MHz at the Boulder residential location (August 31–September 1, 2009).....	31
Figure 20.	Median, mean, and peak measured noise power in a 1-MHz bandwidth at a center frequency of 221.5 MHz at the Boulder residential location (September 3–4, 2009).	31
Figure 21.	Median, mean, and peak measured noise power in a 1-MHz bandwidth at a center frequency of 401 MHz at the Boulder residential location (September 2–3, 2009).	32
Figure 22.	Median, mean, and peak measured noise power in a 1-MHz bandwidth at a center frequency of 112.5 MHz at the Boulder business location (July 21–22, 2009).....	32
Figure 23.	Median, mean, and peak measured noise power in a 1-MHz bandwidth at a center frequency of 221.5 MHz at the Boulder business location (July 20–21, 2009).....	33
Figure 24.	Median, mean, and peak measured noise power in a 1-MHz bandwidth at a center frequency of 401 MHz at the Boulder business location (July 22–23, 2009).....	33
Figure 25.	Median, mean, and peak measured noise power in a 1-MHz bandwidth at a center frequency of 112.5 MHz at the Denver residential location (July 29–30, 2009).....	34
Figure 26.	Median, mean, and peak measured noise power in a 1-MHz bandwidth at a center frequency of 221.5 MHz at the Denver residential location (July 28–29, 2009).....	34
Figure 27.	Median, mean, and peak measured noise power in a 1-MHz bandwidth at a center frequency of 401 MHz at the Denver residential location (July 27–28, 2009).....	35

Figure 28.	Median, mean, and peak measured noise power in a 1-MHz bandwidth at a center frequency of 112.5 MHz at the Denver business location (August 17–18, 2009).....	35
Figure 29.	Median, mean, and peak measured noise power in a 1-MHz bandwidth at a center frequency of 221.5 MHz at the Denver business location (August 18–19, 2009).....	36
Figure 30.	Median, mean, and peak measured noise power in a 1-MHz bandwidth at a center frequency of 401 MHz at the Denver business location (August 19–20, 2009).....	36
Figure 31.	Complementary cumulative distribution of the hourly median values of the median, mean, and peak powers in a 1-MHz bandwidth at a center frequency of approximately 112.5 MHz over both residential locations.	38
Figure 32.	Complementary cumulative distribution of the hourly median values of the median, mean, and peak powers in a 1-MHz bandwidth at a center frequency of approximately 221.5 MHz over both residential locations.	38
Figure 33.	Complementary cumulative distribution of the hourly median values of the median, mean, and peak powers in a 1-MHz bandwidth at a center frequency of 401 MHz over both residential locations.	39
Figure 34.	Complementary cumulative distribution of the hourly median values of the median, mean, and peak powers in a 1-MHz bandwidth at a center frequency of approximately 112.5 MHz over both business locations.	39
Figure 35.	Complementary cumulative distribution of the hourly median values of the median, mean, and peak powers in a 1-MHz bandwidth at a center frequency of approximately 221.5 MHz over both business locations.	40
Figure 36.	Complementary cumulative distribution of the hourly median values of the median, mean, and peak powers in a 1-MHz bandwidth at a center frequency of 401 MHz over both business locations.	40
Figure 37.	Comparison of measured and predicted values of F_{am} and standard deviation of F_{am} for residential locations. ¹⁴	44
Figure 38.	Comparison of measured and predicted values of F_{am} and standard deviation of F_{am} for business locations.....	44
Figure A-1.	Block diagram of the spectrum survey measurement system.....	51
Figure A-2.	Maximum, mean, and median received signal power at the Boulder residential location for Event 1 (104–164 MHz, RBW = 10 kHz, 100 sweeps, sweep time = 300 ms).....	55

Figure A-3. Maximum, mean, and median received signal power at the Denver residential location for Event 1 (104–164 MHz, RBW = 10 kHz, 100 sweeps, sweep time = 300 ms).....	56
Figure A-4. Maximum, mean, and median received signal power at the Boulder business location for Event 1 (104–164 MHz, RBW = 10 kHz, 100 sweeps, sweep time = 300 ms).	57
Figure A-5. Maximum, mean, and median received signal power at the Denver business location for Event 1 (104–164 MHz, RBW = 10 kHz, 100 sweeps, sweep time = 300 ms).	58
Figure A-6. Maximum, mean, and median received signal power at the Boulder residential location for Event 2 (160–180 MHz, RBW = 10 kHz, 500 sweeps, sweep time = 300 ms).....	59
Figure A-7. Maximum, mean, and median received signal power at the Denver residential location for Event 2 (160–180 MHz, RBW = 10 kHz, 500 sweeps, sweep time = 300 ms).....	60
Figure A-8. Maximum, mean, and median received signal power at the Boulder business location for Event 2 (160–180 MHz, RBW = 10 kHz, 500 sweeps, sweep time = 300 ms).	61
Figure A-9. Maximum, mean, and median received signal power at the Denver business location for Event 2 (160–180 MHz, RBW = 10 kHz, 500 sweeps, sweep time = 300 ms).	62
Figure A-10. Maximum, mean, and median received signal power at the Boulder residential location for Event 3 (170–220 MHz, RBW = 100 kHz, 500 sweeps, sweep time = 100 ms).....	63
Figure A-11. Maximum, mean, and median received signal power at the Denver residential location for Event 3 (170–220 MHz, RBW = 100 kHz, 500 sweeps, sweep time = 100 ms).....	64
Figure A-12. Maximum, mean, and median received signal power at the Boulder business location for Event 3 (170–220 MHz, RBW = 100 kHz, 500 sweeps, sweep time = 100 ms).	65
Figure A-13. Maximum, mean, and median received signal power at the Denver business location for Event 3 (170–220 MHz, RBW = 100 kHz, 500 sweeps, sweep time = 100 ms).	66
Figure A-14. Maximum, mean, and median received signal power at the Boulder residential location for Event 4 (216–225 MHz, RBW = 3 kHz, 60 sweeps, sweep time = 900 ms).....	67

Figure A-15. Maximum, mean, and median received signal power at the Denver residential location for Event 4 (216–225 MHz, RBW = 3 kHz, 60 sweeps, sweep time = 900 ms).....	68
Figure A-16. Maximum, mean, and median received signal power at the Boulder business location for Event 4 (216–225 MHz, RBW = 3 kHz, 60 sweeps, sweep time = 900 ms).....	69
Figure A-17. Maximum, mean, and median received signal power at the Denver business location for Event 4 (216–225 MHz, RBW = 3 kHz, 60 sweeps, sweep time = 900 ms).....	70
Figure A-18. Maximum, mean, and median received signal power at the Boulder residential location for Event 5 (225–405 MHz, RBW = 30 kHz, 100 sweeps, sweep time = 100 ms).....	71
Figure A-19. Maximum, mean, and median received signal power at the Denver residential location for Event 5 (225–405 MHz, RBW = 30 kHz, 100 sweeps, sweep time = 100 ms).....	72
Figure A-20. Maximum, mean, and median received signal power at the Boulder business location for Event 5 (225–405 MHz, RBW = 30 kHz, 100 sweeps, sweep time = 100 ms).....	73
Figure A-21. Maximum, mean, and median received signal power at the Denver business location for Event 5 (225–405 MHz, RBW = 30 kHz, 100 sweeps, sweep time = 100 ms).....	74
Figure A-22. Maximum, mean, and median received signal power at the Boulder residential location for Event 6 (400–406 MHz, RBW = 3 kHz, 60 sweeps, sweep time = 900 ms).....	75
Figure A-23. Maximum, mean, and median received signal power at the Denver residential location for Event 6 (400–406 MHz, RBW = 3 kHz, 60 sweeps, sweep time = 900 ms).....	76
Figure A-24. Maximum, mean, and median received signal power at the Boulder business location for Event 6 (400–406 MHz, RBW = 3 kHz, 60 sweeps, sweep time = 900 ms).....	77
Figure A-25. Maximum, mean, and median received signal power at the Denver business location for Event 6 (400–406 MHz, RBW = 3 kHz, 60 sweeps, sweep time = 900 ms).....	78
Figure A-26. Maximum, mean, and median received signal power at the Boulder residential location for Event 7 (400–420 MHz, RBW = 10 kHz, 200 sweeps, sweep time = 300 ms).....	79

Figure A-27. Maximum, mean, and median received signal power at the Denver residential location for Event 7 (400–420 MHz, RBW = 10 kHz, 200 sweeps, sweep time = 300 ms).....	80
Figure A-28. Maximum, mean, and median received signal power at the Boulder business location for Event 7 (400–420 MHz, RBW = 10 kHz, 200 sweeps, sweep time = 300 ms).	81
Figure A-29. Maximum, mean, and median received signal power at the Denver business location for Event 7 (400–420 MHz, RBW = 10 kHz, 200 sweeps, sweep time = 300 ms).	82
Figure A-30. Maximum, mean, and median received signal power at the Boulder residential location for Event 8 (420–450 MHz, RBW = 10 kHz, 100 sweeps, sweep time = 300 ms).....	83
Figure A-31. Maximum, mean, and median received signal power at the Denver residential location for Event 8 (420–450 MHz, RBW = 10 kHz, 100 sweeps, sweep time = 300 ms).....	84
Figure A-32. Maximum, mean, and median received signal power at the Boulder business location for Event 8 (420–450 MHz, RBW = 10 kHz, 100 sweeps, sweep time = 300 ms).	85
Figure A-33. Maximum, mean, and median received signal power at the Denver business location for Event 8 (420–450 MHz, RBW = 10 kHz, 100 sweeps, sweep time = 300 ms).	86
Figure A-34. Maximum, mean, and median received signal power at the Boulder residential location for Event 9 (450–470 MHz, RBW = 10 kHz, 200 sweeps, sweep time = 300 ms).....	87
Figure A-35. Maximum, mean, and median received signal power at the Denver residential location for Event 9 (450–470 MHz, RBW = 10 kHz, 200 sweeps, sweep time = 300 ms).....	88
Figure A-36. Maximum, mean, and median received signal power at the Boulder business location for Event 9 (450–470 MHz, RBW = 10 kHz, 200 sweeps, sweep time = 300 ms).	89
Figure A-37. Maximum, mean, and median received signal power at the Denver business location for Event 9 (450–470 MHz, RBW = 10 kHz, 200 sweeps, sweep time = 300 ms).	90
Figure A-38. Maximum, mean, and median received signal power at the Boulder residential location for Event 10 (470–520 MHz, RBW = 10 kHz, 100 sweeps, sweep time = 300 ms).....	91

Figure A-39. Maximum, mean, and median received signal power at the Denver residential location for Event 10 (470–520 MHz, RBW = 10 kHz, 100 sweeps, sweep time = 300 ms).....	92
Figure A-40. Maximum, mean, and median received signal power at the Boulder business location for Event 10 (470–520 MHz, RBW = 10 kHz, 100 sweeps, sweep time = 300 ms).	93
Figure A-41. Maximum, mean, and median received signal power at the Denver business location for Event 10 (470–520 MHz, RBW = 10 kHz, 100 sweeps, sweep time = 300 ms).	94
Figure A-42. Maximum, mean, and median received signal power at the Boulder residential location for Event 11 (512–812 MHz, RBW = 100 kHz, 200 sweeps, sweep time = 100 ms).....	95
Figure A-43. Maximum, mean, and median received signal power at the Denver residential location for Event 11 (512–812 MHz, RBW = 100 kHz, 200 sweeps, sweep time = 100 ms).....	96
Figure A-44. Maximum, mean, and median received signal power at the Boulder business location for Event 11 (512–812 MHz, RBW = 100 kHz, 200 sweeps, sweep time = 100 ms).	97
Figure A-45. Maximum, mean, and median received signal power at the Denver business location for Event 11 (512–812 MHz, RBW = 100 kHz, 200 sweeps, sweep time = 100 ms).	98
Figure A-46. Maximum, mean, and median received signal power at the Boulder residential location for Event 12 (806–906 MHz, RBW = 10 kHz, 60 sweeps, sweep time = 300 ms).....	99
Figure A-47. Maximum, mean, and median received signal power at the Denver residential location for Event 12 (806–906 MHz, RBW = 10 kHz, 60 sweeps, sweep time = 300 ms).....	100
Figure A-48. Maximum, mean, and median received signal power at the Boulder business location for Event 12 (806–906 MHz, RBW = 10 kHz, 60 sweeps, sweep time = 300 ms).	101
Figure A-49. Maximum, mean, and median received signal power at the Denver business location for Event 12 (806–906 MHz, RBW = 10 kHz, 60 sweeps, sweep time = 300 ms).	102
Figure A-50. Maximum, mean, and median received signal power at the Boulder residential location for Event 13 (900–920 MHz, RBW = 10 kHz, 100 sweeps, sweep time = 300 ms).....	103

Figure A-51. Maximum, mean, and median received signal power at the Denver residential location for Event 13 (900–920 MHz, RBW = 10 kHz, 100 sweeps, sweep time = 300 ms).....	104
Figure A-52. Maximum, mean, and median received signal power at the Boulder business location for Event 13 (900–920 MHz, RBW = 10 kHz, 100 sweeps, sweep time = 300 ms).	105
Figure A-53. Maximum, mean, and median received signal power at the Denver business location for Event 13 (900–920 MHz, RBW = 10 kHz, 100 sweeps, sweep time = 300 ms).	106
Figure A-54. Maximum, mean, and median received signal power at the Boulder residential location for Event 14 (920–960 MHz, RBW = 10 kHz, 300 sweeps, sweep time = 300 ms).....	107
Figure A-55. Maximum, mean, and median received signal power at the Denver residential location for Event 14 (920–960 MHz, RBW = 10 kHz, 300 sweeps, sweep time = 300 ms).....	108
Figure A-56. Maximum, mean, and median received signal power at the Boulder business location for Event 14 (920–960 MHz, RBW = 10 kHz, 300 sweeps, sweep time = 300 ms).	109
Figure A-57. Maximum, mean, and median received signal power at the Denver business location for Event 14 (920–960 MHz, RBW = 10 kHz, 300 sweeps, sweep time = 300 ms).	110
Figure A-58. Maximum, mean, and median received signal power at the Boulder residential location for Event 15 (960–1060 MHz, RBW = 100 kHz, 500 sweeps, sweep time = 100 ms).....	111
Figure A-59. Maximum, mean, and median received signal power at the Denver residential location for Event 15 (960–1060 MHz, RBW = 100 kHz, 500 sweeps, sweep time = 100 ms).....	112
Figure A-60. Maximum, mean, and median received signal power at the Boulder business location for Event 15 (960–1060 MHz, RBW = 100 kHz, 500 sweeps, sweep time = 100 ms).....	113
Figure A-61. Maximum, mean, and median received signal power at the Denver business location for Event 15 (960–1060 MHz, RBW = 100 kHz, 500 sweeps, sweep time = 100 ms).....	114

TABLES

	Page
Table 1. Description of noise measurement locations	9
Table 2. Measured system gain and noise figure at each measurement frequency and location	24
Table 3. Statistics of the hourly medians of the mean noise power for residential locations	41
Table 4. Statistics of the hourly medians of the mean noise power for business locations	41
Table 5. Major differences between measurements used in the ITU Model and measurements taken for this study	42
Table 6. Comparison of measured and predicted values of F_{am} for residential locations ¹⁴	43
Table 7. Comparison of measured and predicted values of F_{am} for business locations.....	43
Table A-1. Spectrum analyzer and preselector parameters for spectrum survey measurements.....	53

WIDEBAND MAN-MADE RADIO NOISE MEASUREMENTS IN THE VHF AND LOW UHF BANDS

Jeffery A. Wepman and Geoffrey A. Sanders¹

Man-made radio noise measurements were conducted in a 1.16-MHz bandwidth at 112.5, 221.5, and 401 MHz at two residential and two business locations in the Boulder/Denver, Colorado, area. The measurement frequencies and bandwidth were selected using the results of a spectrum survey performed over the 104–1060-MHz frequency range. The noise measurement data were collected as a complex baseband noise data record (consisting of six million in-phase (I) and quadrature-phase (Q) samples) every 10 minutes over a 24-hour period for each frequency and location. The data were processed to provide various statistical descriptions of the noise such as amplitude probability distributions (APDs). Median values of the antenna noise figure F_{am} were determined for each measurement frequency and environment type and compared to predicted values from existing man-made radio noise models. The measured values of F_{am} , while larger than the values predicted by the International Telecommunication Union (ITU) man-made radio noise model, were still within one standard deviation of the predicted values. Further noise measurements are recommended in a greater number of locations to provide more statistically significant results.

Key words: man-made noise; man-made radio noise; impulsive noise; Gaussian noise; noise measurements; spectrum measurements; spectrum survey; antenna noise factor; external noise factor; amplitude probability distributions; International Telecommunications Union (ITU) radio noise model

1 INTRODUCTION

Having an accurate model of man-made radio noise at very high frequency (VHF) and ultra high frequency (UHF)² is of interest in the design and evaluation of radio communication systems and wireless networks [1]. While an International Telecommunications Union (ITU) model for man-made radio noise is available today [2], this model is based on measurements that were taken in the 1960s and 1970s.

¹ The authors are with the Institute for Telecommunication Sciences, National Telecommunications and Information Administration, U.S. Department of Commerce, Boulder, CO 80305.

² The VHF band is from 30 to 300 MHz and the UHF band is from 300 to 3000 MHz.

The proliferation of computers, cellular telephones, wireless networks, and other electronic devices as well as increases in spectrum crowding, aging of the power distribution infrastructure, and enhancements to auto ignition systems suggest that the man-made radio noise environment may have changed since the 1970s. Because of these significant changes in technology, it is suspected that the ITU model for man-made radio noise may no longer be accurate. Noise measurements taken in the 1990s also raised questions about the accuracy of the ITU model [3], [4].

This report has three primary objectives. The first is to introduce a new, wideband noise measurement system suitable for measuring man-made radio noise in bandwidths more comparable to those used in modern wideband communication systems. The second objective is to present results from some initial man-made radio noise measurements taken at VHF and UHF and to compare these results to the current ITU model [2]. Building on the results of these initial measurements, the third objective is to help identify areas that warrant further study.

Section 2 of this report presents some key background information to provide a context for this measurement study. A discussion of noise parameters that have been traditionally used to express noise power measurements is presented. Models that are currently used to predict noise power are also given. The section also includes a look at some of the relevant man-made noise measurement studies previously undertaken.

Judicious selection of both appropriate measurement locations and frequencies was a necessary and critical prerequisite to taking the noise measurements. Section 3 discusses the selection of locations for making the noise measurements. The selection of the specific measurement frequencies and bandwidths is addressed in Section 4. This process was complicated by the requirement of taking relatively wide bandwidth noise measurements. A spectrum survey and subsequent data analysis were required, along with the development of a swept spectrum measurement system to aid in the selection of frequencies and bandwidths for the noise measurements. Details of the spectrum survey including the measurement system, procedure, and results are provided in the Appendix. The results are presented as maximum, mean, and median received signal power for the entire frequency range measured (104–1060 MHz).

The noise measurement system and procedure for making the measurements is given in Section 5. The data analysis is covered in Section 6. Some example amplitude probability distributions (APDs) of individual noise data records are given along with an example time domain display of a noise data record. The statistical summary data includes the median, mean, and peak noise power levels over a 24-hour time period at each measurement location and frequency. Complementary cumulative distributions of the hourly median values of the median, mean and peak power are given for each frequency and environment type. Median values of the antenna noise figure are determined for each measurement frequency and environment type. These values are compared to those predicted by the ITU model. Section 7 provides a brief summary of the report and some conclusions about the results of the data analysis and the comparison between these results and the predicted values from the ITU model. Some recommendations for further study are also offered.

2 BACKGROUND

Man-made radio noise was studied extensively in the 1960s and 1970s and radio noise in general has been studied for even longer. Therefore, there is a wealth of knowledge that is relevant to noise measurements conducted today. This section provides some of this background information, such as a description of noise parameters commonly used to quantify noise power, noise power models that have been developed to predict measured noise power, and previous noise measurements that have been undertaken.

2.1 Description of Noise Parameters

The characterization of the man-made radio noise environment traditionally has been given in terms of the noise power received by an antenna of a radio frequency (RF) receiving system. Typically, noise power is presented in terms of an antenna noise figure. In this section, commonly used noise parameters are described.

To describe these noise parameters, it is helpful to consider a model of an RF receiving system as shown in Figure 1 [5].

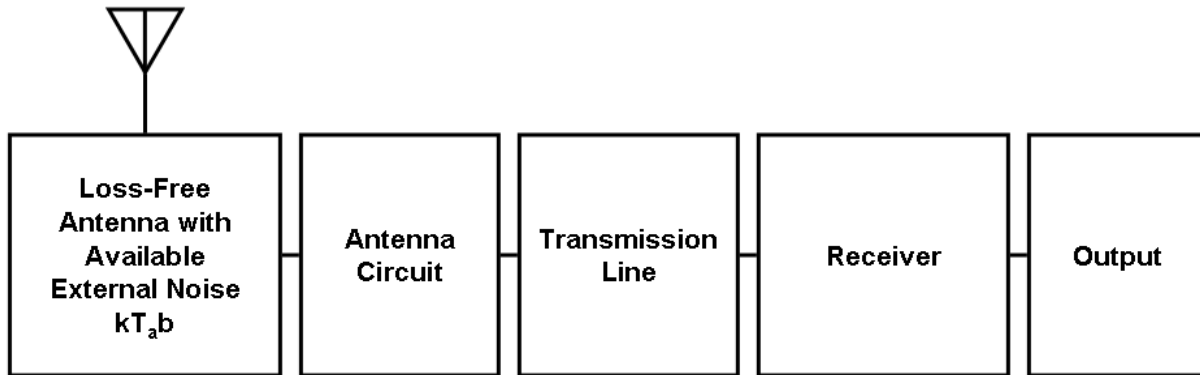


Figure 1. Model of an RF receiving system.

The mean overall measured system noise power, p , can be expressed in terms of the overall system noise factor, f , by

$$p = f k T_0 b \quad (1)$$

where

k = Boltzmann's constant = 1.38×10^{-23} joules/K,

T_0 = reference temperature = 288 K,

b = receiver noise equivalent bandwidth in Hz.

Expressing (1) in decibels yields

$$P = F + 10 \log_{10}(kT_0 b) \quad (2)$$

where

$P = 10 \log_{10} p$ = mean overall measured system noise power in dB and

$F = 10 \log_{10} f$ = overall system noise figure in dB.

Using Friis' method of combining noise factors in cascade [6], the overall system noise factor can be expressed as

$$f = f_a + (l_c - 1) \frac{T_c}{T_0} + l_c(l_t - 1) \frac{T_t}{T_0} + l_c l_t (f_r - 1) \quad (3)$$

where

l_c = antenna circuit loss,

l_t = transmission line loss,

T_c = actual temperature of the antenna circuit in K,

T_t = actual temperature of the transmission line in K,

f_r = receiver noise factor and

f_a = antenna noise factor.

Now, since the noise factor associated with the antenna circuit loss is given as

$$f_c = 1 + (l_c - 1) \frac{T_c}{T_0} \quad (4)$$

and the noise factor associated with the transmission line loss is given as

$$f_t = 1 + (l_t - 1) \frac{T_t}{T_0} \quad (5)$$

if $T_c = T_t = T_0$, then (3) can be written as

$$f = f_a - 1 + f_c f_t f_r. \quad (6)$$

If the antenna circuit and transmission line are assumed to be lossless, (6) reduces to

$$f = f_a + f_r - 1 \quad (7)$$

providing a relationship between the overall system noise factor f , the antenna noise factor f_a , and the receiver noise factor f_r . A lossless antenna circuit and transmission line are assumed for the measurements taken for this report. This assumption is valid because:

- The quarter-wave monopole antenna used for each frequency was tuned to achieve a minimum voltage standing wave ratio (VSWR) of less than 1.25:1 in all cases.
- The noise diode calibration at the output terminals of the antenna removes the effects of any transmission line loss.

Some of the final data statistics presented in this report, under certain conditions, are given in terms of the antenna noise figure F_a (where $F_a = 10 \log_{10} f_a$) as determined from the overall system noise factor f and (7). Values of F_a can be converted to the mean external noise power available from an equivalent lossless antenna, P_n , by $P_n = F_a + 10 \log_{10} (kT_0 b)$. This will be discussed in greater detail in Section 6.2.

2.2 Man-Made Noise Models

The current ITU model of man-made radio noise power [2] provides predicted values of F_{am} (median of F_a values) for frequencies ranging from 250 kHz to 250 MHz and is given as

$$F_{am} = c - d \log_{10}(f_0) \quad (8)$$

where f_0 is the center frequency in MHz, $d = 27.7$ dB/MHz, and c is 76.8 dB, 72.5 dB, and 67.2 dB for business, residential, and rural environments, respectively.

Hagn [7] suggested using the ITU Model for frequencies below 200 MHz but proposed a different model for frequencies above 200 MHz.³ The Hagn model is also given as in (8) except $d = 15.8$ dB/MHz and c is 49.4 dB, 45.2 dB, and 39.2 dB for business, residential, and rural environments, respectively. Figure 2 shows a plot of the predicted F_{am} values versus frequency in business, residential, and rural locations for both the ITU and Hagn models.

³ Measurements by Lauber and Bertrand [8] showed that the Hagn model was more accurate than the ITU model for frequencies above 200 MHz.

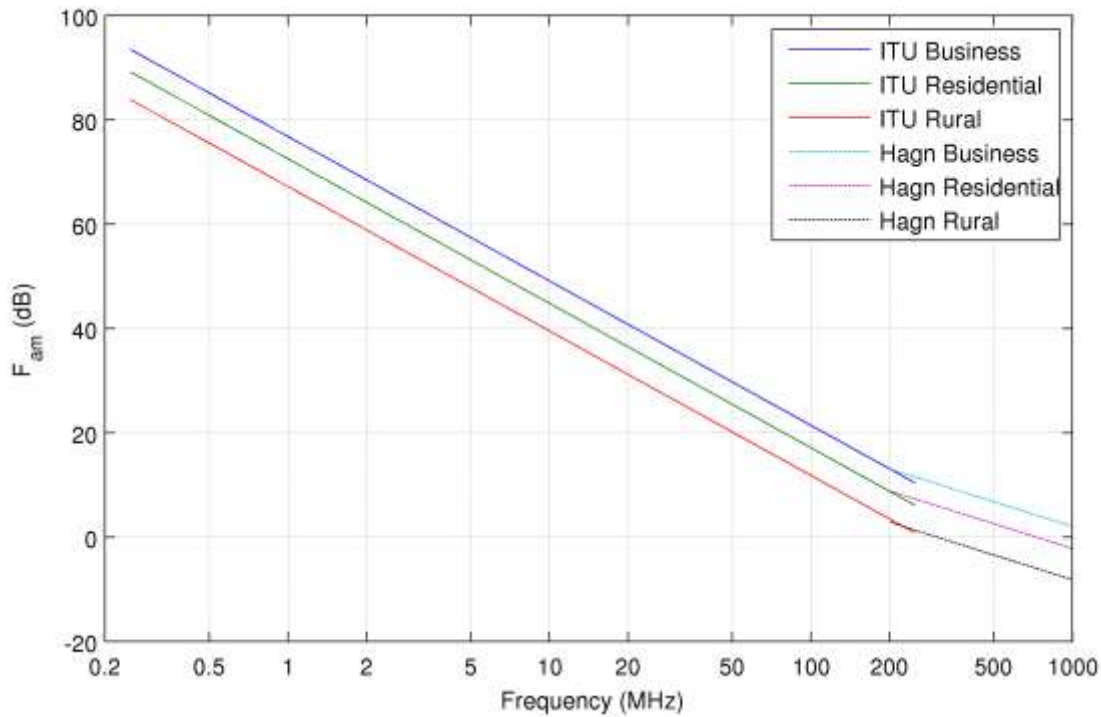


Figure 2. Predicted F_{am} values versus frequency for both the ITU and Hagn models.

2.3 Previous Noise Measurements

The ITU model is based on measurements taken in the 1960s and 1970s by Spaulding and Disney [6]. The measurements consisted of mobile measurement runs taken in 23 business, 38 residential, and 31 rural areas in Colorado, Maryland, Texas, Virginia, Washington, Wyoming, and the District of Columbia. The duration of each run varied from about 15 minutes to over one hour. The measurements were made in a 4-kHz noise equivalent bandwidth at 10 different frequencies from 250 kHz to 250 MHz. Short vertical monopole antennas, mounted on the aluminum roof of the measurement van were used for the measurements. The aluminum roof served as a ground plane for the antennas.

Due to the concern that the ITU model was possibly no longer accurate, further man-made noise measurements were made at the Institute for Telecommunication Sciences (ITS) in the 1990s [3], [4]. Two separate measurement campaigns were performed.

In the first campaign, measurements were performed in a variety of locations including six business, two residential, and four rural areas. Additional measurements were also taken to observe noise emissions from automobiles, electrical power networks and electronic equipment. All measurements were conducted with a stationary measurement system. The measurements were taken in a 32-kHz, 3-dB bandwidth at 137.5 MHz using a vertical, quarter-wave monopole antenna mounted on a ground plane. The duration of the measurements was less than one hour in the rural locations, more than 24 hours in the residential locations, and varied from one to more

than 24 hours in the business locations. Values of F_{am} computed from these measurements were found to be within one standard deviation of the values predicted by the ITU model for the business and rural locations. However, for the residential locations, measured values of F_{am} were well below those predicted by the ITU model.

For the second measurement campaign, measurements were taken in a 30-kHz, 3-dB bandwidth at 137.5, 402.5, and 761 MHz. Vertical, quarter-wave monopoles were mounted on a ground plane and tuned to each measurement frequency. The measurements were performed in two residential and two business locations in the Boulder/Denver, Colorado, area. Again, all measurements were conducted with a stationary measurement system. The duration of the measurements at each location was 24 hours. It was not possible to compute accurate F_{am} values from the 402.5 and 761 MHz measurements because the measured noise power was too close to system noise. The value of F_{am} computed from the 137.5 MHz measurements in the business locations was found to be very similar to that computed from the previous ITS 137.5 MHz noise measurements and also within one standard deviation of the value predicted by the ITU model. For the residential locations, values of F_{am} computed from the 137.5 MHz measurements were again well below those predicted by the ITU model.

In 2006, man-made noise measurements were conducted in the United Kingdom by MASS Consultants Limited in five urban, five industrial, eight suburban, and seven rural locations [9]. All measurements were conducted with a stationary measurement system. The measurements were taken in a 1-MHz bandwidth at 209.5 and 425 MHz using vertically-polarized, tuned dipole antennas at a height of 1.5 m above ground. At each location, measurements were conducted for approximately 24 hours. Values of F_{am} computed from the 209.5 MHz measurements were within one standard deviation of those predicted by the ITU model for the urban, suburban, and rural locations.⁴ Values of F_{am} computed from the 425 MHz measurements in the urban, suburban, and rural location were larger than those predicted by the Hagn model.

⁴ The types of measurement environments in the MASS study may be somewhat different from those used for the development of the ITU model. The urban, suburban, and rural locations described in the MASS study probably correspond to the business, residential, and rural locations defined in the ITU model. The industrial locations defined in the MASS study probably do not directly correspond to an environment type in the ITU model.

3 NOISE MEASUREMENT LOCATION SELECTION

The locations for conducting the noise measurements in this study were chosen to represent, as closely as possible, typical residential and business areas as defined in [6]. A business area, as defined in [6], is “any area where the predominant usage throughout the area is for any type of business. This includes stores and offices, industrial parks, large shopping centers, main streets or highways lined with various business enterprises, etc.” A residential area, as defined in [6], is “any area used predominantly for single or multiple family dwellings with a density of at least two single-family units per acre and no large or busy highways.” Several constraints, imposed by the noise measurement system vehicle, limited the choice of locations in this measurement study.

The noise measurements were conducted using the ITS Radio Spectrum Measurement Science 4th Generation (RSMS-4G) Measurement Vehicle. A photograph of the measurement vehicle is shown in Figure 3.



Figure 3. Photograph of the RSMS-4G measurement vehicle.

This vehicle provided some tremendous benefits for making measurements, including a high-degree of RF shielding (60 dB) between the measurement equipment and the antenna, AC power (from either external shore power, an external generator, or a built-in diesel generator), temperature control, and shelter. However, the vehicle also imposed some constraints on the measurements. The location needed to be able to accommodate the large RSMS-4G vehicle, which is roughly 9 m (29 ft) long, 2.6 m (8.5 ft) wide, and 3.4 m (11.5 ft) tall. Further, permission needed to be obtained to park the truck in the same location 24 hours each day for at

least three consecutive days. The large size of the vehicle also precluded any practical mobile measurements.

Since the vast majority of locations could not provide AC power to the vehicle, the vehicle’s built-in diesel generator was used to supply AC power for the equipment. Previous noise measurement system characterization measurements were taken in a radio quiet area in Boulder Canyon. The noise measurement system detected no appreciable radio noise from the built-in diesel generator. However, location selection required consideration of the audible noise produced by the generator. Since the measurements were taken over 24-hour time periods, this was a particular concern in residential locations. Security of the measurement vehicle, equipment, and personnel was also taken into account in location selection. Since the noise measurements were primarily automated and did not require measurement personnel to be present most of the time, security guards were employed to protect the vehicle and equipment.

Consideration of all of the constraints on selection of measurement locations led to the choice of one residential location and one business location in Boulder, Colorado, and one residential and one business location in Denver, Colorado.⁵ Table 1 lists a description of these locations. Aerial photographs⁶ of these locations, as shown in Figures 4–7, provide a better portrayal of the types of measurement environments.

Table 1. Description of noise measurement locations

Location	Description of Location
Residential Boulder	North edge of U.S. Dept. of Commerce Boulder Laboratories campus immediately adjacent to the residential area at King Ave. and 22 nd St.
Business Boulder	Downtown Boulder near Canyon Blvd. and 16 th St.
Residential Denver	Urban St. near West Colfax Ave. in Lakewood, Colorado
Business Denver	Downtown Denver near Champa and 21 st St.

⁵ The residential locations selected in this study were not strictly residential as defined above and in [6]; they were residential with some nearby businesses or busy roads. The residential location in Boulder, while adjacent to a strictly residential area, was also close to the U.S. Department of Commerce Boulder Laboratories. The residential location in Denver, while near several houses and on the edge of a strictly residential area, was also close to a large street with some businesses.

⁶ Data available from U.S. Geological Survey, Earth Resources Observation and Science (EROS) Center, Sioux Falls, SD.



Figure 4. Aerial photograph of residential measurement location in Boulder (courtesy of the U.S. Geological Survey). The marker near the bottom of the photograph shows the location of the residential Boulder spectrum survey measurements discussed in Section 4 and described in the Appendix.

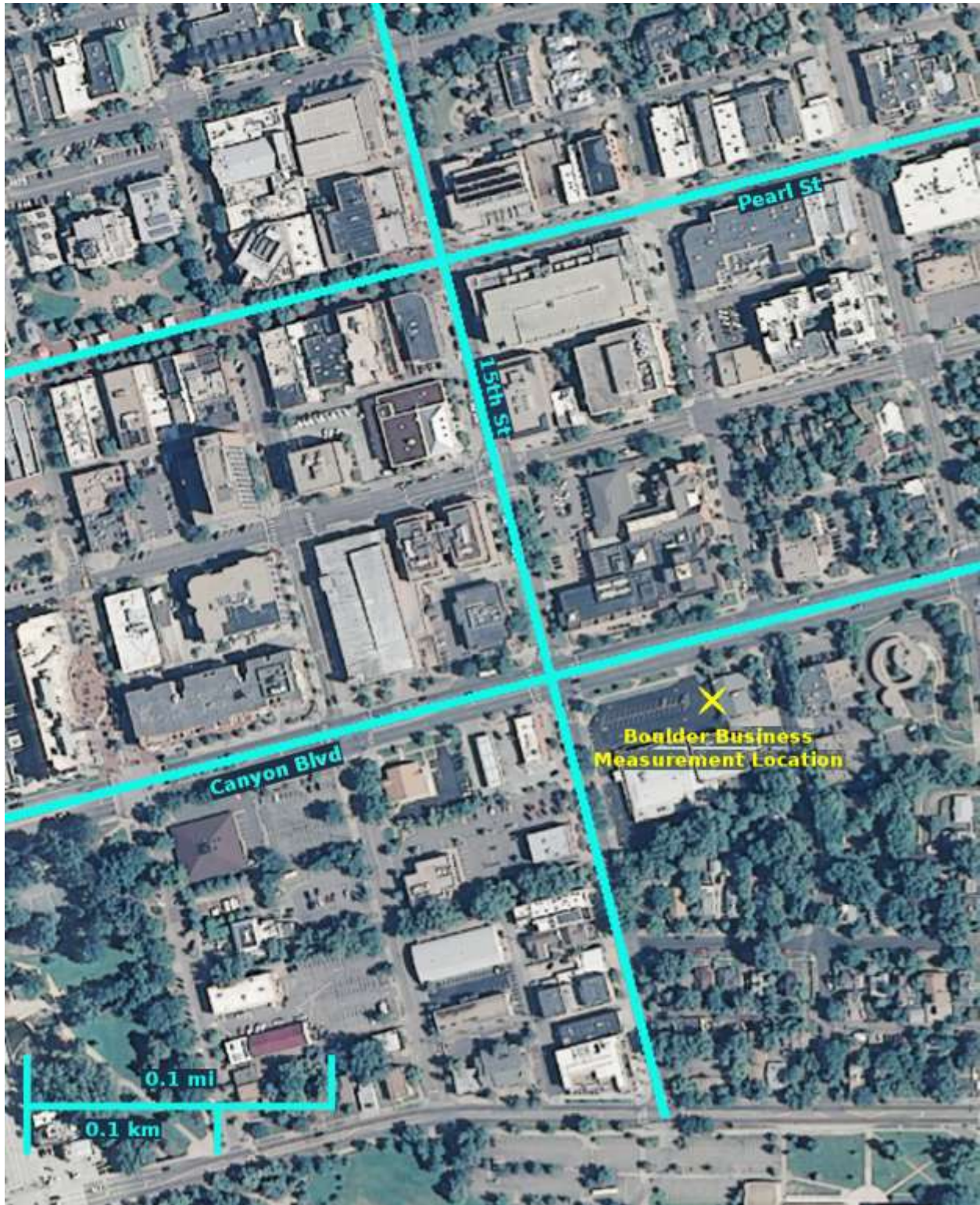


Figure 5. Aerial photograph of business measurement location in Boulder (courtesy of the U.S. Geological Survey).

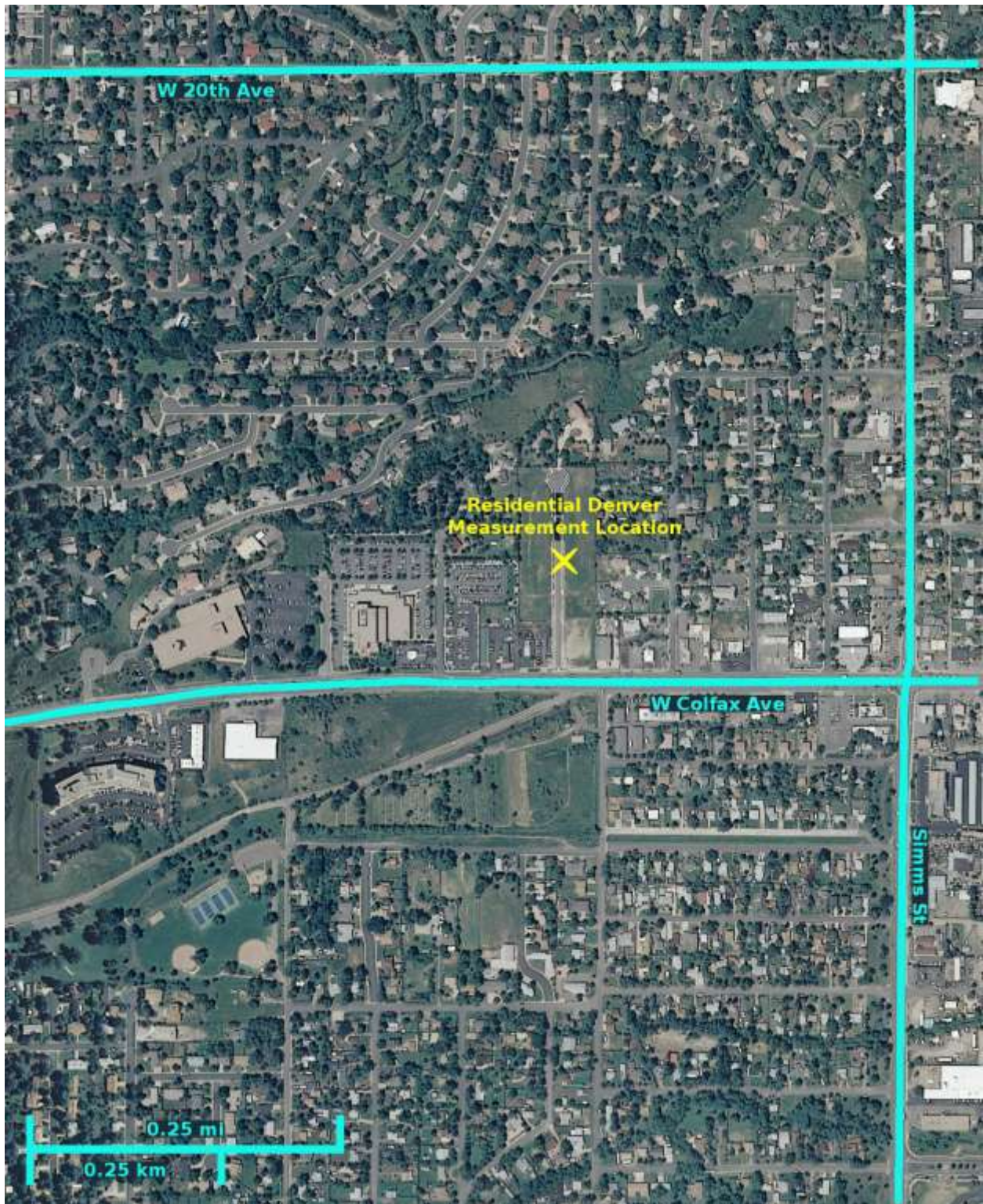


Figure 6. Aerial photograph of residential measurement location in Denver (courtesy of the U.S. Geological Survey).

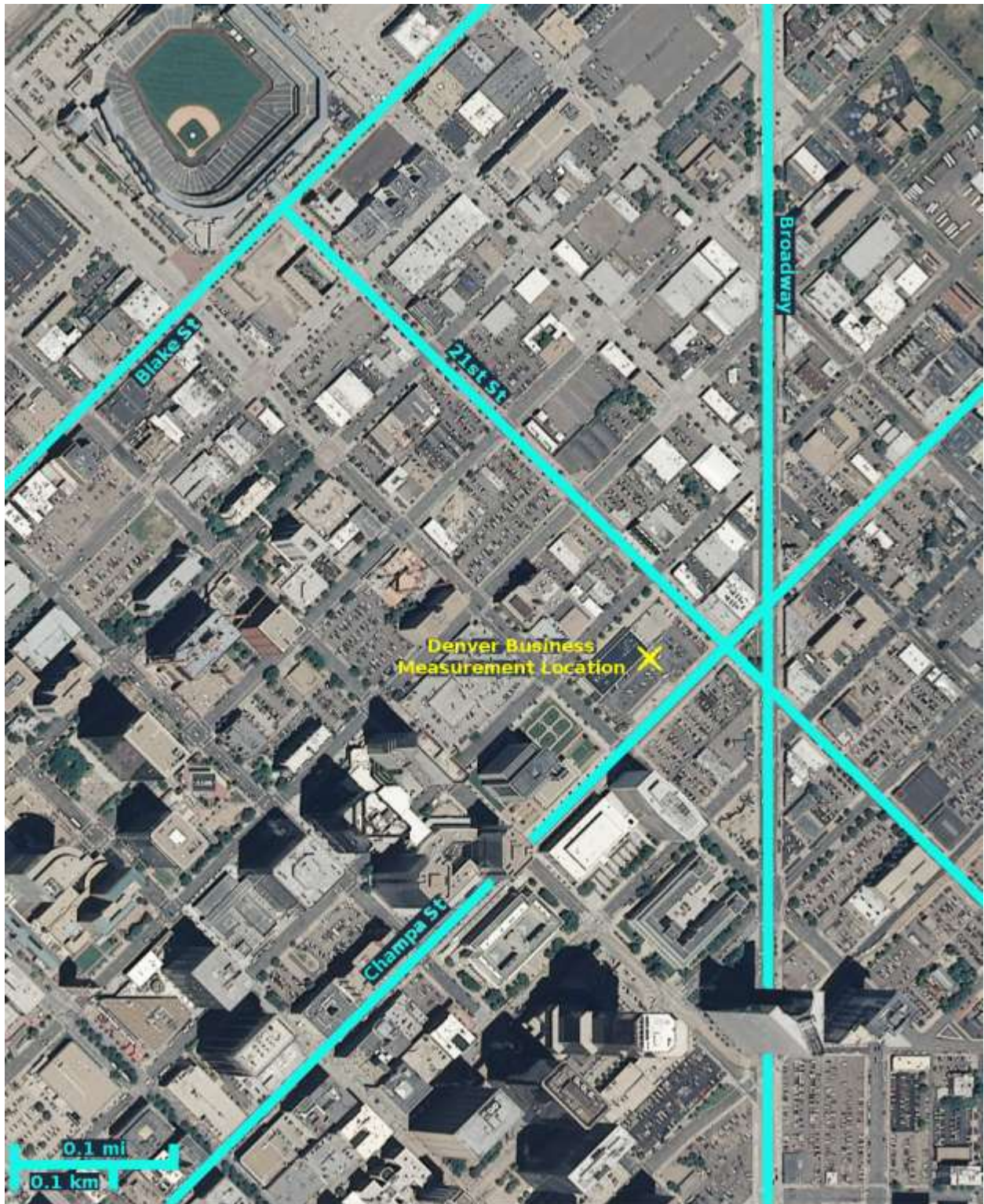


Figure 7. Aerial photograph of business measurement location in Denver (courtesy of the U.S. Geological Survey).

4 NOISE MEASUREMENT FREQUENCY AND BANDWIDTH SELECTION

The selection of appropriate frequencies and bandwidths between 100 and 1000 MHz at which to perform the noise measurements required a good understanding of the radio environment at the proposed measurement locations. Since recent spectrum survey measurements in these areas were not available, a spectrum survey of the radio environment was required. To accomplish this, an automated swept spectrum measurement system was developed for frequencies between 100 and 1100 MHz. A spectrum survey was then conducted at the four measurement locations proposed for the noise measurements. Details of the spectrum survey measurement system, measurement procedure, and results are provided in the Appendix.

4.1 Noise Measurement Bandwidth Selection

Before selection of the noise measurement frequencies, the bandwidth to be used in the noise measurements needed to be considered. Only relatively narrowband noise measurements (30 kHz or less) had been made in the past at ITS. There was considerable interest in making noise measurements in much wider bandwidths. Data taken in wide bandwidths can be processed directly or filtered to narrower bandwidths and then further processed. Therefore, data taken in wide bandwidths is more versatile than data taken in narrow bandwidths. However, there are significant challenges in making wideband noise measurements. The wider the bandwidth used for noise measurements, the more difficult it becomes to ensure that the noise measurements meet the requirement of being essentially free from intentionally radiated signals, and the more susceptible the measurements are to overload. Furthermore, if wideband noise data is going to be filtered to narrower bandwidths for statistical data processing such as APDs or mean power values, a longer data capture time (and hence more data storage) is required compared to that required for statistical processing of only the wideband data. The longer data capture time is required to ensure a sufficient number of independent samples for the computation of the statistics for the filtered noise data.

While wideband noise measurements were desirable and the noise measurement system can support measurements in bandwidths as wide as 36 MHz, it was difficult to find areas of the spectrum (particularly in the 100–200-MHz range) more than 1 MHz wide with no (or even very few) low-power intentionally radiated signals. Therefore, a 1-MHz measurement bandwidth was selected for the wideband noise measurements.

4.2 Noise Measurement Frequency Selection

The received signal power versus frequency data shown in Figures A-2 to A-61 in the Appendix were analyzed to determine three optimal frequencies at which to conduct the noise measurements. Ideally, these three frequencies would be spaced approximately an octave apart to provide a good characterization of how noise power varies with frequency. The selection of optimal frequencies included the consideration of the number and power levels of signals within and adjacent to a 1-MHz bandwidth (the bandwidth used for the wideband noise measurements). Consideration was also given to the types and database listings of licensed transmitters both within and outside the 1-MHz bandwidth. Where possible, to be able to best compare results,

selection of frequencies near those studied in previous noise measurement efforts at ITS was attempted [3], [4].

In the selection of the first frequency, 137.5 MHz was considered as it had been used in previous noise measurements at ITS in the mid- to late 1990s [3], [4]. Those measurements, however, were conducted in a 30-kHz bandwidth. It was not possible to find 1 MHz of spectrum around 137.5 MHz that was free from intentional emitters. However, Figures A-2–A-5 show that spectrum exists between 108 and 118 MHz that has some 1-MHz wide areas relatively free from intentional emitters. This band is allocated for VHF omnidirectional range (VOR) aeronautical navigation beacons [10]. Figure 8 shows an expanded view of the received signal power versus frequency for all four measurement locations from 110 to 115 MHz. The resolution bandwidth (RBW), number of sweeps, and duration of each sweep are also given. Analyzing the spectrum in Figures A-2–A-5 and Figure 8, and using sectional aeronautical charts to identify the locations and operating frequencies of the VORs around the Denver area, a suitable noise measurement frequency was found at 112.5 MHz. (Note that VOR signals in the Denver area can be seen in the median plot in Figure 8.)

The frequency at the next octave would be 225 MHz. This is at the end of an amateur radio band and therefore was unsuitable for the noise measurements. Looking at the received signal power versus frequency data for all four measurement locations from 216 to 225 MHz in Figures A-14–A-17 and the expanded view of the spectrum from 219 to 224 MHz in Figure 9, 221.5 MHz was identified as the best possible frequency to use for the second noise measurement frequency. This frequency falls within a band that is used for private land mobile radio and radiolocation [10].

The selection of the final noise measurement frequency was based on finding a frequency close to 402.5 MHz. This frequency was also used for previous noise measurements at ITS in the late 1990s [4] and it is roughly an octave above 221.5 MHz. However, after examining the received signal power versus frequency data for all four measurement locations from 400 to 406 MHz in Figures A-22–A-25 and the expanded view of the spectrum from 400 to 404 MHz in Figure 10, 401 MHz was chosen for the final noise measurement frequency. The 1 MHz of spectrum centered at 401 MHz includes bands allocated for meteorological aids; space operation and research; and meteorological, mobile, and earth exploration satellites [10].

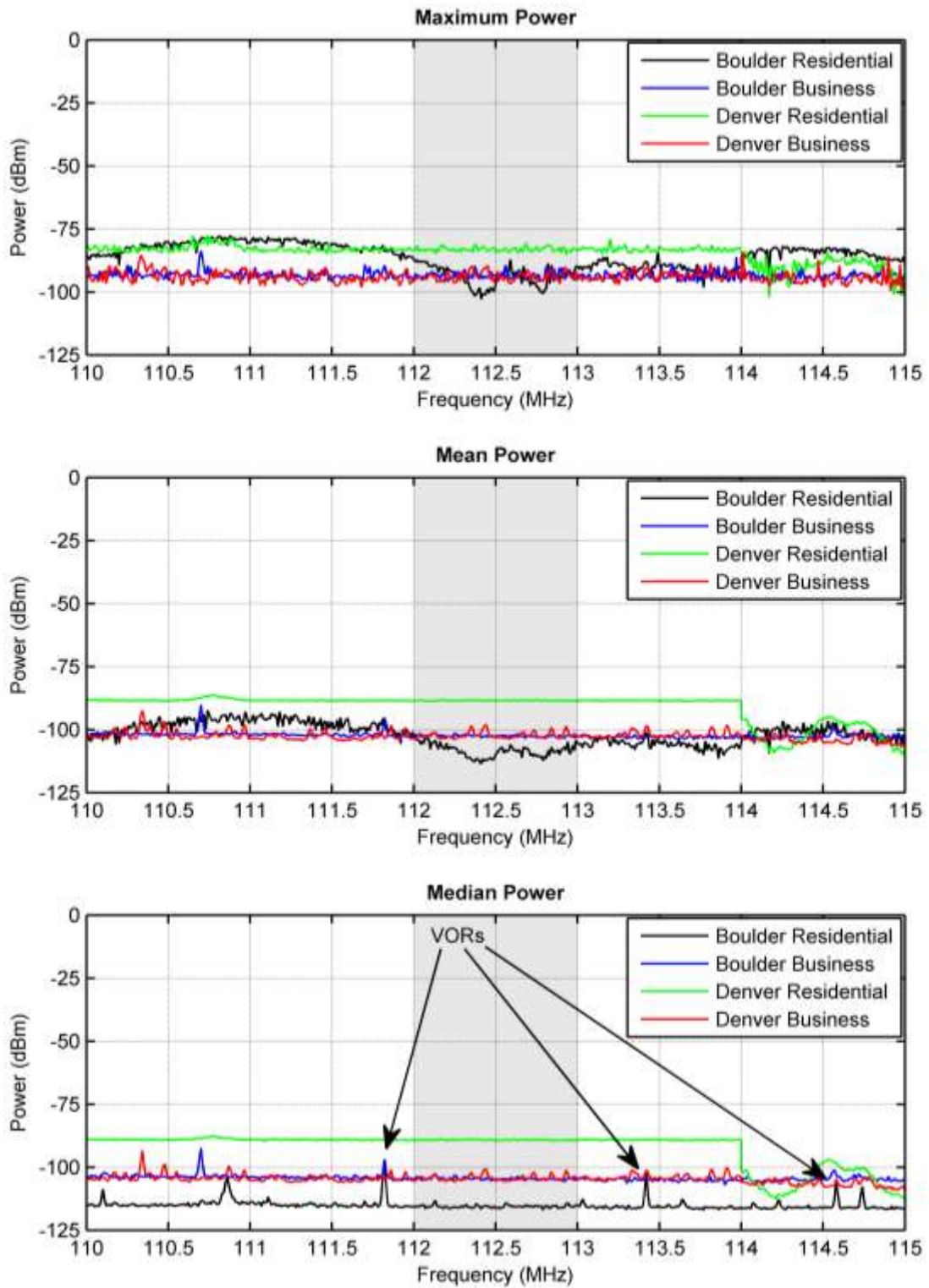


Figure 8. Maximum, mean, and median received signal power at all measurement locations for 110–115 MHz (RBW = 10 kHz, 100 sweeps, sweep time = 300 ms).

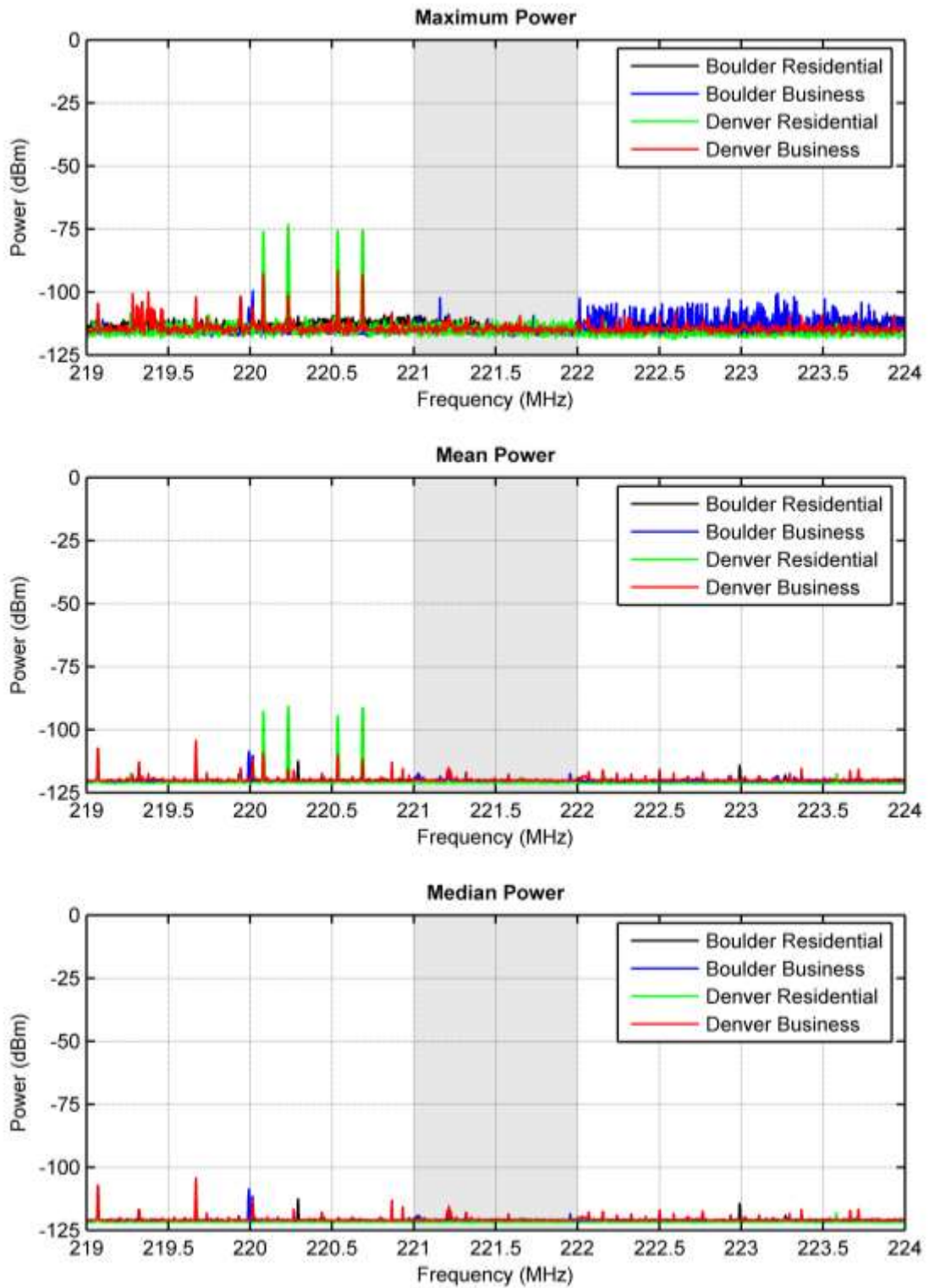


Figure 9. Maximum, mean, and median received signal power at all measurement locations for 219–224 MHz (RBW = 3 kHz, 60 sweeps, sweep time = 900 ms).

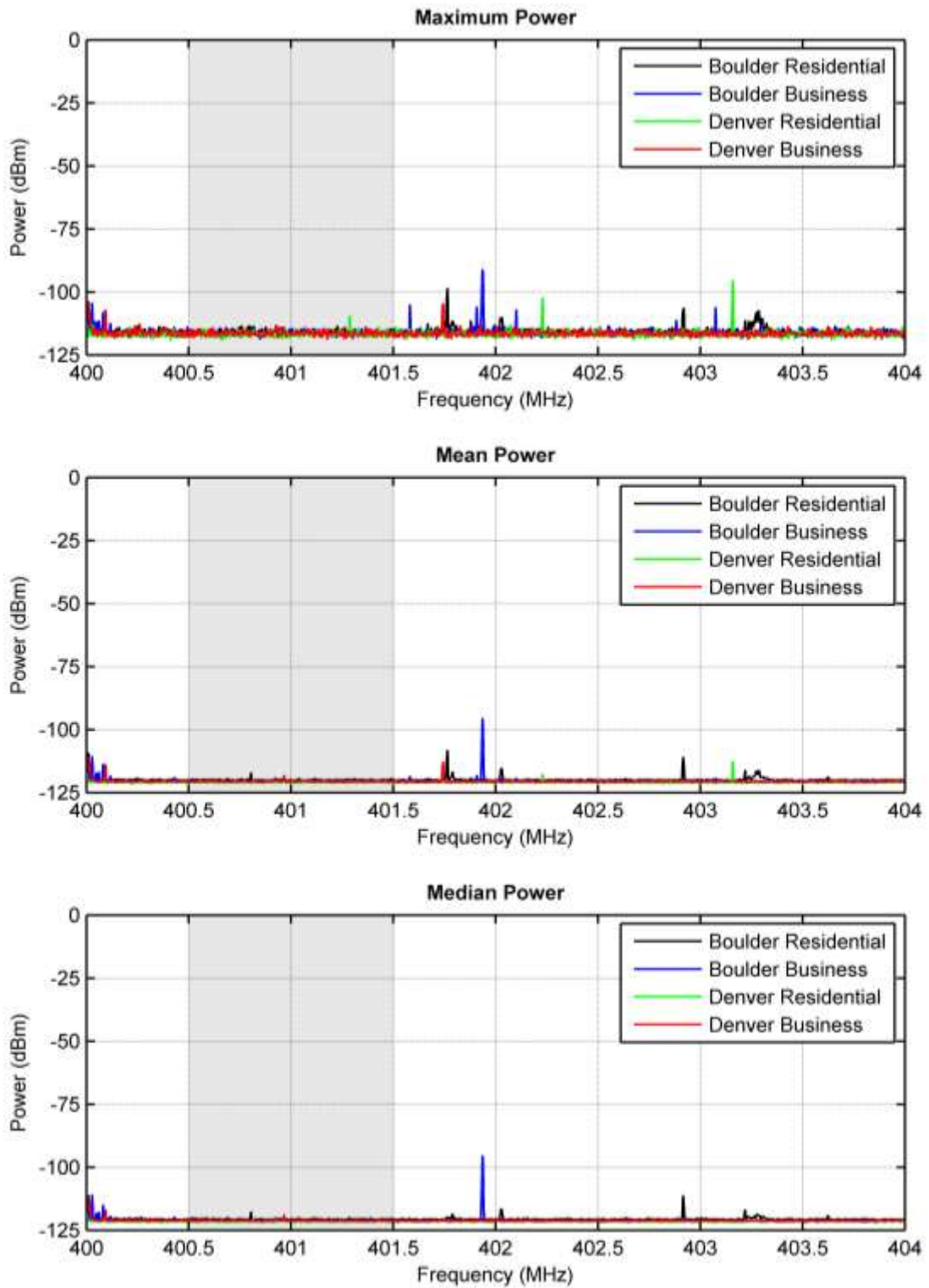


Figure 10. Maximum, mean, and median received signal power at all measurement locations for 400–404 MHz (RBW = 3 kHz, 60 sweeps, sweep time = 900 ms).

5 NOISE MEASUREMENTS

The noise measurement system and how it is optimized and verified are described in this section. The procedure used to collect the noise measurement data at all of the measurement locations and frequencies is then detailed.

5.1 Noise Measurement System

The noise measurements presented in this report were taken using a new, automated, wideband noise measurement system developed by ITS. Figure 11 shows a block diagram of the noise measurement system. The system consists of an antenna, ITS custom-built preselector, vector signal analyzer (VSA), thermostat control unit, and two personal computers.

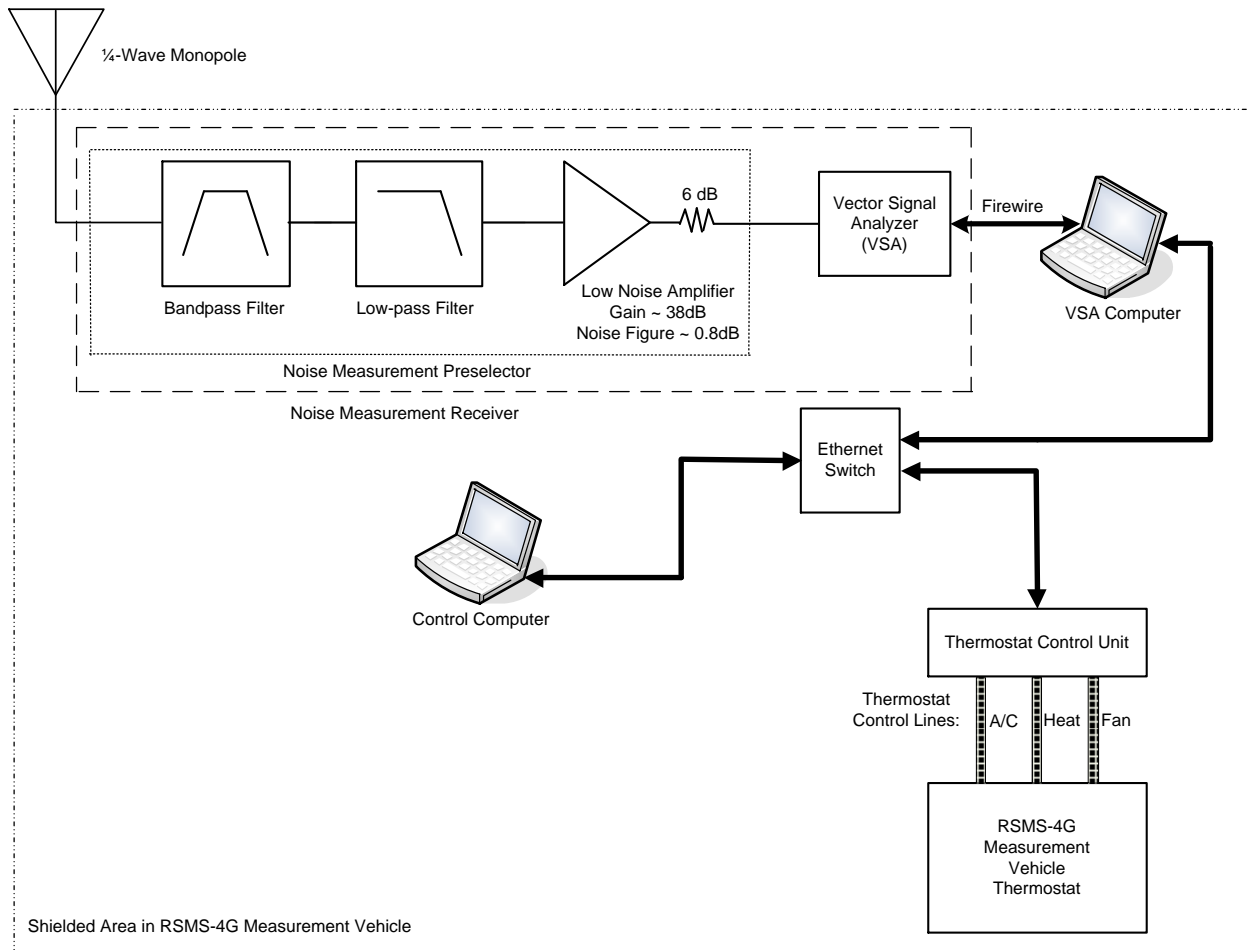


Figure 11. Block diagram of the noise measurement system installed in the RSMS-4G measurement vehicle.

For each distinct measurement frequency, a separate quarter-wave monopole antenna is required. Each antenna is carefully tuned to the measurement frequency and mounted on a circular ground plane with a diameter of approximately 1.3 m that is attached to the roof of the RSMS-4G

vehicle. The ground plane diameter corresponds to roughly 0.5, 1.0, and 1.7 wavelengths at 112.5, 221.5, and 401 MHz, respectively. An indication of the frequency response of the antennas can be seen from the plots of VSWR versus normalized frequency shown in Figure 12.

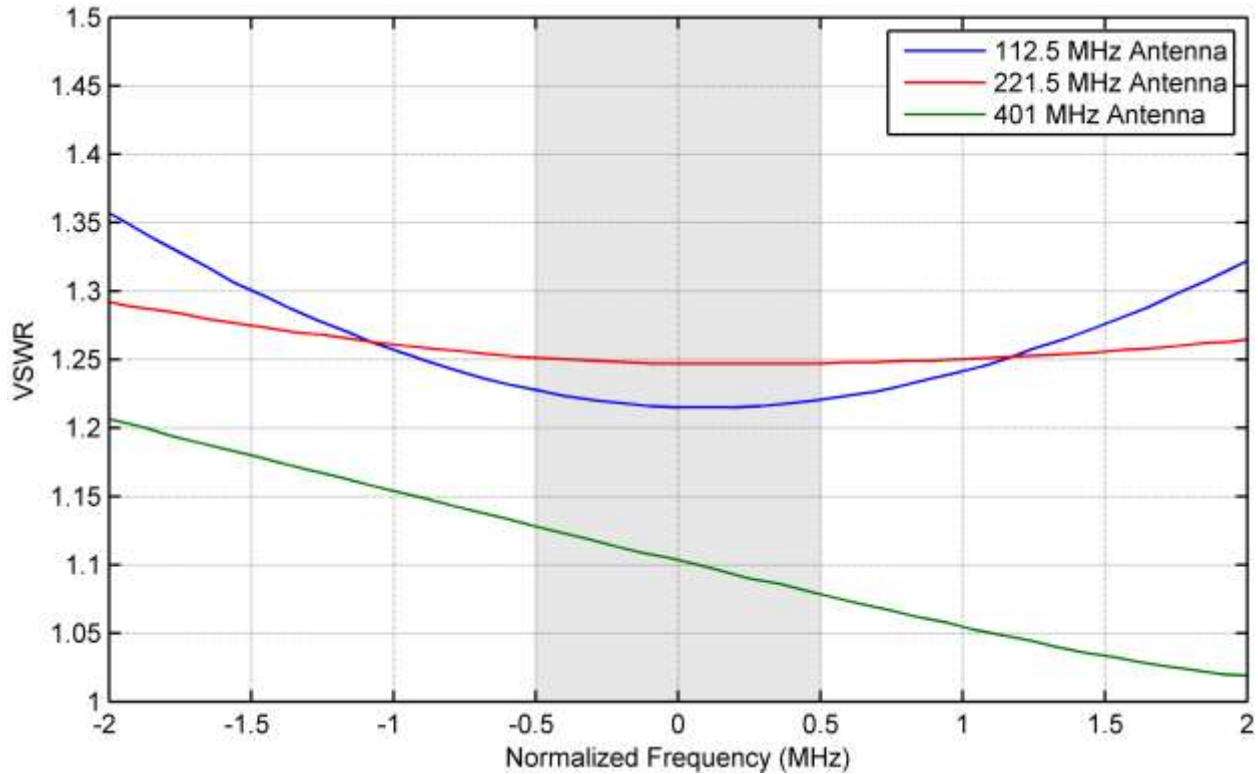


Figure 12. VSWR versus normalized frequency for the quarter-wave monopole antennas.

Man-made noise is believed to arrive at the receive antenna at relatively low elevation angles and from widely distributed directions [11]. The quarter-wave monopole antenna mounted on a circular ground plane was chosen for the noise measurements in this study because it provides an omnidirectional, azimuthal pattern and good gain at the horizon and at relatively low elevation angles. Using the same antenna type for different noise measurement studies makes it easier to provide a comparison of the results. This was another reason why quarter-wave monopoles over a ground plane were used; noise measurements at ITS in the 1990s [3], [4] used the same antenna type. Electrically short monopoles over a ground plane, which also have an omnidirectional, azimuthal pattern and a similar elevation pattern as the quarter-wave monopole, were used for the measurements on which the current ITU model for man-made noise is based [6].

The custom built preselector consists of a fixed-cavity bandpass filter centered on the measurement frequency; a fixed, low-pass filter with a cutoff frequency just above the bandpass filter stopband (to attenuate repeated bandpass responses); a low-noise amplifier; and some attenuators to adjust the gain of the overall preselector. All of these components are housed inside an RF shielded box.

For each measurement frequency, the appropriate fixed bandpass and low-pass filters are installed in the preselector shielded box; changing frequencies requires that a different set of filters be installed. Fixed bandpass filters are used instead of tunable ones to achieve a very steep roll-off and low insertion loss. The bandpass filters have an insertion loss of less than 1.9 dB over a bandwidth of at least 1 MHz and an attenuation of 50–60 dB beyond ± 5 MHz from the center frequency. The 1-MHz passband amplitude variation is less than 0.25 dB with a deviation from linear phase less than $\pm 5^\circ$.

The core of the new measurement system is the VSA. This instrument is capable of recording digitized in-phase (I) and quadrature (Q) samples in up to 36 MHz of bandwidth. The ability to record I and Q data, properly sampled at a rate above Nyquist, makes it possible to process the noise data in ways that were not possible with many previous noise measurement systems that only recorded amplitude data. With the I and Q data it is possible not only to obtain noise amplitude statistics such as APDs, but also to fully characterize the time and frequency domain characteristics of the noise data. Properly sampled data can also be filtered to narrower bandwidths. In addition, the I and Q data are valuable because they can be used in simulations. The VSA is controlled by commercial software operating on a dedicated personal computer as shown in Figure 11.

The thermostat control unit consists of three Ethernet-controlled electro-mechanical relays. These relays are placed in-line with the RSMS-4G measurement vehicle thermostat control lines for the fan, air conditioner (A/C), and heater. The fan, A/C, and heater are disabled by the noise measurement software during noise data acquisition. This eliminates any possibility of the noise measurement system measuring unintentional RF emissions from this equipment.

The noise measurement software operates on a personal computer, labeled as the control computer in Figure 11. The software controls both the VSA and the thermostat control unit. The software allows the user to set the VSA measurement frequency, bandwidth (span), number of data points to collect, input range, and other parameters. Once the measurement is started, it will automatically collect data at user-defined time intervals for a user-specified duration. The capability to perform and display results of noise diode calibrations, spectrum captures, and single, manual noise measurement data captures is also included in the software.

For the noise measurements taken in this study, the measurement system was installed in the RSMS-4G measurement vehicle as discussed in Section 3. Figure 13 shows a photograph of the noise measurement system equipment set up inside the measurement vehicle.

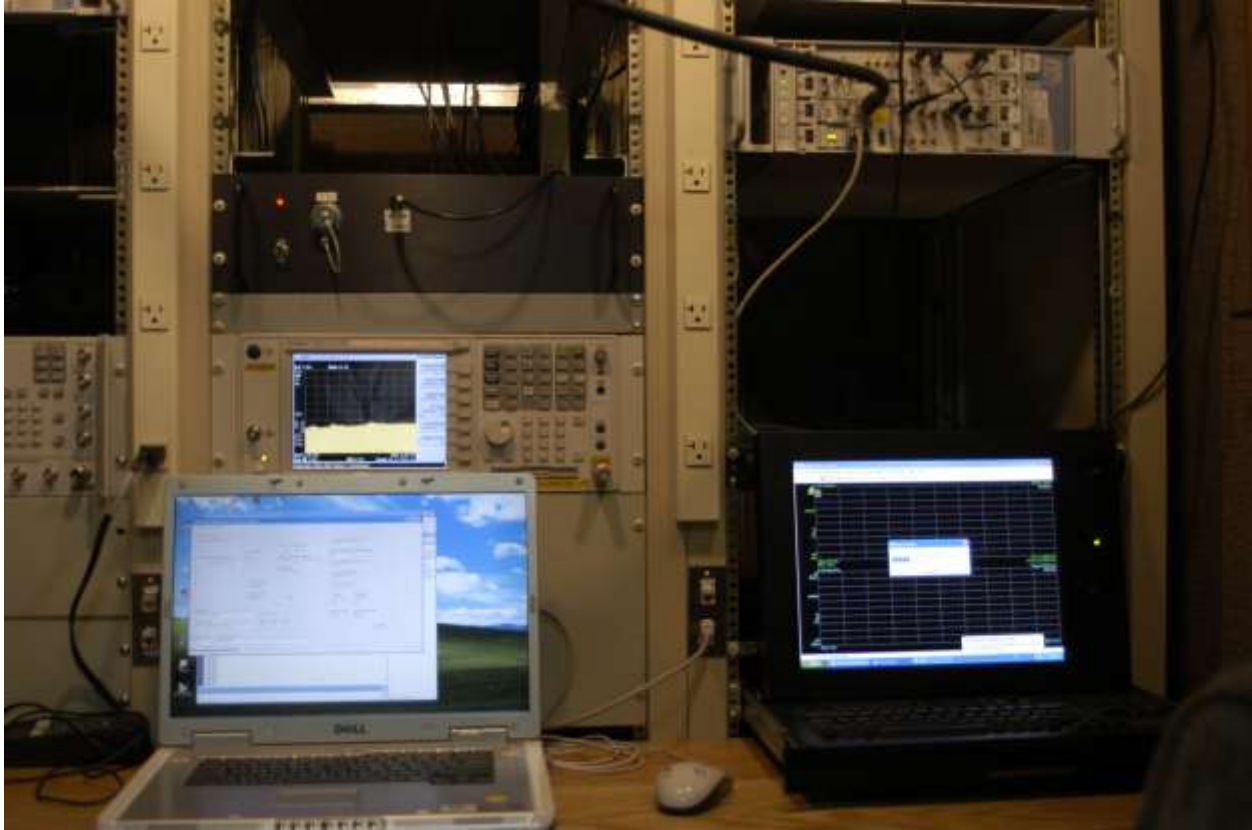


Figure 13. Photograph of the noise measurement system installed in the RSMS-4G measurement vehicle.

5.2 Noise Measurement System Optimization and Verification

Assuming an input range setting of -30 dBm on the VSA⁷ in the noise measurement system, the preselector gain was adjusted, with the use of attenuators, such that the overall measurement system dynamic range was maximized while maintaining a noise figure of approximately 3 to 4 dB over the selected noise measurement frequencies. In order to avoid VSA overloads from impulsive noise in the field, it was necessary to increase the input attenuation in the front end of the VSA by 15 dB⁸. This improved the overall dynamic range of the noise measurement system by 13 dB but degraded the sensitivity by 2 dB. Therefore, the resulting noise figure of the overall system varied from 5 to 6 dB over the selected noise measurement frequencies with a dynamic range of approximately 69 dB.

The measurement system was set up to determine the variation in receiver noise figure F_r over a 24-hour period. To accomplish this, the antenna was disconnected and replaced by a 50Ω load.

⁷ The input range setting on the VSA controls its sensitivity and dynamic range. A setting of -30 dBm provides an optimal balance between good VSA sensitivity and high dynamic range.

⁸ The input attenuation in the front end of the VSA is increased by 15 dB by increasing the input range setting on the VSA from -30 dBm to -15 dBm.

The preselector was configured with the bandpass and low-pass filters for measurements at a 112.5 MHz center frequency. The receiver noise figure was measured in a 1-MHz bandwidth over a 24-hour period. The variation in the receiver noise figure was seen to be less than ± 0.25 dB. Measurements of the receiver noise figure at both 221.5 and 401 MHz showed a similar variation.

5.3 Noise Measurement Procedure

The noise measurements were conducted at the four locations described in Section 3. At each location, before beginning the measurements, the preselector was configured with the proper bandpass and low-pass filters corresponding to the desired measurement frequency. Next, the quarter-wave monopole antenna tuned to the correct frequency was installed on the ground plane mounted on the roof of the vehicle. The equipment was turned on and allowed to warm up for at least 30 minutes. Using a commercial cable and antenna analyzer, the antenna VSWR was measured to help verify that the antenna was working properly. After verifying proper antenna operation and ensuring that the equipment had been sufficiently warmed up, the noise measurement software was initiated.

Before starting the noise measurements, the signal environment around the measurement center frequency was observed using the VSA spectrum display with a span of 36 MHz (the maximum VSA span) and an input range of -30 dBm. The VSA display was first observed to determine the occurrence of any overloads. As mentioned in Section 5.2, it was necessary to increase the input attenuation in the front end of the VSA by 15 dB to prevent VSA overloads due to impulsive noise.

Once the input range was set, the VSA spectrum display was checked for any obvious signals within a measurement span of 1.16 MHz about the center frequency. If there were noticeable signals within this span then the VSA measurement center frequency was adjusted slightly (550 kHz at most) so the signals would occur outside of the span.⁹ Care was taken to keep the entire measurement span within the RF filter's flat magnitude response and relatively linear phase region. The frequency allocations of the bands the measurement span encompassed were also taken into consideration.

The gain and noise figure of the system were then determined by performing a noise diode calibration as described in Section A.2.

The system gain and noise figure values are used to verify the proper operation of the measurement system. The resulting measured system gain and noise figure values for each measurement frequency and location are shown in Table 2.

⁹ For better readability of this report, the center frequencies used for the measurements are stated as being taken at the nominal center frequencies of 112.5, 221.5, and 401 MHz even when the actual measurement frequencies were slightly different.

Table 2. Measured system gain and noise figure at each measurement frequency and location

Location	Approx. Center Frequency					
	112.5 MHz		221.5 MHz		401 MHz	
	Gain (dB)	Noise Figure (dB)	Gain (dB)	Noise Figure (dB)	Gain (dB)	Noise Figure (dB)
Boulder Residential	32.7	5.1	32.5	5.3	32.2	6.0
Denver Residential	32.2	5.5	32.4	5.4	32.0	6.0
Boulder Business	32.6	5.5	32.1	5.5	32.2	6.0
Denver Business	32.7	5.1	32.1	5.6	32.2	6.0

Following the noise diode calibration, single noise data record captures, both with a 50 Ω dummy load and with the quarter-wave monopole antenna, were performed to ensure that the system was working properly. First, the antenna was replaced by a 50 Ω dummy load and a single noise data record was captured using the manual measurement capability within the noise measurement software. Next, the antenna was reconnected and another noise data record was captured. The APDs of both captures were then computed and displayed using the noise measurement software. APDs provide a convenient way of displaying the amplitude characteristics of noise. Explanations of APDs and how they are computed are given in [12] and [13].

The APD corresponding to the 50 Ω load capture was expected to be a straight line with the same slope as, but higher amplitude than, an APD generated from simulated complex Gaussian noise with a thermal noise power within the receiver bandwidth. The APD corresponding to the 50 Ω load capture was expected to be higher in amplitude than the APD of complex Gaussian noise by the noise figure of the measurement system. The APD corresponding to the capture with the antenna connected was seen to vary considerably depending on the location, frequency, and time of the capture.

After confirmation that the measurement system was working properly, the noise measurement software was set up to collect noise data automatically for a 24-hour period. The measurements were set up so that every 10 minutes a noise data record consisting of six million I and Q data samples was taken in a 1.16-MHz VSA span.¹⁰ The reason that six million data samples were collected is that it ensures that one million independent data samples are available to compute APDs. This is covered in more detail during the discussion of APDs in Section 6.1.

The 24-hour automated noise measurements were then initiated. Before leaving the measurement system unattended, the measurements were observed for at least 20 minutes to ensure that VSA overloads were not occurring and that the air conditioner, heater, and fan did not run during the data acquisition. Once the 24-hour data collection was complete, the data were saved to a portable external hard drive as a backup.

¹⁰ The 1.16-MHz VSA span is the closest cardinal span available on the VSA to the desired 1-MHz noise measurement bandwidth. VSA cardinal spans use hardware decimation filters while other VSA spans use additional software filtering. Cardinal spans are used since they provide much faster recording of the data.

If a VSA overload occurred for a particular six-million-sample data capture, it was thrown out and not included in the data analysis. At most locations and frequencies either no VSA overloads occurred at all or one VSA overload occurred out of 144 data captures. The most VSA overloads occurred at a center frequency of 112.5 MHz at the Boulder residential location where a VSA overload occurred in 9 out of 144 data captures.

6 DATA ANALYSIS

The first type of data analysis examines characteristics of the individual noise data records. The second type of data analysis examines noise power statistics over a 24-hour period.

As mentioned previously, a noise data record consists of six million I and Q noise data samples that were collected in a 1.16-MHz VSA span every 10 minutes over a 24-hour time period for each frequency and location. Before analyzing the data, each noise data record is filtered in software using a low-pass finite impulse response (FIR) filter with a 0.01 dB ripple, 500-kHz bandwidth (1-MHz double-sided bandwidth) that provides a 60 dB double-sided bandwidth of 1.16 MHz. Note that frequencies in the noise data record obtained from the VSA between 1.16 MHz and the double-sided Nyquist frequency of 1.484375 MHz can contain aliased components. These aliased components have already been attenuated by at least 20 dB by the VSA. The low-pass FIR filter ensures that any aliased components are attenuated by at least 80 dB.

The I and Q data samples in each noise data record represent complex envelope voltage values of the noise. These samples are converted to magnitude values and scaled by a factor of $1/\sqrt{2}$ to ensure the correct total average power [14] and form a scaled-magnitude noise data record.

6.1 Time Domain Characteristics and APDs of Individual Noise Data Records

First, the time domain characteristics of the individual noise data records are examined. The samples in the scaled-magnitude noise data records are converted to power received at the input to the VSA in dBm. The overall system noise power, at the antenna output terminals, is obtained by subtracting the gain of the measurement system in dB (defined as the gain from the antenna output terminals to the input of the VSA) from the noise power at the input to the VSA (see Figure 11).

Figure 14 provides an example of a time domain plot showing 60 ms of a noise data record taken at the residential Boulder location at a center frequency of 112.5 MHz at 0349 on September 1, 2009. In this plot it is possible to see evidence of 60 Hz unintentional emissions from the AC power distribution system. Evidence of 60 Hz unintentional emissions is seen in at least some of the noise data records at every measurement location and frequency. Harmonics of 60 Hz are also noted in many of the noise data records.

Next, APDs of the individual noise data records are examined. To compute the APD, the six million data samples in each scaled-magnitude data record are first decimated by a factor of six to ensure that the resulting samples are independent of correlation introduced by the measurement system. The first L samples out of the remaining one million samples (where L is the number of taps in the FIR filter) are discarded to ensure that the filter has settled. An APD is then computed [13] using the remaining samples. The amplitude values in the APD are converted into values of overall system noise power following the same procedure described above for the time domain characteristics. Figures 15–18 show example APDs along with the APD of the measured receiver noise power as a reference.

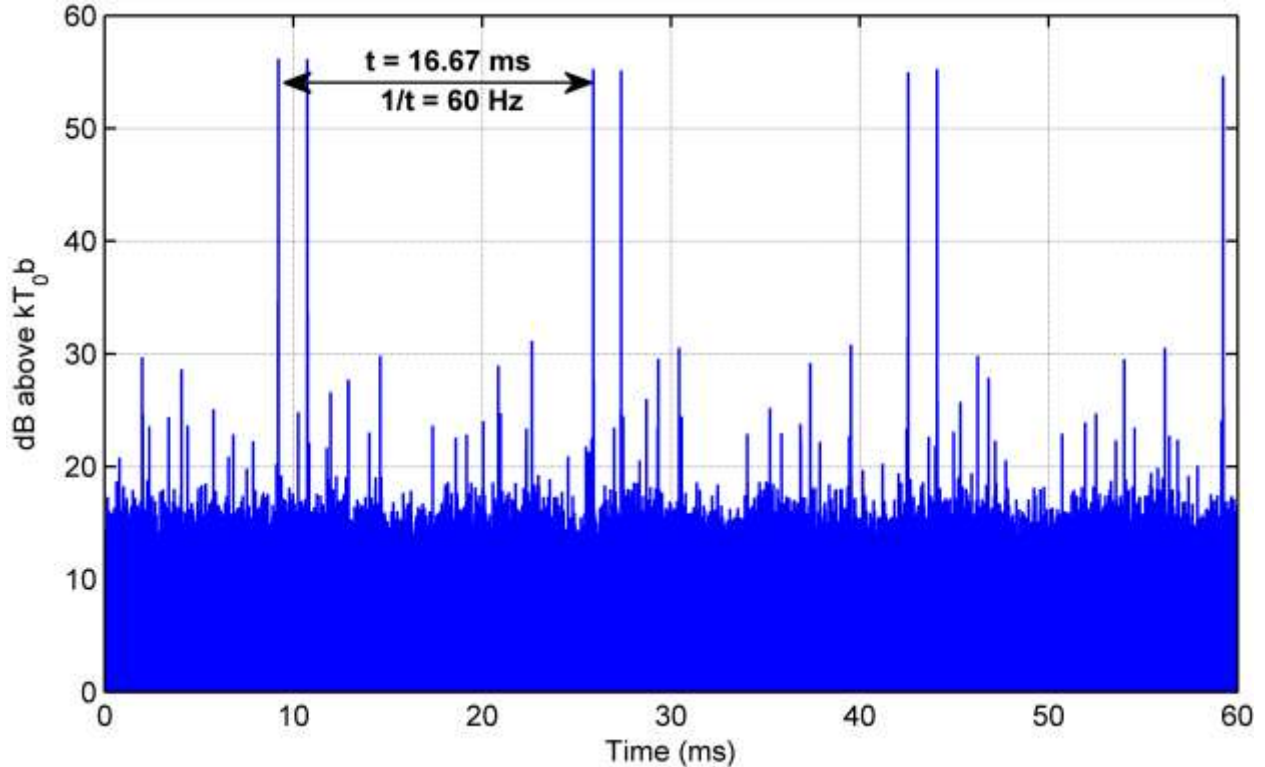


Figure 14. Example time domain plot showing 60 ms of a noise data record from the residential Boulder location at 0349 on September 1, 2009 with a 112.5-MHz center frequency and 1.16-MHz span.

Figure 15 shows the APD from the same noise data record used to produce the time-domain plot seen in Figure 14. Figures 16–18 provide example APDs from other noise measurement locations and frequencies. In the example APD in Figure 15, with a 112.5-MHz center frequency, note the increased power levels at percent exceeding ordinate values corresponding to the reciprocal of 60 Hz and 120 Hz (1.6 % and 0.8 %, respectively). This indicates the presence of noise from the AC power distribution system. This is not seen in the APDs at higher frequencies (Figures 16 and 17).

Impulsive noise is present in the vast majority of the noise data records. At the 401-MHz measurement frequency and residential measurement locations, Gaussian noise without impulsive noise is observed more often than at the other measurement frequencies, but still only occasionally. Figures 15–17 provide good examples of what impulsive noise looks like in an APD. Figure 18 shows what appears to be primarily Gaussian noise that is elevated substantially above the measured receiver noise power.

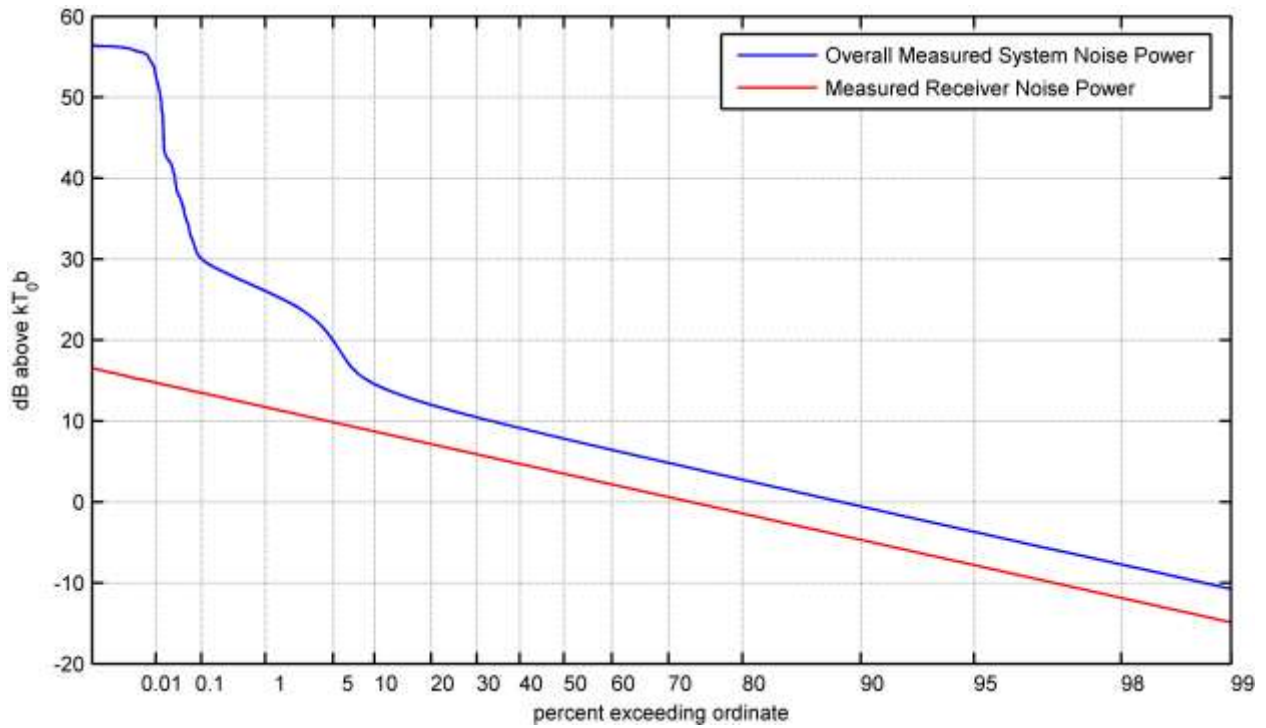


Figure 15. Example APD from the residential Boulder location at 0349 on September 1, 2009 with a 112.5-MHz center frequency and 1.16-MHz span.

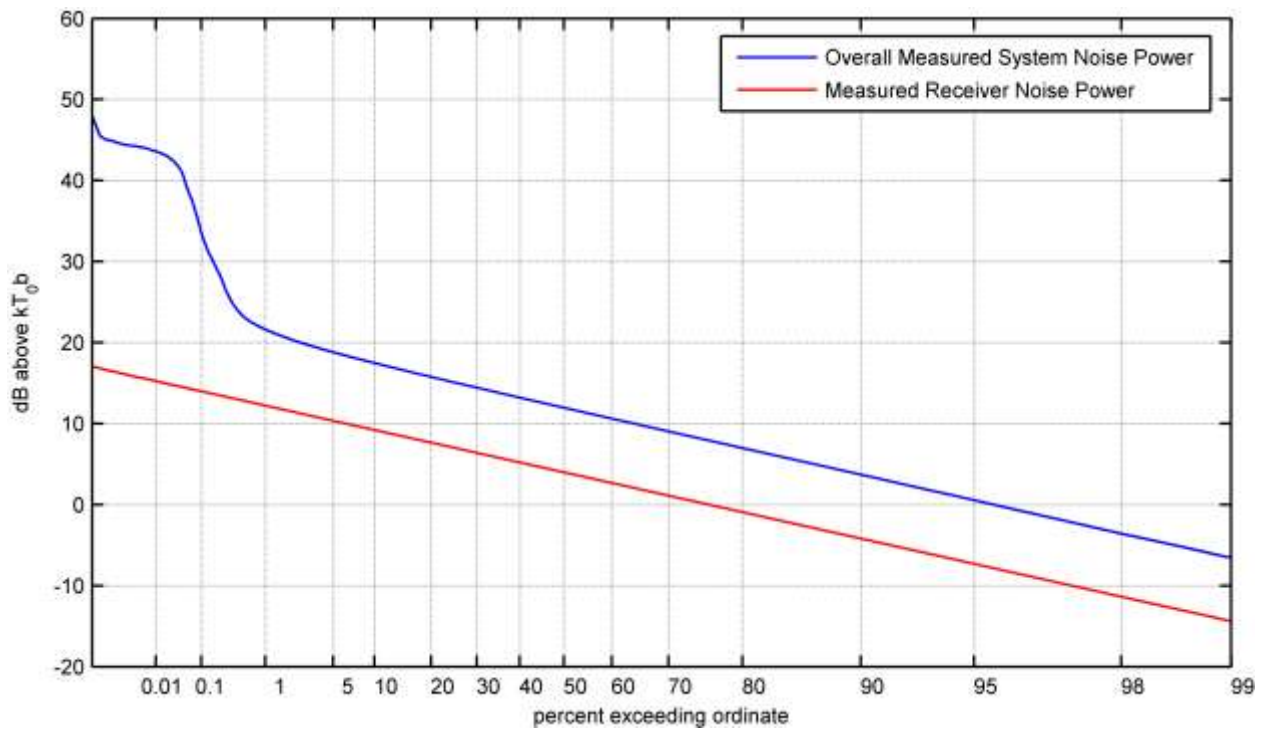


Figure 16. Example APD from the Denver business location at 0723 on August 19, 2009 with a 221.5-MHz center frequency and 1.16-MHz span.

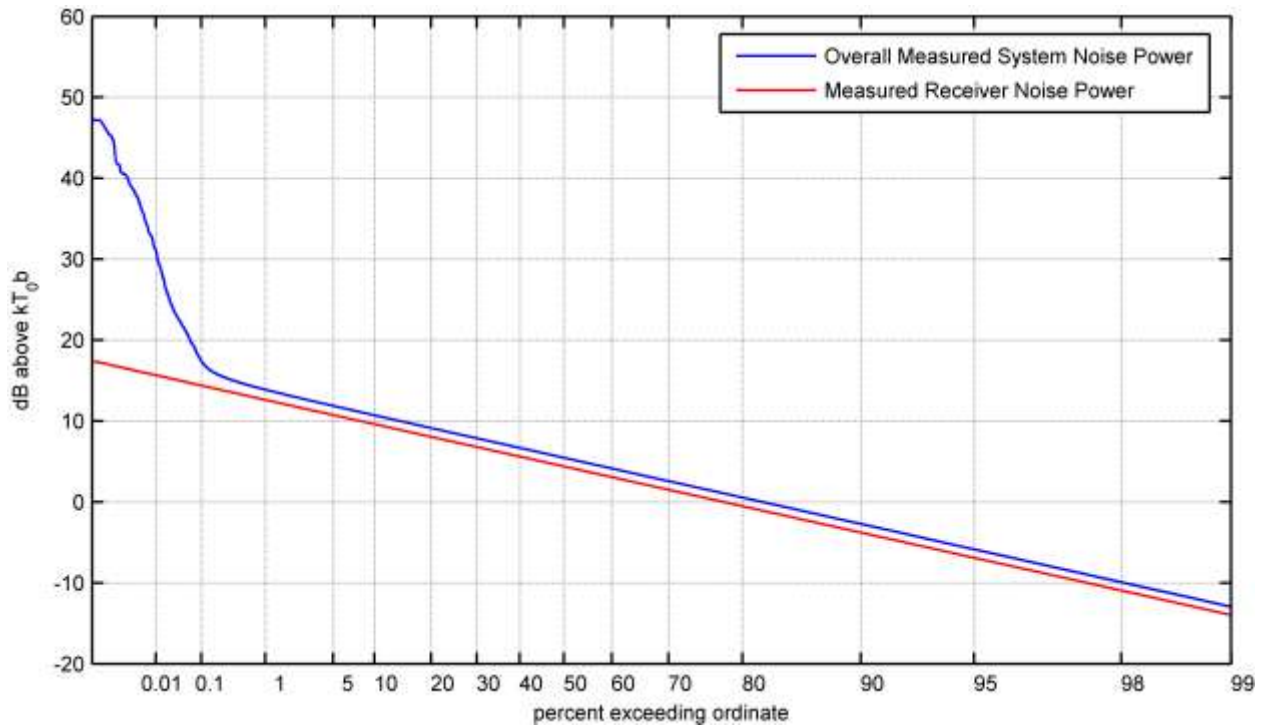


Figure 17. Example APD from the Boulder business location at 1211 on July 22, 2009 with a 401-MHz center frequency and 1.16-MHz span.

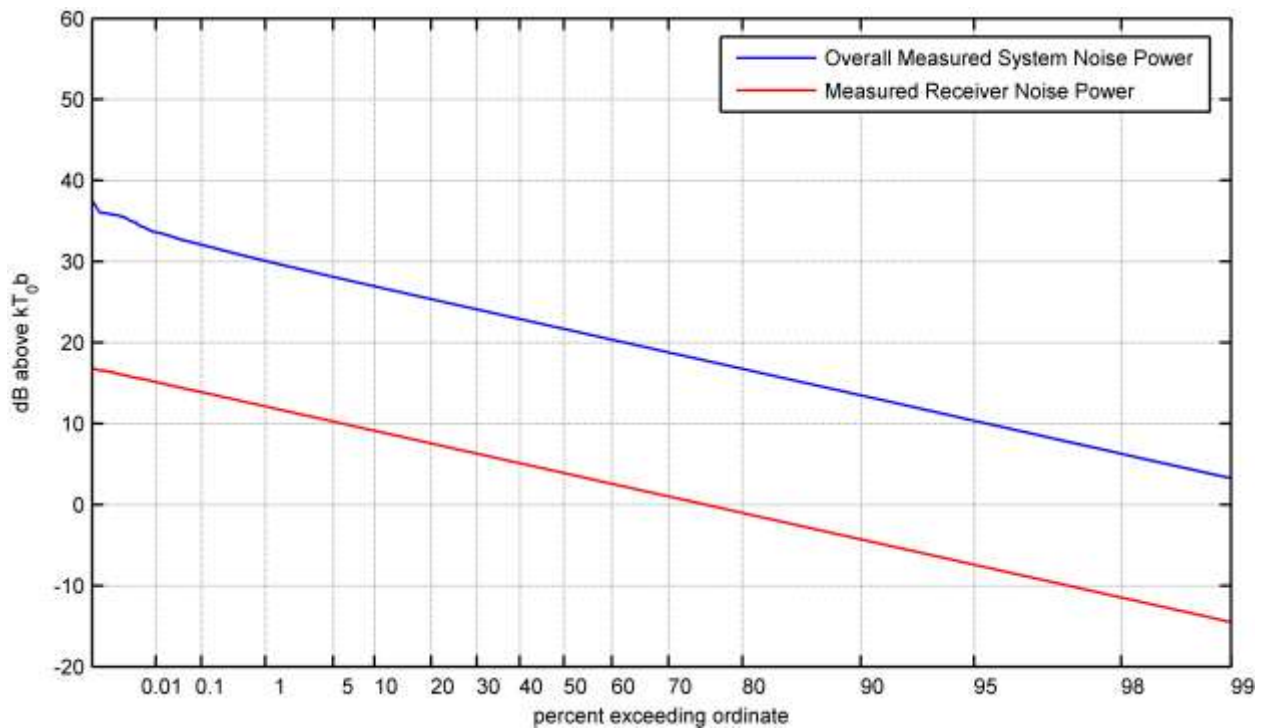


Figure 18. Example APD from the Denver residential location at 2319 on July 29, 2009 with a 112.5-MHz center frequency and 1.16-MHz span.

6.2 Median, Mean, and Peak Noise Power Analysis

The first type of data processing for statistically summarizing all of the noise data collected provides the median, mean, and peak power of the overall measured system noise power (expressed in dB above kT_{ob}) for each scaled-magnitude noise data record collected. Note that for the purposes of this report, as in [3] and [4], the peak noise power is defined as the noise power level exceeded 0.01% of the time.

The procedure for computing the median, mean, and peak noise power follows that for computing the APD as described in Sections 6 and 6.1, with the exception that median, mean, and peak noise power values are computed instead of the APD for each scaled-magnitude noise data record. Figures 19–30 show the median, mean, and peak noise power (bottom, middle, and top curves of each figure, respectively) for each noise data record taken every 10 minutes over a 24-hour period and for each measurement frequency and location.

The mean and peak noise power plots in Figures 19–30 typically show, as would be expected, that the noise power is higher during the day than during the night. At most of the frequencies and locations the noise is clearly non-Gaussian, as the peak noise power is more than 10 dB greater than the mean noise power. (For complex Gaussian noise, the peak noise power is 9.6 dB greater than the mean noise power.) The noise appears as if it may be Gaussian during the nighttime hours (between 2000 and 0800) for the 401-MHz data at the residential location in Boulder (Figure 21) and during some of the time between 0200 and 0600 for the 401-MHz data at the residential location in Denver (Figure 27).

The mean noise power was substantially higher than the system noise power (the system noise power was between 5 and 5.5 dB above kT_{ob}) for the measurements around 112.5 MHz at all locations. At around 221.5 MHz, the mean noise power was substantially higher than the system noise power (the system noise power was approximately 5.5 dB above kT_{ob}) at the business locations at all times of the day, at the residential location in Boulder between 1000 and 2000, and at the residential location in Denver only at certain times between 1000 and 1600. The mean noise power was close to or slightly above the system noise power (the system noise power was 6.0 dB above kT_{ob}) for the measurements at 401 MHz at all locations. For the 401-MHz measurements, the mean noise power was slightly higher in the business locations than in the residential locations and also slightly higher during business hours than during non-business hours.

The median power generally varied less than the mean or peak power for almost all of the frequencies and locations. An exception to this is for the 112.5-MHz residential location in Denver (Figure 25) where the mean and median power vary similarly. The peak power varied significantly for all frequencies and locations.

Man-made radio noise power is often characterized by analyzing how the noise power statistics (such as mean power) vary over time and between locations and also by computing statistics (such as the median) of these noise power statistics [3], [4], and [6]. Therefore, the median, mean, and peak noise power statistics were used as a starting point for further analysis.

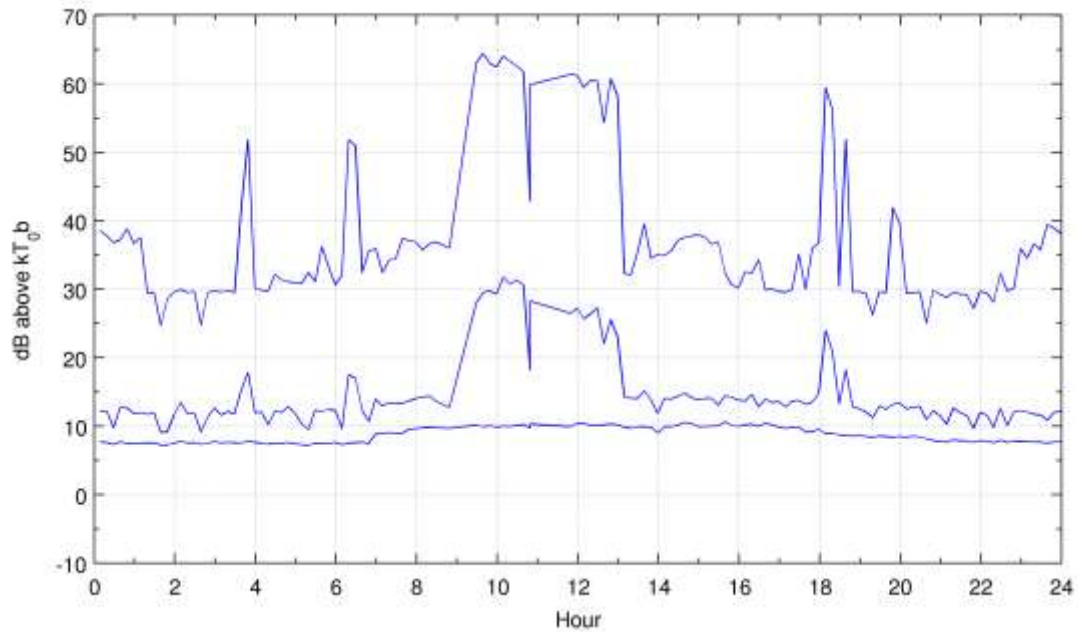


Figure 19. Median, mean, and peak measured noise power in a 1-MHz bandwidth at a center frequency of 112.5 MHz at the Boulder residential location (August 31–September 1, 2009).

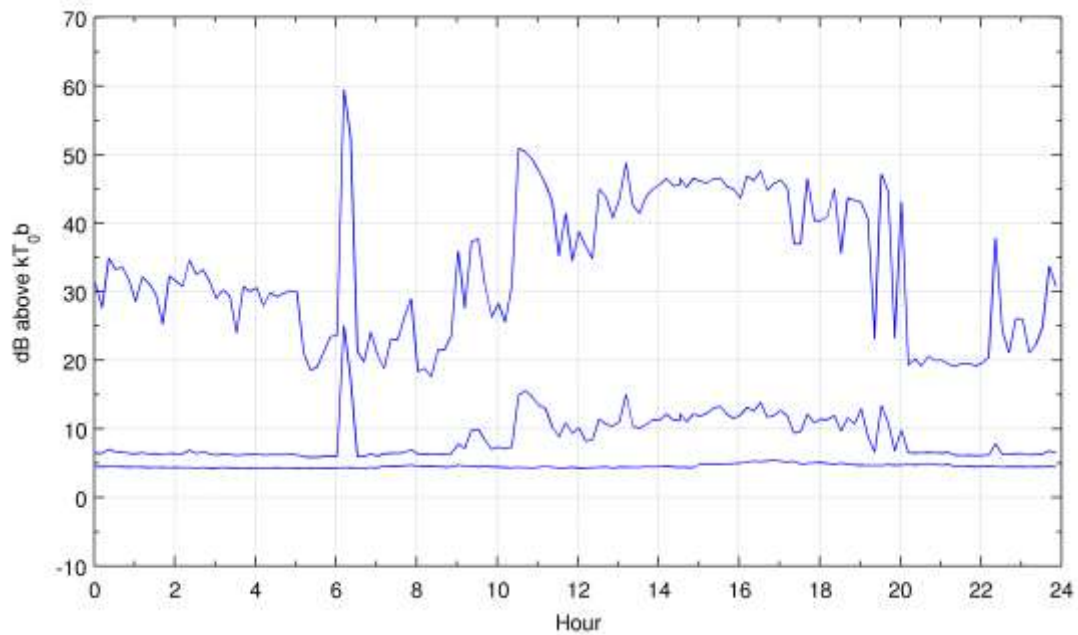


Figure 20. Median, mean, and peak measured noise power in a 1-MHz bandwidth at a center frequency of 221.5 MHz at the Boulder residential location (September 3–4, 2009).

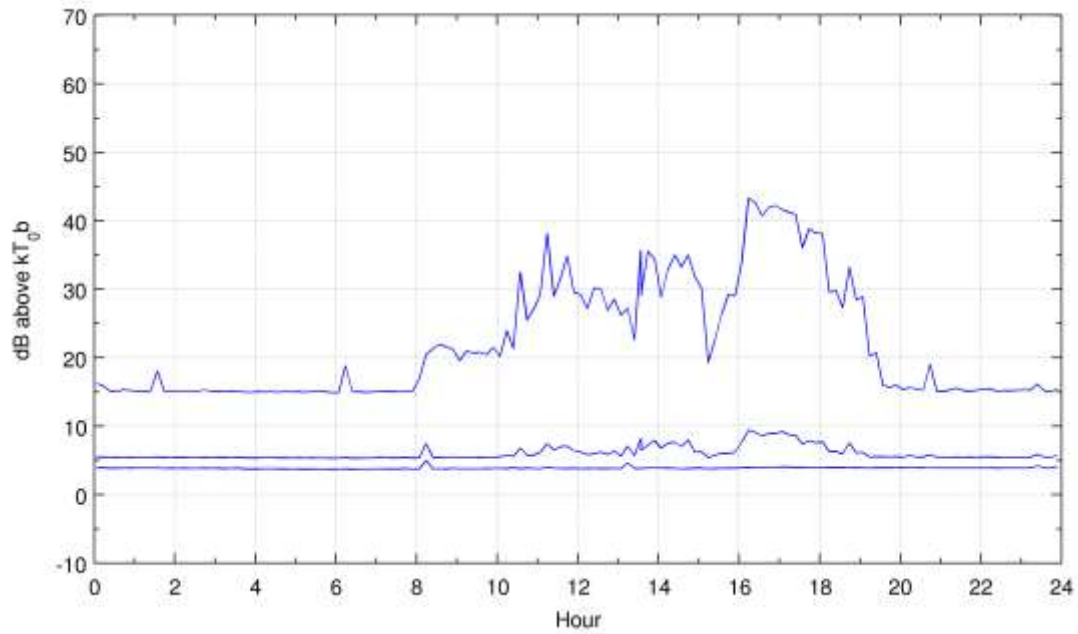


Figure 21. Median, mean, and peak measured noise power in a 1-MHz bandwidth at a center frequency of 401 MHz at the Boulder residential location (September 2–3, 2009).

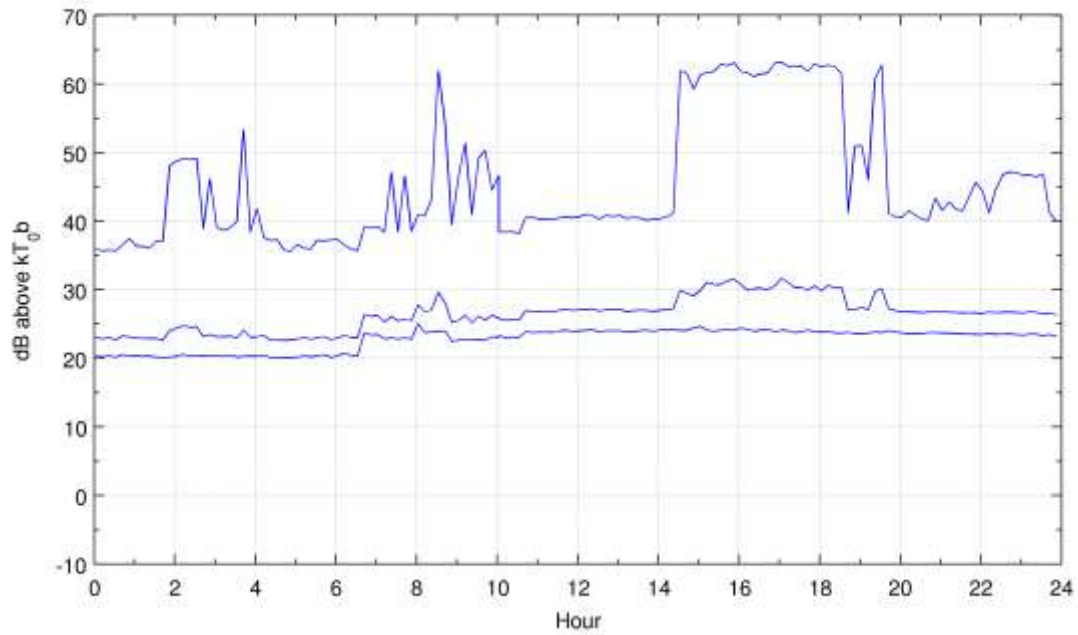


Figure 22. Median, mean, and peak measured noise power in a 1-MHz bandwidth at a center frequency of 112.5 MHz at the Boulder business location (July 21–22, 2009).

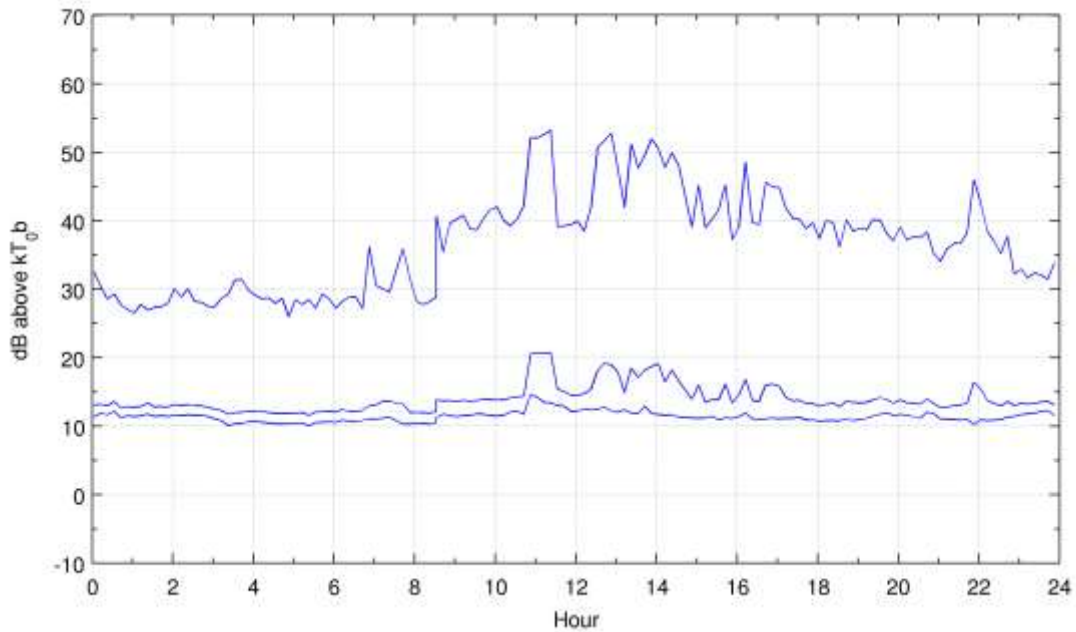


Figure 23. Median, mean, and peak measured noise power in a 1-MHz bandwidth at a center frequency of 221.5 MHz at the Boulder business location (July 20–21, 2009).

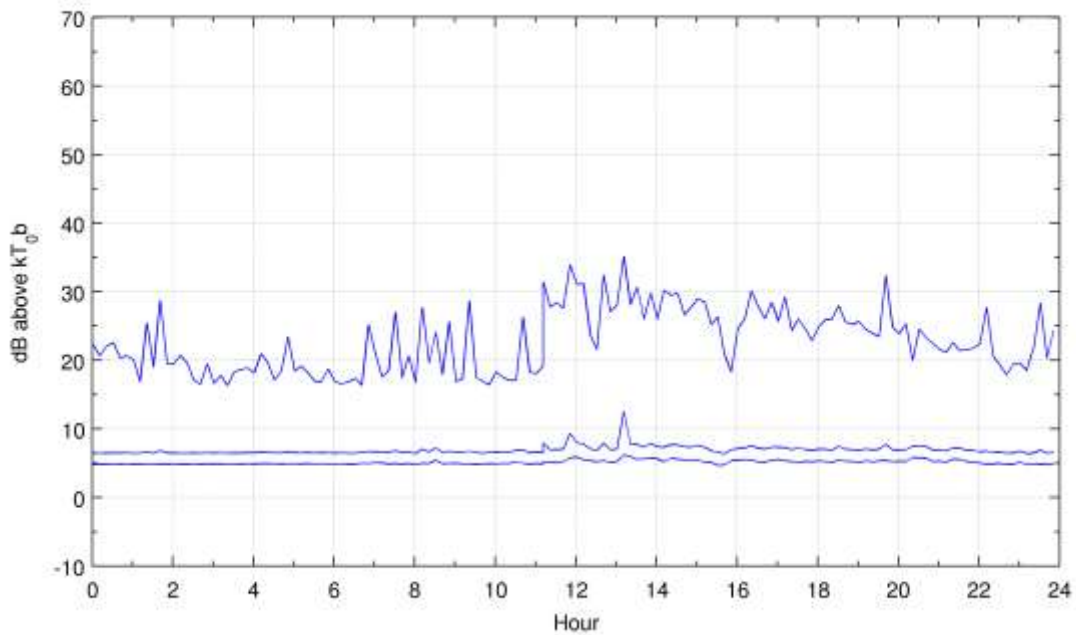


Figure 24. Median, mean, and peak measured noise power in a 1-MHz bandwidth at a center frequency of 401 MHz at the Boulder business location (July 22–23, 2009).

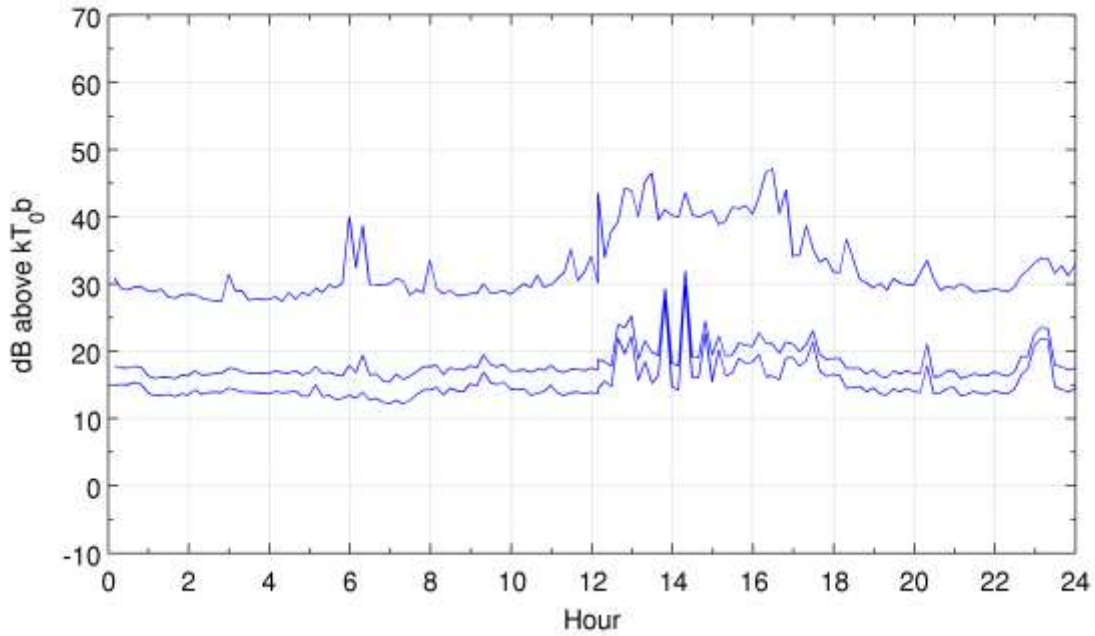


Figure 25. Median, mean, and peak measured noise power in a 1-MHz bandwidth at a center frequency of 112.5 MHz at the Denver residential location (July 29–30, 2009).

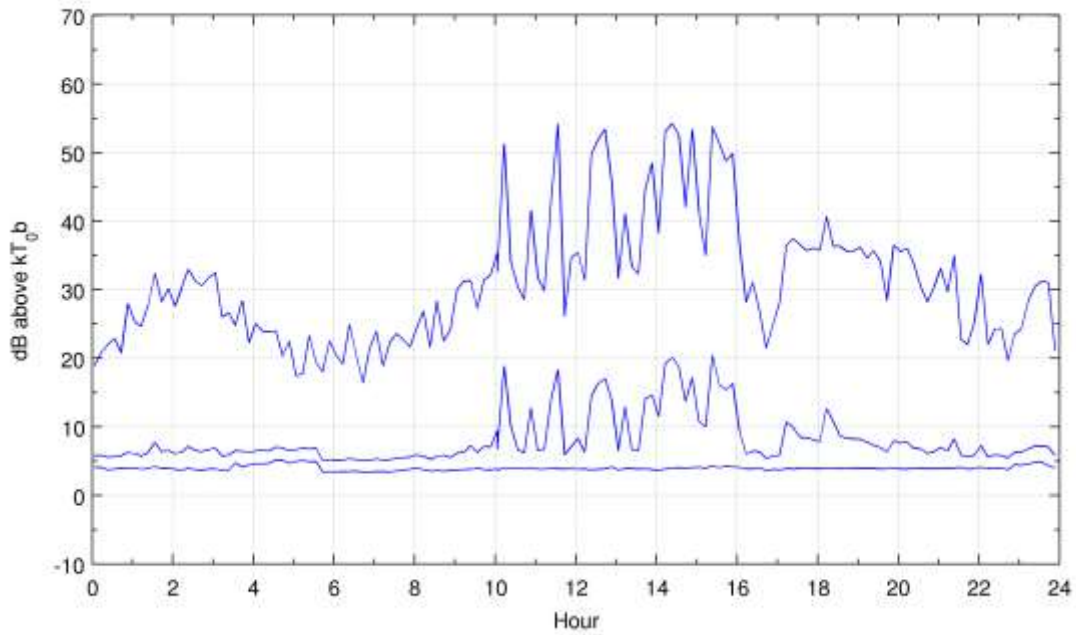


Figure 26. Median, mean, and peak measured noise power in a 1-MHz bandwidth at a center frequency of 221.5 MHz at the Denver residential location (July 28–29, 2009).

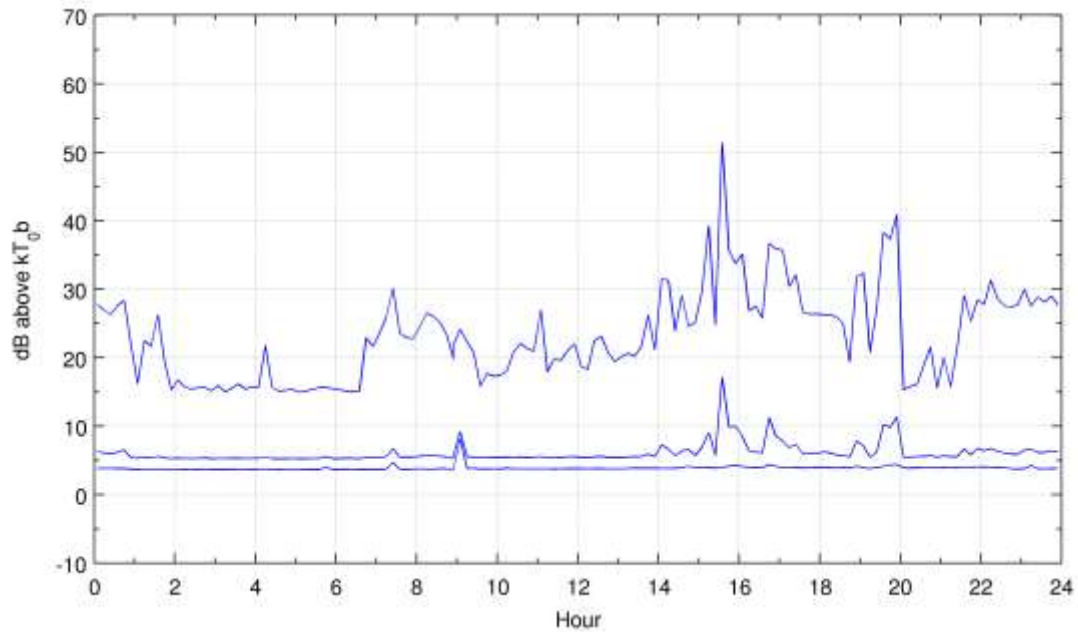


Figure 27. Median, mean, and peak measured noise power in a 1-MHz bandwidth at a center frequency of 401 MHz at the Denver residential location (July 27–28, 2009).

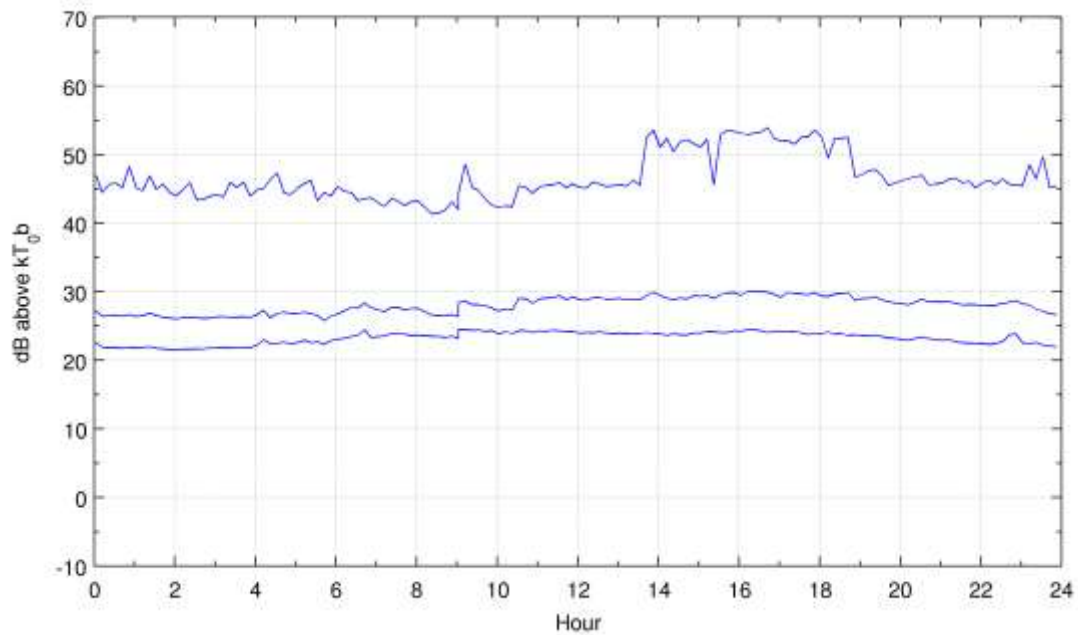


Figure 28. Median, mean, and peak measured noise power in a 1-MHz bandwidth at a center frequency of 112.5 MHz at the Denver business location (August 17–18, 2009).

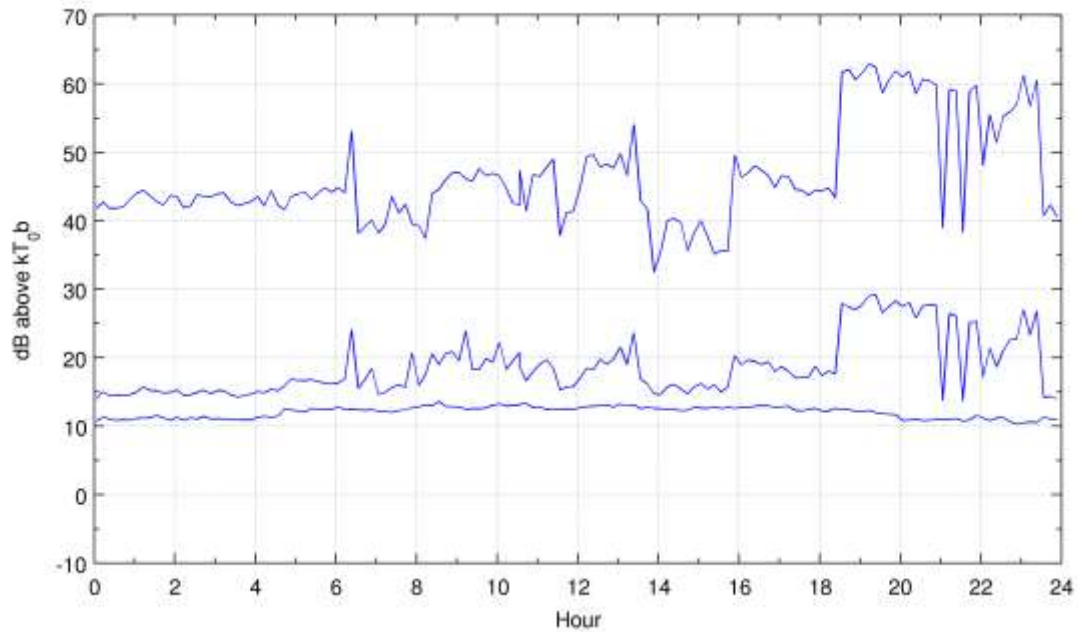


Figure 29. Median, mean, and peak measured noise power in a 1-MHz bandwidth at a center frequency of 221.5 MHz at the Denver business location (August 18–19, 2009).

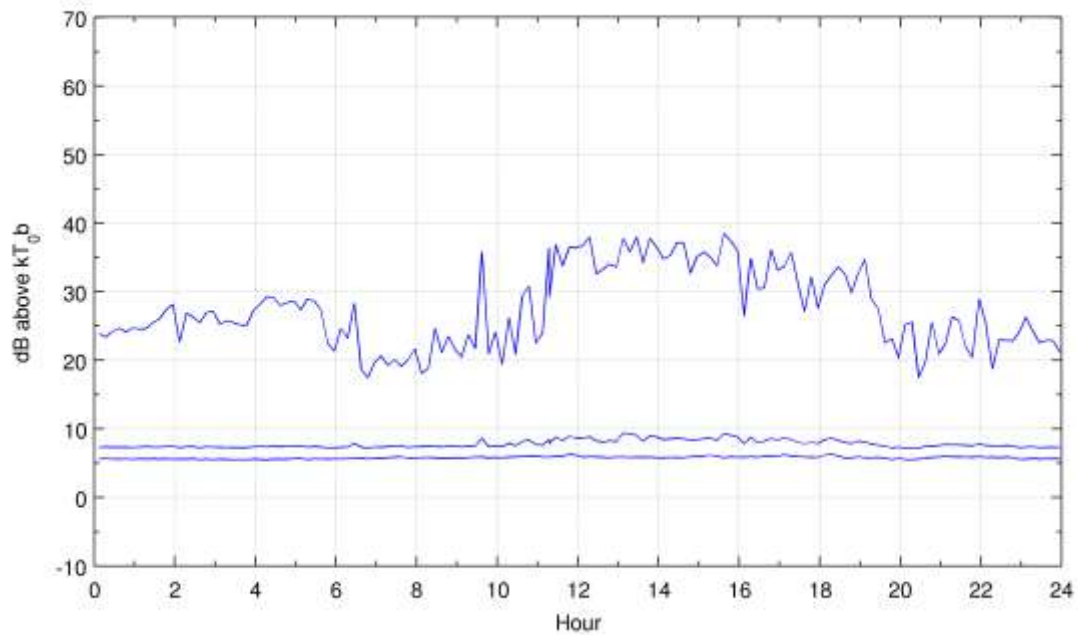


Figure 30. Median, mean, and peak measured noise power in a 1-MHz bandwidth at a center frequency of 401 MHz at the Denver business location (August 19–20, 2009).

6.3 Complementary Cumulative Distributions of Hourly Median Noise Power

To further analyze the data, first, an hourly median value is determined for the median, mean, and peak noise power for each noise data record that was taken every 10 minutes over a 24-hour period for each frequency and location.¹¹ Then the complementary cumulative distribution of the hourly median values is determined for each frequency and location type (residential and business). Data from both residential locations are grouped together and data from both urban locations are grouped together for this analysis. The complementary cumulative distribution of the hourly median values of the median, mean, and peak powers are plotted on normal probability paper in Figures 31–36 as the bottom, middle, and top curves of each figure, respectively.

On normal probability paper, Gaussian-distributed data appears as a straight line with the slope indicating the standard deviation. The hourly medians of the mean powers appear to be roughly Gaussian distributed for both the 401-MHz residential and urban locations as seen in Figures 33 and 36. General conclusions about the distributions at other frequencies are not readily apparent.

6.4 Statistics of the Hourly Medians of Mean Noise Power

The most useful statistic, from a standpoint of being able to compare with results from previous noise measurement studies, is the median of the hourly medians of the mean powers denoted as F_m [4]. This statistic can be found from the 50% point on the complementary cumulative distribution plots of the mean power (middle curve in Figures 31–36).

Tables 3 and 4 show the values for both F_m and the standard deviation of the hourly medians of the mean powers (σ) for each measurement frequency. When $F_m > (F_r + 0.5 \text{ dB})$, values of F_{am} are obtained from values of F_m by applying (7). Requiring $F_m > (F_r + 0.5 \text{ dB})$ ensures that the variation in F_{am} due to variation in F_r is less than $\pm 0.75 \text{ dB}$. This can be shown using (7) with an F_r of 5 or 6 dB and a variation in F_r of $\pm 0.25 \text{ dB}$.¹² Note that the larger F_m is compared to F_r , the less impact variation in F_r has on F_{am} . Values of F_{am} and the corresponding standard deviation σ_a , when applicable, are also shown in Tables 3 and 4.

The values shown in the first four columns of Tables 3 and 4 were derived from the data taken over 24 hours for each frequency. Because the mean noise power is typically highest during business hours (0800–1700) and the data taken to develop the ITU man-made radio noise model [2] and [6] was only taken during business hours, additional values of F_{am} and σ_a are also computed from data taken only during business hours. These additional values are also shown in Tables 3 and 4.

¹¹ Because the hourly median is computed based on six values, the median is found by taking the third and fourth ranked values and averaging them.

¹² Recall from Section 5.2 that the variation in F_r was measured and found to be less than $\pm 0.25 \text{ dB}$.

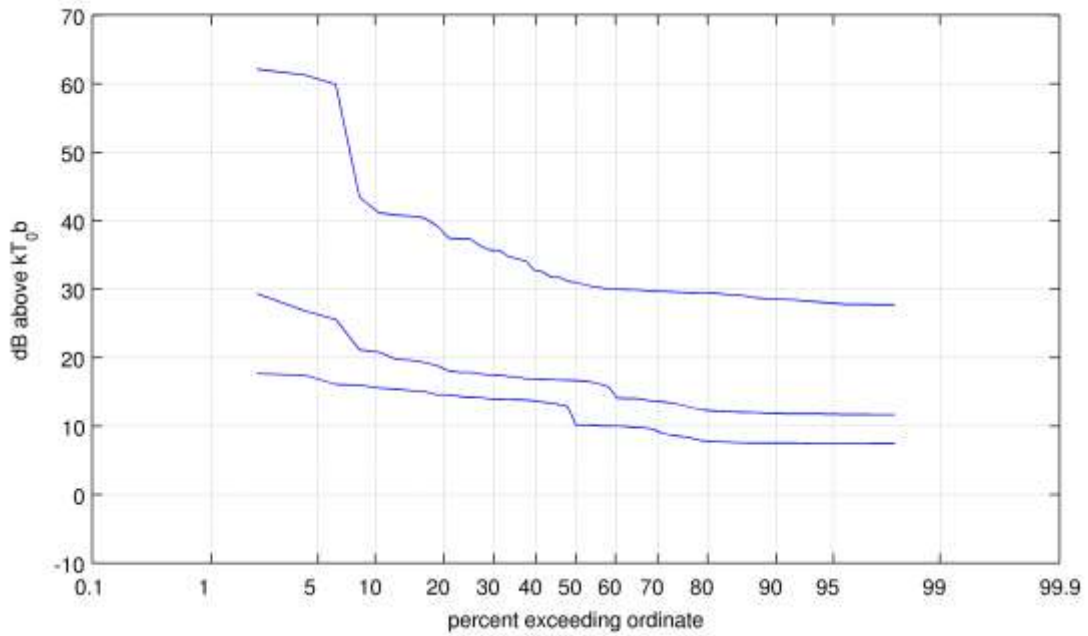


Figure 31. Complementary cumulative distribution of the hourly median values of the median, mean, and peak powers in a 1-MHz bandwidth at a center frequency of approximately 112.5 MHz over both residential locations.

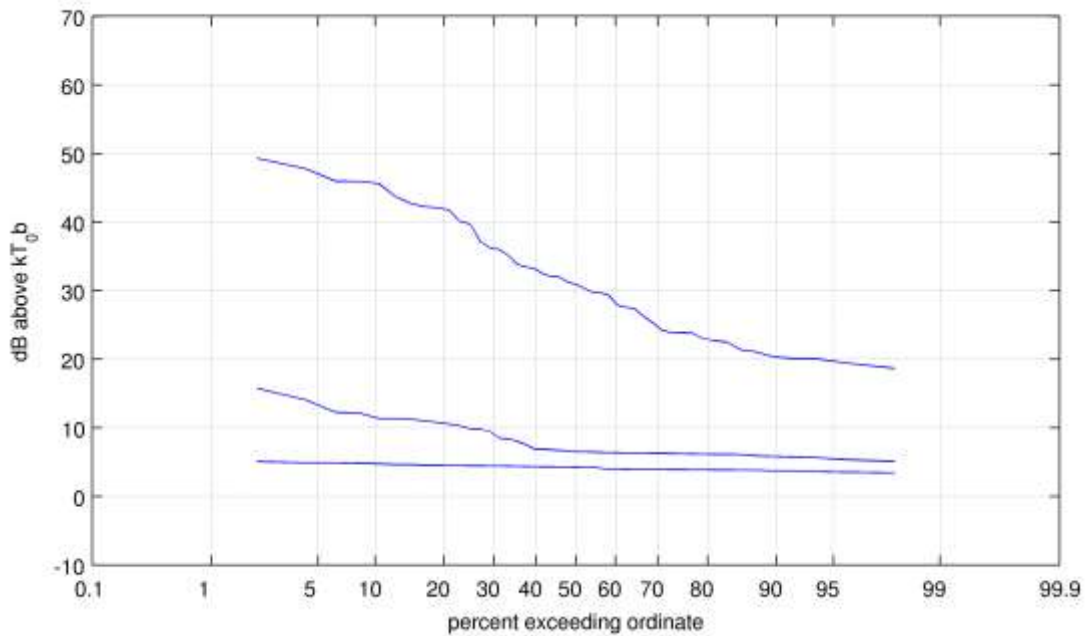


Figure 32. Complementary cumulative distribution of the hourly median values of the median, mean, and peak powers in a 1-MHz bandwidth at a center frequency of approximately 221.5 MHz over both residential locations.

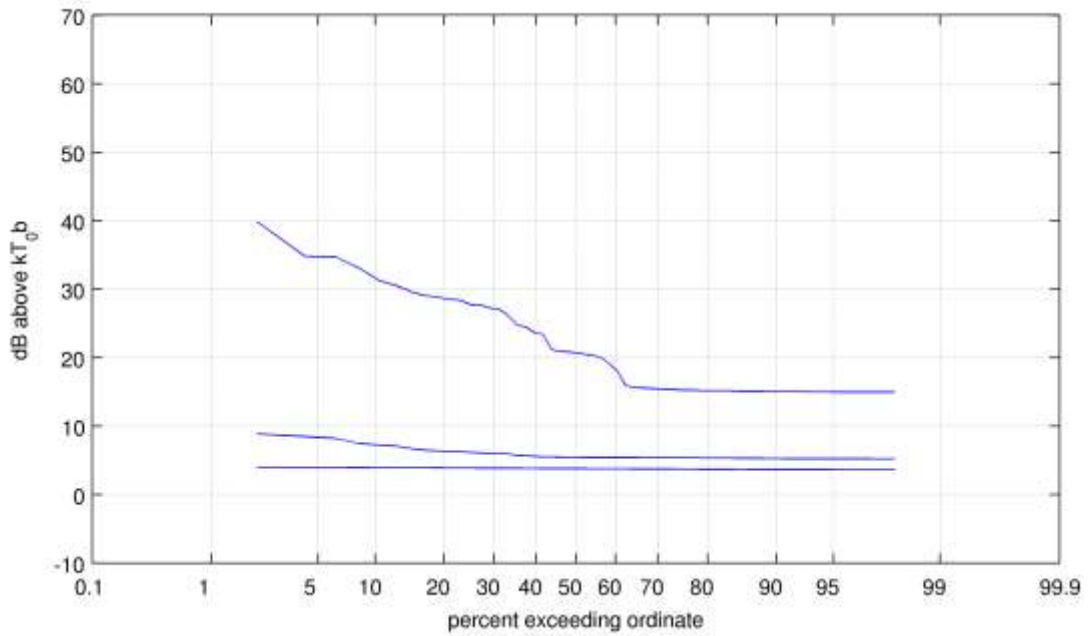


Figure 33. Complementary cumulative distribution of the hourly median values of the median, mean, and peak powers in a 1-MHz bandwidth at a center frequency of 401 MHz over both residential locations.

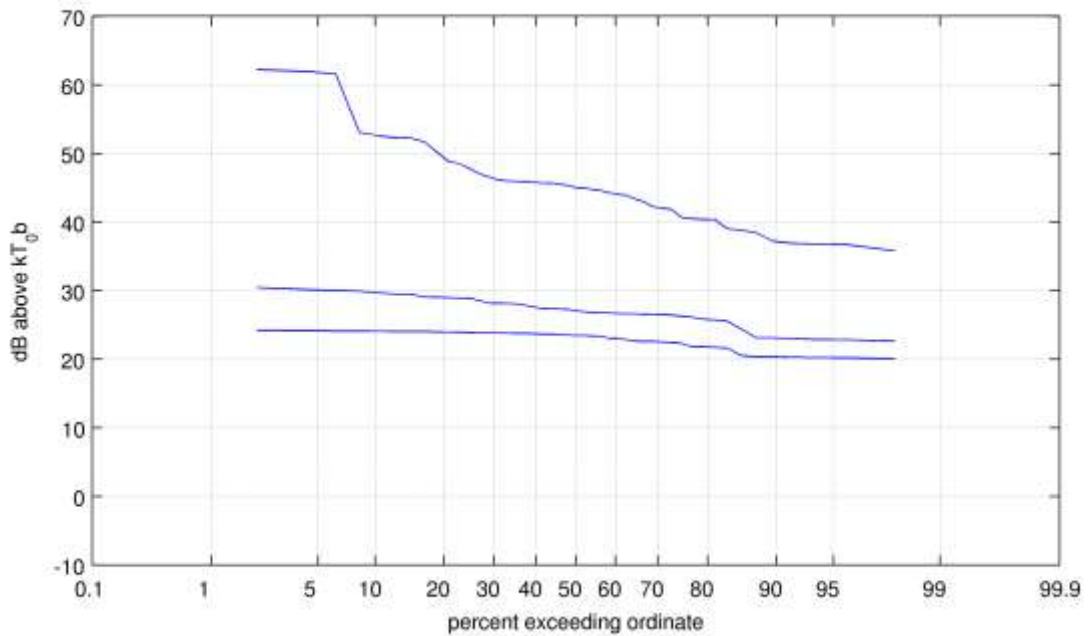


Figure 34. Complementary cumulative distribution of the hourly median values of the median, mean, and peak powers in a 1-MHz bandwidth at a center frequency of approximately 112.5 MHz over both business locations.

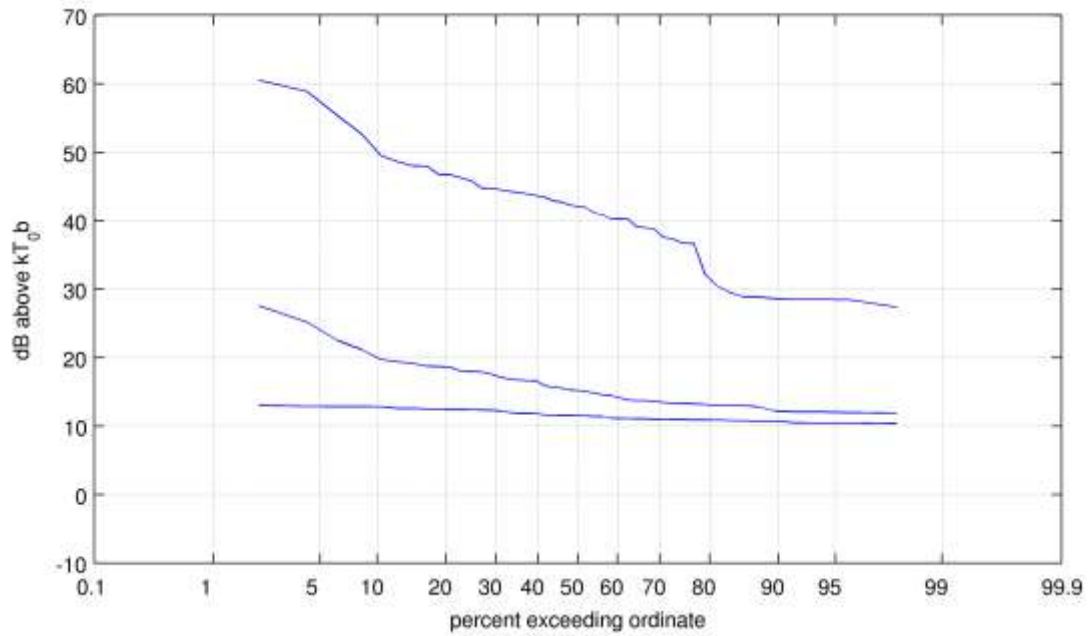


Figure 35. Complementary cumulative distribution of the hourly median values of the median, mean, and peak powers in a 1-MHz bandwidth at a center frequency of approximately 221.5 MHz over both business locations.

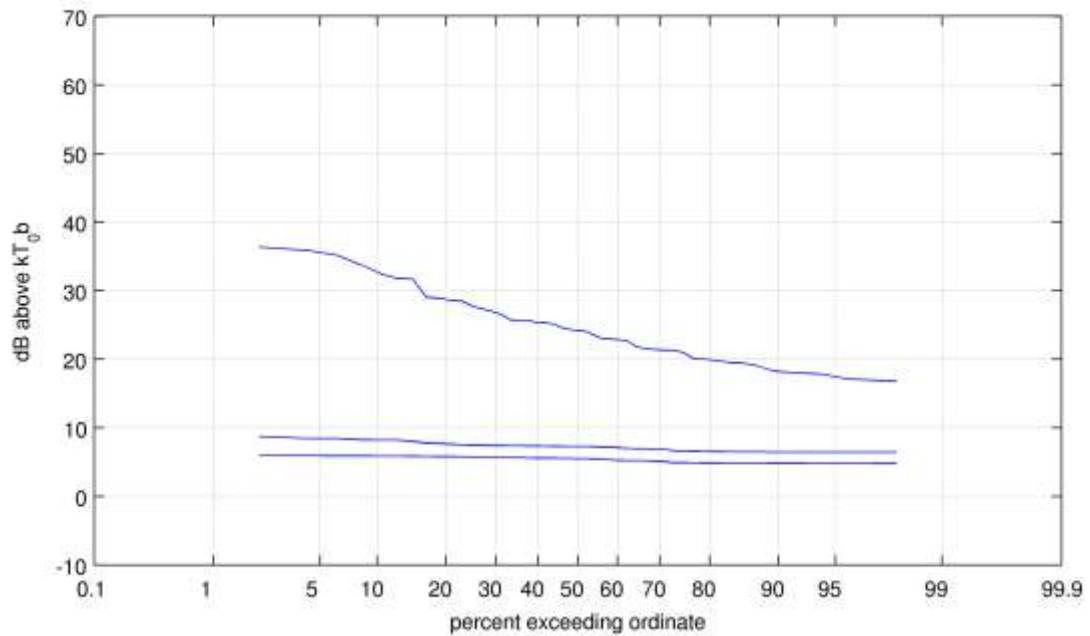


Figure 36. Complementary cumulative distribution of the hourly median values of the median, mean, and peak powers in a 1-MHz bandwidth at a center frequency of 401 MHz over both business locations.

Table 3. Statistics of the hourly medians of the mean noise power for residential locations

Frequency (MHz)	Time of Day for Data Collection					
	0000–2400		0000–2400		0800–1700	
	F_m (dB)	σ (dB)	F_{am} (dB)	σ_a (dB)	F_{am} (dB)	σ_a (dB)
112.5	16.7	4.4	16.5	4.6	18.2	5.5
221.5	6.6	2.9	3.3	4.3	9.3	4.7
401	5.5	1.0	†	†	†	†

† Values of F_{am} and σ_a are not computed because not all of the hourly medians of the mean powers are greater than 0.5 dB above the receiver noise figure F_r .

Table 4. Statistics of the hourly medians of the mean noise power for business locations

Frequency (MHz)	Time of Day for Data Collection					
	0000–2400		0000–2400		0800–1700	
	F_m (dB)	σ (dB)	F_{am} (dB)	σ_a (dB)	F_{am} (dB)	σ_a (dB)
112.5	27.2	2.1	27.2	2.2	28.1	1.5
221.5	15.3	3.8	14.9	4.0	16.7	2.4
401	7.3	0.7	3.8	1.5	4.1	1.6

Several trends become apparent when looking at the data in Tables 3 and 4. For both residential and business locations, as expected, F_{am} decreases with increasing frequency. Note that for the 401 MHz case, for the residential locations, F_m was too small (relative to F_r) to obtain a good estimate of F_{am} . Also as expected, for a given frequency, F_{am} is significantly larger in the business locations than in the residential locations. Finally, as might be surmised by studying the plots of the median, mean, and peak noise power variation over 24 hours (Figures 19–30), values of F_{am} are larger for data taken just over the business hours as compared to those taken over all hours.

6.5 Comparison of Measured Results with Models

The current ITU model showing median values of man-made radio noise power is based on measurements that were taken from 1966 to 1971. These measurements were briefly described in Section 2.3; a more detailed description is found in [6]. One of the primary objectives of the current measurement study is to help determine if levels of man-made radio noise have changed since the measurements used for development of the ITU man-made radio noise model were made. In this section, the results of the current measurement study are compared to those predicted by the ITU model. Before comparing the results, it is important to understand the differences in how the measurement data were collected and processed.

The measurements used to develop the ITU model were taken with a measurement system that records a root mean square (rms) envelope voltage (among other parameters) every 10 seconds in a 4-kHz equivalent noise bandwidth. An effective antenna noise figure F_a is determined from each rms voltage. The data were processed by first separating the data according to environment type (business, residential, or rural). For each mobile measurement run, the median F_a (F_{am}), the ratio of the upper decile to F_{am} (D_u), and the ratio of F_{am} to the lower decile (D_l) were computed for each of the eight frequencies measured. (The frequencies ranged from 0.25 to 250 MHz.) Linear regression was used on the F_{am} values for all measurement runs and for all frequencies within an environment type to determine the best straight line approximation of F_{am} as a function of frequency. For each frequency within an environment type, the standard deviation of F_{am} values was calculated providing an indication of the variation in F_{am} from location to location [6]. The expected variation of the F_a values about F_{am} within the hour for a location was found by taking the rms of all the D_u values and the rms of all of the D_l values for each location and frequency within an environment type. Table 5 summarizes some of the major differences between the measurements taken for the data used in developing the ITU model and the measurements taken in this study.

Table 5. Major differences between measurements used in the ITU Model and measurements taken for this study

Measurements for this Study	Measurements Used in ITU Model
1-MHz 0.25 dB bandwidth	4-kHz noise equivalent bandwidth
Fixed location measurements	Mobile measurements
Few locations measured for a relatively long time duration at each location	Many locations measured for relatively short duration mobile measurement runs
Duration of measurement at each location = 24 hours	Duration of measurement runs = 15 min to more than 1 hour
F_{am} = median of hourly medians of F_a	F_{am} = linear regression of medians of F_a

To provide a better comparison between the results of the current measurement study and the ITU model, the measurement data from the current study was reprocessed using a filter with a 4-kHz noise equivalent bandwidth instead of the 1-MHz filter.¹³

Tables 6 and 7 show the comparison between F_{am} and its standard deviation σ_a from this study (for the 4-kHz filtered data taken over only the business hours) and F_{am} and its standard deviation σ_{aL} (location variability) from the data used in the ITU model for the residential and business environments, respectively.¹⁴ Values of σ_{aL} are found by using linear interpolation of the measured standard deviation values found in Table 1 of [6]. Tables 6 and 7 also show F_{am} values for the Hagn model.

¹³ Specifically, before reprocessing the data, each noise data record was filtered using a low-pass FIR filter with a 0.01 dB, 1.88-kHz bandwidth (3.76 kHz double-sided bandwidth) that provides a 60 dB double-sided bandwidth of 4.35 kHz (see Section 6).

¹⁴ Recall that measured values of F_{am} and σ_a from this study were determined from data taken in residential locations that were not strictly residential. The predicted values from the ITU model are for strictly residential locations.

Table 6. Comparison of measured and predicted values of F_{am} for residential locations¹⁴

Approx. Center Frequency (MHz)	Current Measurements		ITU Model		Hagn Model
	F_{am} (dB)	σ_a (dB)	F_{am} (dB)	σ_{aL} (dB)	F_{am} (dB)
112.5	17.8	5.9	15.7	2.7	‡
221.5	8.9	4.8	7.5	2.8	8.1
401	*	*	†	†	4.0

* Values of F_{am} and σ_a are not computed because not all of the hourly medians of the mean powers are greater than 0.5 dB above the receiver noise figure F_r .

† Values of F_{am} for frequencies above 250 MHz are not defined in the ITU Model.

‡ Hagn [7] recommends using values of F_{am} predicted by the ITU Model for frequencies below 200 MHz.

Table 7. Comparison of measured and predicted values of F_{am} for business locations

Approx. Center Frequency (MHz)	Current Measurements		ITU Model		Hagn Model
	F_{am} (dB)	σ_a (dB)	F_{am} (dB)	σ_{aL} (dB)	F_{am} (dB)
112.5	28.1	1.4	20.0	8.4	‡
221.5	15.5	2.5	11.8	4.7	12.3
401	*	*	†	†	8.3

* Values of F_{am} and σ_a are not computed because not all of the hourly medians of the mean powers are greater than 0.5 dB above the receiver noise figure F_r .

† Values of F_{am} for frequencies above 250 MHz are not defined in the ITU Model.

‡ Hagn [7] recommends using values of F_{am} predicted by the ITU Model for frequencies below 200 MHz.

To facilitate the comparison, Figures 37 and 38 provide a graphical representation of the F_{am} data given in Tables 6 and 7. Also included in these figures are values of F_{am} from the 137.5 MHz measurements taken by ITS from 1996 to 1997 [3] and from the 209.5 and 425 MHz measurements taken in the United Kingdom by MASS Consultants Limited in 2006 [9].

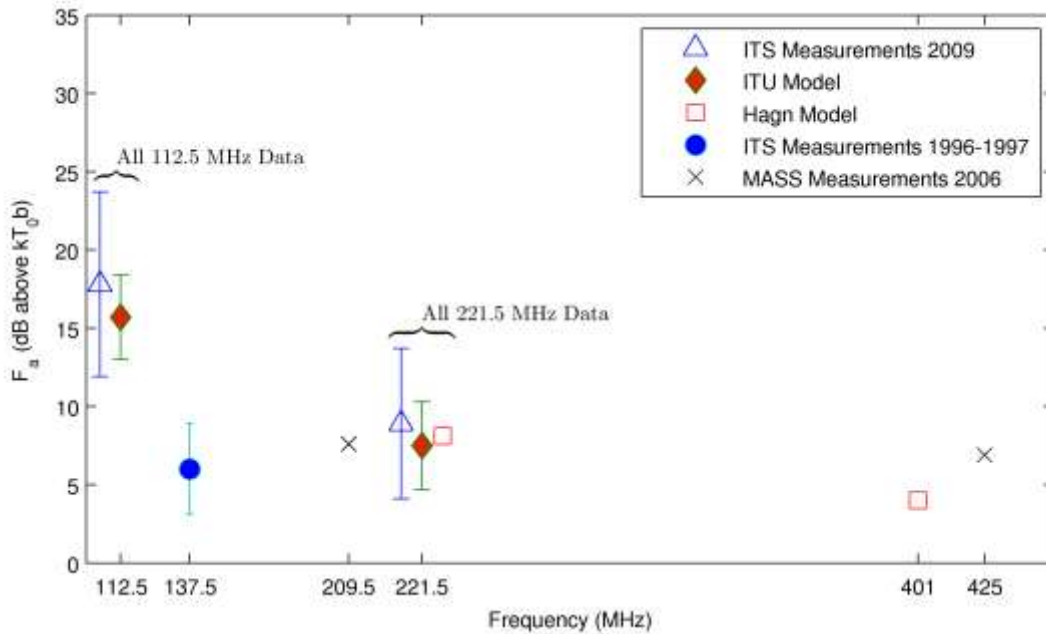


Figure 37. Comparison of measured and predicted values of F_{am} and standard deviation of F_{am} for residential locations.¹⁴

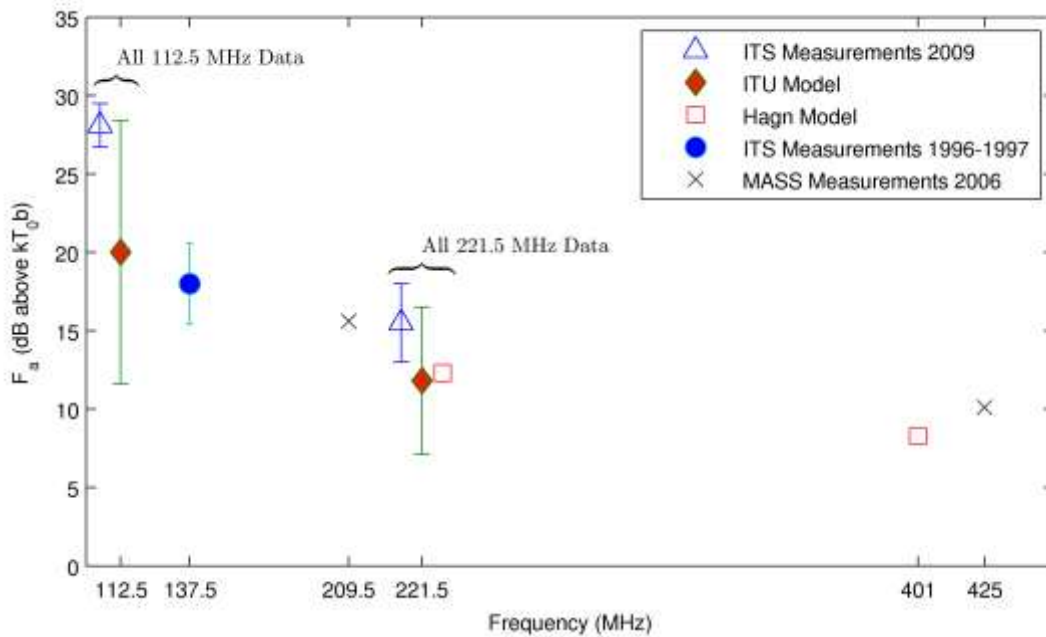


Figure 38. Comparison of measured and predicted values of F_{am} and standard deviation of F_{am} for business locations.

For the business locations at 112.5 and 221.5 MHz, measured values of F_{am} found in this study, for the 4-kHz filtered data, were larger than predicted with the ITU and Hagn models. However, the measured values of F_{am} are within a standard deviation of F_{am} from the ITU model.

For the residential locations, the measured values of F_{am} , for the 4-kHz filtered data, were also larger at 112.5 and 221.5 than predicted with the ITU and Hagn models. However, for the residential locations, the measured values and the values predicted from the models were closer to agreement than for the business locations. The measured values of F_{am} are clearly within one standard deviation of F_{am} from the ITU model. (Note that the standard deviation is much smaller for the residential locations than for the business locations in the ITU model.)

For both the business and residential locations at 401 MHz, values of F_{am} and σ_a are not computed for the 4-kHz filtered data because not all of the hourly medians of the mean powers are greater than 0.5 dB above the receiver noise figure F_r .

A quantitative assessment of within the hour variation of F_a values was not performed for this study. Therefore, no comparison for within the hour variation is given. However, within the hour variation of F_a values can be observed qualitatively from the mean noise power curves in Figures 19–30. Each mean noise power curve shows six measured values of F_a per hour over a 24-hour period for a particular frequency and location. Over many of the hourly intervals, F_a does not change much; however, a few hourly intervals do show significant variation in F_a .

7 SUMMARY AND CONCLUSIONS

This report discussed an initial set of man-made radio noise measurements that were taken in the Boulder/Denver, Colorado, area in the summer of 2009. The measurement locations were chosen to represent as closely as possible typical residential and business areas as defined in [6]. One residential and one business location in Boulder and one residential and one business location in Denver were selected.

The selection of appropriate frequencies between 100 and 1000 MHz at which to perform the noise measurements required a good understanding of the radio environment at the proposed measurement locations. Since recent spectrum survey measurements in these areas were not available, a spectrum survey of the radio environment was performed. Based on the subsequent analysis of the spectrum survey data, noise measurement frequencies of 112.5, 221.5, and 401 MHz were selected.

While wideband noise measurements were desirable and the noise measurement system could support measurements in up to a 36-MHz bandwidth, it was difficult to find areas of the spectrum (particularly in the 100–200-MHz range) more than 1 MHz wide with no (or even very few) low-power intentionally radiated signals. Therefore, a 1-MHz measurement bandwidth was selected for the wideband noise measurements.

The noise measurements presented in this report were taken using the new, automated, wideband noise measurement system developed by ITS and installed in the ITS RSMS-4G measurement vehicle. This vehicle provided significant advantages for making measurements, including a high-degree of RF shielding (60 dB) between the measurement equipment and the antenna, AC power (from either external shore power, an external generator, or a built-in diesel generator), temperature control, and shelter. Noise measurement data were collected in a 1.16-MHz VSA span at all locations and frequencies.

The data were analyzed to show the characteristics of individual noise data records and to provide various statistical descriptions of the noise. Some example APDs of individual noise data records were given along with an example time domain display of a noise data record clearly showing the presence of 60 Hz noise indicative of unintentional emissions from the AC power distribution system. The statistical summary data included the median, mean, and peak noise power levels over a 24-hour time period at each measurement location and frequency. Complementary cumulative distributions of the hourly median values of the median, mean and peak power were also given for each frequency and environment type. Finally, median values of the antenna noise figure F_{am} were determined for each measurement frequency and environment type and compared to those predicted by the ITU model and, alternatively, the Hagn model.

For the business locations at 112.5 and 221.5 MHz, this study found that measured values of F_{am} were larger than predicted with the ITU and Hagn models. However, the measured values of F_{am} were still within a standard deviation of F_{am} from the predicted values using the ITU model.

For the residential locations, the measured values of F_{am} were also larger at 112.5 and 221.5 MHz than predicted with the ITU and Hagn models. However, for the residential locations, the measured values and the values predicted from the models were closer to agreement than for

the business locations. The measured values of F_{am} were clearly within one standard deviation of F_{am} as predicted by the ITU model. (Note that the predicted standard deviation values for the residential locations in the ITU model are much smaller than those for the business locations.)

The measurements taken for this study, while collected over a 24-hour period, were only from two separate locations for each environment type and frequency. It is possible that the specific measurement locations chosen for this noise measurement study unduly influenced the measured F_{am} values. The business locations that were selected were in downtown areas and these locations may have higher noise levels than other business locations as defined in Section 3 and [6]. The measurement vehicle was located near some overhead power lines in both the Denver and Boulder business locations.

The residential locations selected in this study were not strictly residential; they were residential with some nearby businesses or busy roads. The residential location in Boulder, while adjacent to an exemplary residential area, was also close to the U.S. Department of Commerce Boulder Laboratories. The residential location in Denver, while near several houses and on the edge of a residential area, was also close to a large street with some businesses. It was also line-of-sight to FM and television broadcast antennas located nearby on Lookout Mountain in Golden, Colorado. Therefore, the noise levels measured in residential locations for this study may have been higher than in more strictly residential locations.

Based on these factors, it is recommended that further noise measurements be taken in a greater number of locations to provide some more statistically significant results and therefore a better comparison to the values predicted by the existing models.

8 ACKNOWLEDGEMENTS

The authors would like to thank the following individuals for their efforts in helping achieve the objectives of this study. Robert Achatz and Roger Dalke provided invaluable advice and guidance during the planning and execution of the measurements and the data analysis. Raian Kaiser determined appropriate measurement locations and handled all of the many logistics involved in the selection and use of those locations. Ms. Kaiser also contributed much needed support in performing some of the spectrum survey and noise measurements. A special thanks goes to Randy Hoffman who had the foresight, vision, and drive to establish a modern noise measurement program at ITS. Mr. Hoffman was also instrumental in the development of the software used in making the spectrum survey measurements. Without the assistance of these individuals, this work would not have been possible.

9 REFERENCES

- [1] L. Barclay, "Radio noise: Recent considerations of man-made noise," in *Proc International Symposium on Advanced Radio Technologies/ ClimDiff 2008*, Boulder, Colorado, Jun. 2–4, 2008, pp. 17–24 (NTIA Special Pub SP-08-452, Jun. 2008).
- [2] ITU-R Recommendation P.371-10 (10/2009), "Radio noise," Recommendations of the ITU, Radiocommunication Sector.
- [3] R. J. Achatz, Y. Lo, P. B. Papazian, R. A. Dalke, and G. A. Hufford, "Man-made noise in the 136 to 138-MHz VHF meteorological satellite band," NTIA Report 98-355, Sep. 1998.
- [4] R. J. Achatz and R. A. Dalke, "Man-made noise power measurements at VHF and UHF frequencies," NTIA Report 02-390, Dec. 2001.
- [5] A. D. Spaulding, "Man-made noise: The problem and recommended steps toward solution," OT Report 76-85, Apr. 1976.
- [6] A. D. Spaulding and R. T. Disney, "Man-made radio noise part 1: Estimates for business, residential, and rural areas," OT Report 74-38, Jun. 1974.
- [7] G. H. Hagn, "Man-made radio noise and interference," in *Proc. of the 1987 AGARD Conference*, No. 420, Lisbon, Portugal, Oct. 26–30, 1987, pp. 5.1–5.15.
- [8] W.R. Lauber and J.M. Bertrand, "Man-made noise level measurements of the UHF radio environment," in *Proc. of the 1984 IEEE National Symposium on EMC*, San Antonio, TX, Apr. 24–26, 1984, pp. 185–192.
- [9] A.J. Wagstaff and N.P. Merricks, "Autonomous interference monitoring system phase 2 final report, vol. 1—summary report, issue 1," MASS Consultants Limited MC/SC0585/REP016/1, Mar. 2007.
- [10] National Telecommunications and Information Administration, "Manual of regulations and procedures for federal radio frequency management (Redbook)," May 2010 Revision of the Jan. 2008 Edition.
- [11] R. Dalke, "Radio noise," in *The Wiley Encyclopedia of Electrical and Electronics Engineering*, J.G. Webster, Ed., New York: John Wiley & Sons, Inc. 1999, vol. 18, p. 134.
- [12] W. A. Kissick, Editor, "The temporal and spectral characteristics of ultrawideband signals," NTIA Report 01-383, Jan. 2001.
- [13] M. Cotton, R. Achatz, J. Wepman, and B. Bedford, "Interference potential of ultrawideband signals Part 1: Procedures to characterize ultrawideband emissions and measure interference susceptibility of C-band satellite digital television receivers," NTIA Report TR-05-419, Feb. 2005.

- [14] L. W. Couch II, *Digital and Analog Communications Systems*, Upper Saddle River, NJ: Prentice-Hall, Inc. 1993, pp. 244–255.

APPENDIX: SPECTRUM SURVEY MEASUREMENTS

This appendix describes a spectrum survey measurement system and measurement procedure used in conducting a spectrum survey from 104 MHz to 1060 MHz. The spectrum survey was performed to help select appropriate frequencies and bandwidths at which to perform the noise measurements. The results of the spectrum survey are provided as a series of plots of the maximum, mean, and median received signal power versus frequency for each of the frequency ranges measured.

A.1 Spectrum Survey Measurement System

The spectrum survey measurement system was designed to conduct automated measurements from 104 MHz to 1060 MHz. A block diagram of the system is shown in Figure A-1.

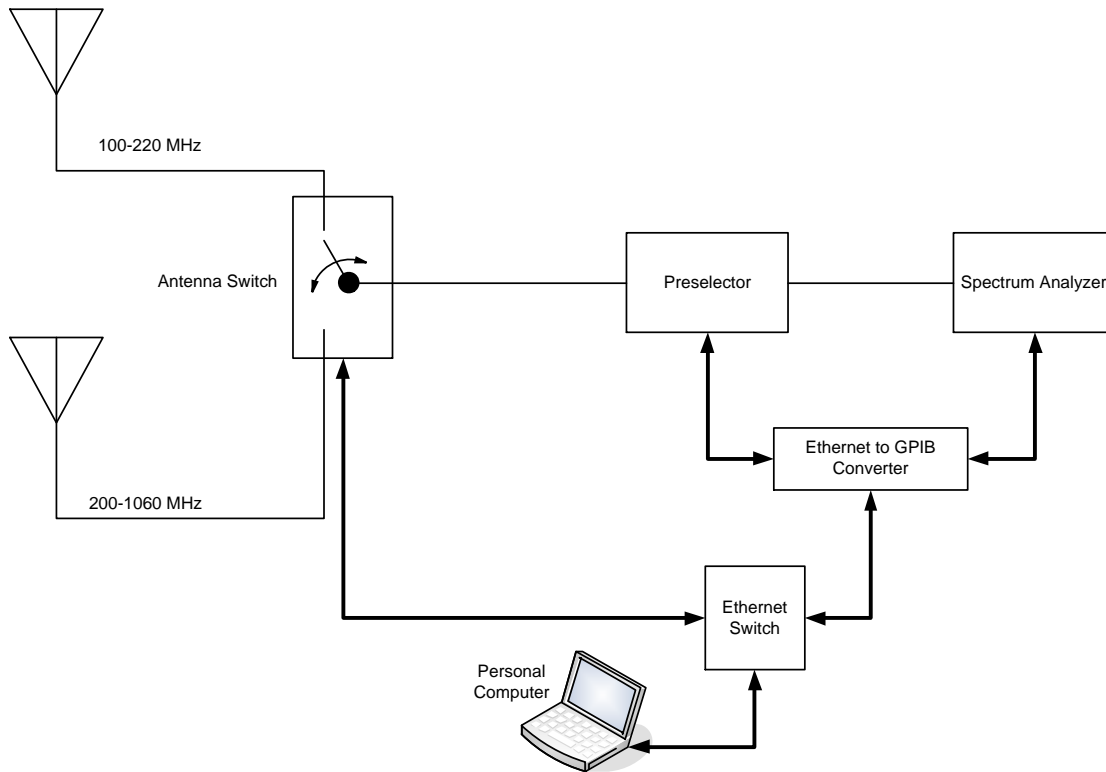


Figure A-1. Block diagram of the spectrum survey measurement system.

The measurement system consists of two omnidirectional discone antennas; an ITS-designed, software-controlled RF antenna switch; and a legacy, commercial off-the-shelf RF preselector and spectrum analyzer. A personal computer (PC) is used to operate ITS-developed custom software that controls the preselector, spectrum analyzer, and antenna switch.

The software automatically controls the antenna switch so that one discone antenna or the other is selected depending on the frequencies to be measured. The received signal is filtered and amplified by the preselector. The appropriate preselector filter is automatically selected based on the measurement frequency range. The preselector also contains an attenuator that can be used

when large signals are present. The filter attenuates out-of-band signals and, along with the attenuator, helps prevent potential front-end overload. The amplifier improves the system sensitivity. After preselection, the received signal is measured by the spectrum analyzer. Received signal power versus frequency data from the spectrum analyzer is then transferred to and stored in files on the PC.

The measurement system was installed in the RSMS-4G measurement vehicle. This vehicle, also used for the noise measurements, is described in Section 3.

A.2 Spectrum Survey Measurement Procedure

The spectrum survey measurements were conducted at the same four measurement locations proposed for the noise measurements.¹ At each location, to begin the measurements, the measurement equipment was turned on and allowed to warm up for at least 30 minutes. After equipment warm-up, the swept spectrum measurement control software was initiated. A noise diode calibration was then performed using the Y-factor method described in [A-1] and [A-2] and implemented in the measurement software. The noise diode calibration is performed by replacing one antenna at a time with a noise diode. The measurement software automates the noise diode calibration by measuring the received noise power of the measurement system as a function of frequency first with the noise diode powered on and then with the noise diode powered off. The system gain and noise figure as a function of frequency are then computed via the measurement software from the noise-diode-on and noise-diode-off received power values. The system gain and noise figure values are used to verify the proper operation of the measurement system. During proper operation, over the 104–1060 MHz frequency range, the noise figure varied from approximately 11 to 16 dB and the gain varied from approximately 16 to 14 dB.

The actual spectrum survey measurements were taken automatically and would run for most of the day at each measurement location, typically during business hours. To accomplish this, the desired spectrum survey measurements were set up in a table that the measurement software uses to carry out the measurements. The table, called an event table, consists of parameters used to set up the spectrum analyzer and preselector to perform swept measurements over a user-defined frequency range.

To measure the spectrum from 104 MHz to 1060 MHz, the frequency range is first divided into fifteen smaller frequency sub bands (called events) as shown in Table A-1. Each event is further divided into a certain number of equally spaced measurement spans. Measurements are taken by setting the spectrum analyzer and preselector to sweep over each span. Each span is measured multiple times by taking multiple sweeps. The number of sweeps per span and the sweep time for each sweep is given in Table A-1 for each event. Each sweep of the spectrum analyzer is set

¹ The spectrum survey and noise measurements at the residential location in Boulder were actually taken in slightly different areas on the U.S Department of Commerce Boulder Laboratories Campus. The spectrum survey measurements were taken on the south side of the Campus immediately adjacent to the residential area at Dartmouth Ave. and Kenwood Dr. The noise measurements were taken on the north side of the Campus immediately adjacent to the residential area at King Ave. and 22nd St.

up to store $N = 1001$ points (1001 values of received power). The resolution bandwidth (RBW) of the spectrum analyzer is set to maintain the ratio

$$(N - 1) \cdot RBW = Span \quad (A-1)$$

and sample detection is used. Therefore, each sweep provides received power versus frequency data where a value of received power is recorded every RBW Hz for the entire span.

The relationship between the span, RBW, and sweep time is given as

$$Sweep\ Time = \frac{k \cdot Span}{(RBW)^2} \quad (A-2)$$

To ensure that the intermediate frequency (IF) filters have sufficient time to settle, values of k should be at least 2 to 3 [A-3].

Measurements were repeated automatically at different times during the day for events that covered frequency bands whose spectrum usage was expected to change with time during the day. These events, called dynamic events, include bands used by mobile radios and airborne radars. Events that covered frequency bands whose spectrum usage was expected to remain relatively constant with time during the day were only measured once a day. These events, called static events, include bands used by commercial radio and television. In general, the static events required fewer sweeps per span than the dynamic events. For the most part, the parameters used for the events in Table A-1 were developed by following the procedures and tables in [A-1].

Table A-1. Spectrum analyzer and preselector parameters for spectrum survey measurements

Event	Start Frequency (MHz)	Stop Frequency (MHz)	# of Spans	Span (MHz)	RBW (kHz)	# of Sweeps per Span	Sweep Time (ms)	# of Times per Day
1	104	164	6	10	10	100	300	2
2	160	180	2	10	10	500	300	3
3	170	220	1	50	100	500	100	1
4	216	225	3	3	3	60	900	2
5	225	405	6	30	30	100	100	1
6	400	406	2	3	3	60	900	1
7	400	420	2	10	10	200	300	3
8	420	450	3	10	10	100	300	2
9	450	470	2	10	10	200	300	3
10	470	520	5	10	10	100	300	3
11	512	812	3	100	100	200	100	1
12	806	906	10	10	10	60	300	2
13	900	920	2	10	10	100	300	2
14	920	960	4	10	10	300	300	3
15	960	1060	1	100	100	500	100	3

To clarify how measurements are taken for a given event, consider Event 1 in Table A-1. This event provides for the measurement of the 104–164-MHz frequency range. This event is measured by taking 100 sweeps of each of the six 10-MHz spans within the 104–164-MHz frequency range with an RBW = 10 kHz and a sweep time of 300 ms.

A.3 Spectrum Survey Measurement Results

Once all the spectrum survey data from each of the four measurement locations were collected, the maximum, mean, and median power levels at each frequency were calculated and plotted for each event. The measurement system gain was used to determine the power levels referenced to the output of the antenna terminals. Figures A-2 to A-61 show the maximum, mean, and median received signal power (referenced to the output of the antenna terminals) versus frequency for each of the 15 events given in Table A-1.

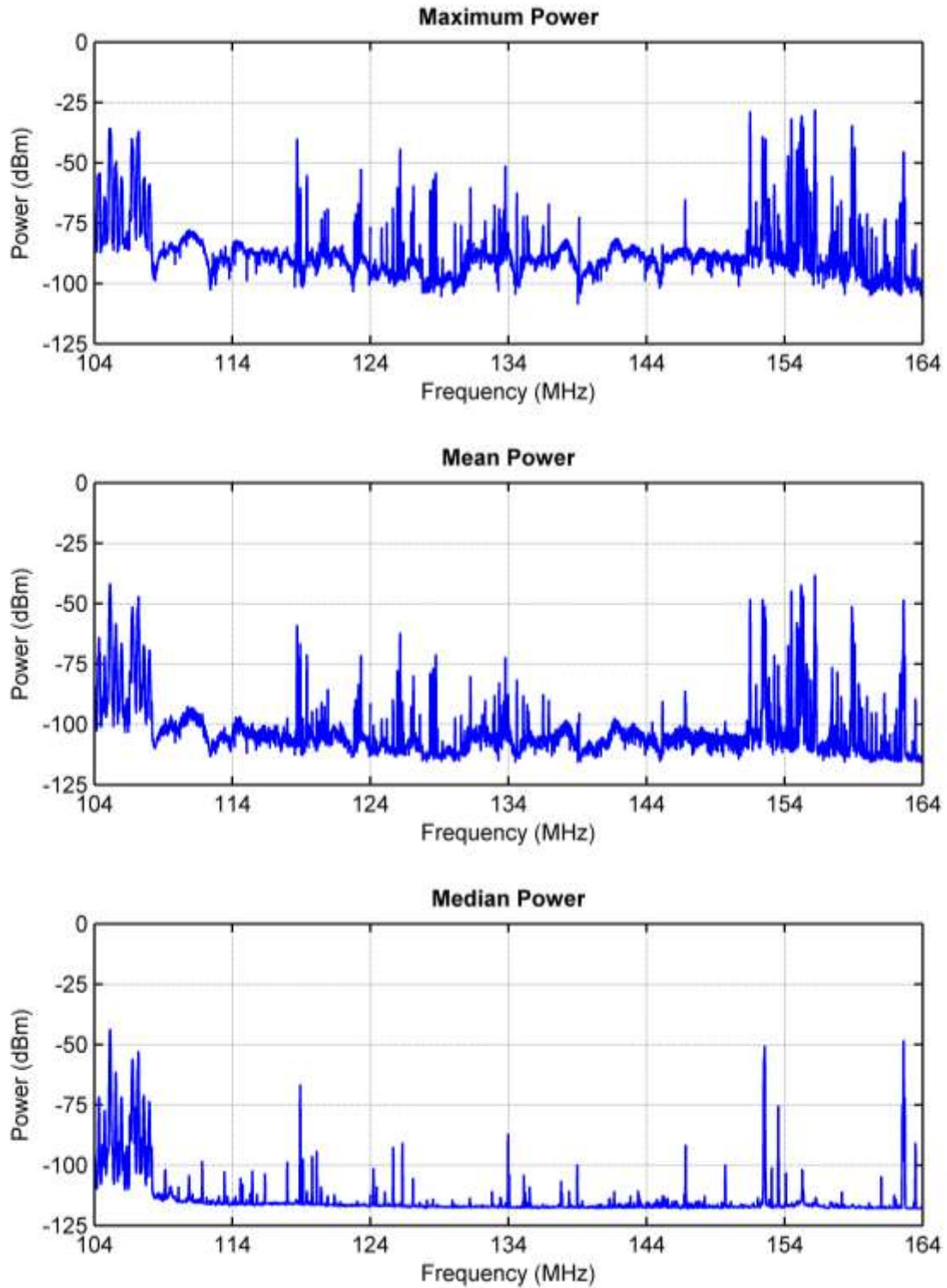


Figure A-2. Maximum, mean, and median received signal power at the Boulder residential location for Event 1 (104–164 MHz, RBW = 10 kHz, 100 sweeps, sweep time = 300 ms).

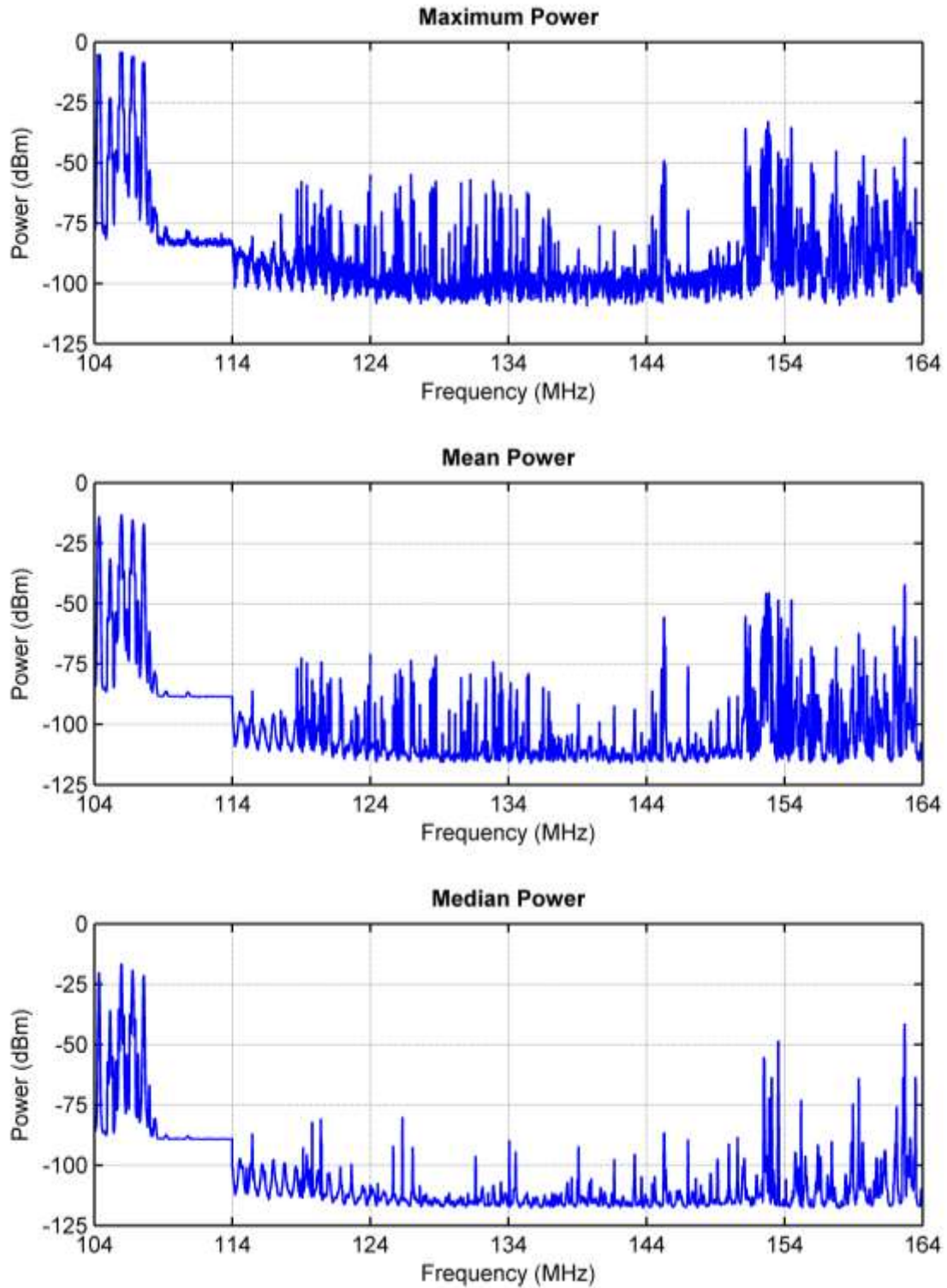


Figure A-3. Maximum, mean, and median received signal power at the Denver residential location for Event 1 (104–164 MHz, RBW = 10 kHz, 100 sweeps, sweep time = 300 ms).

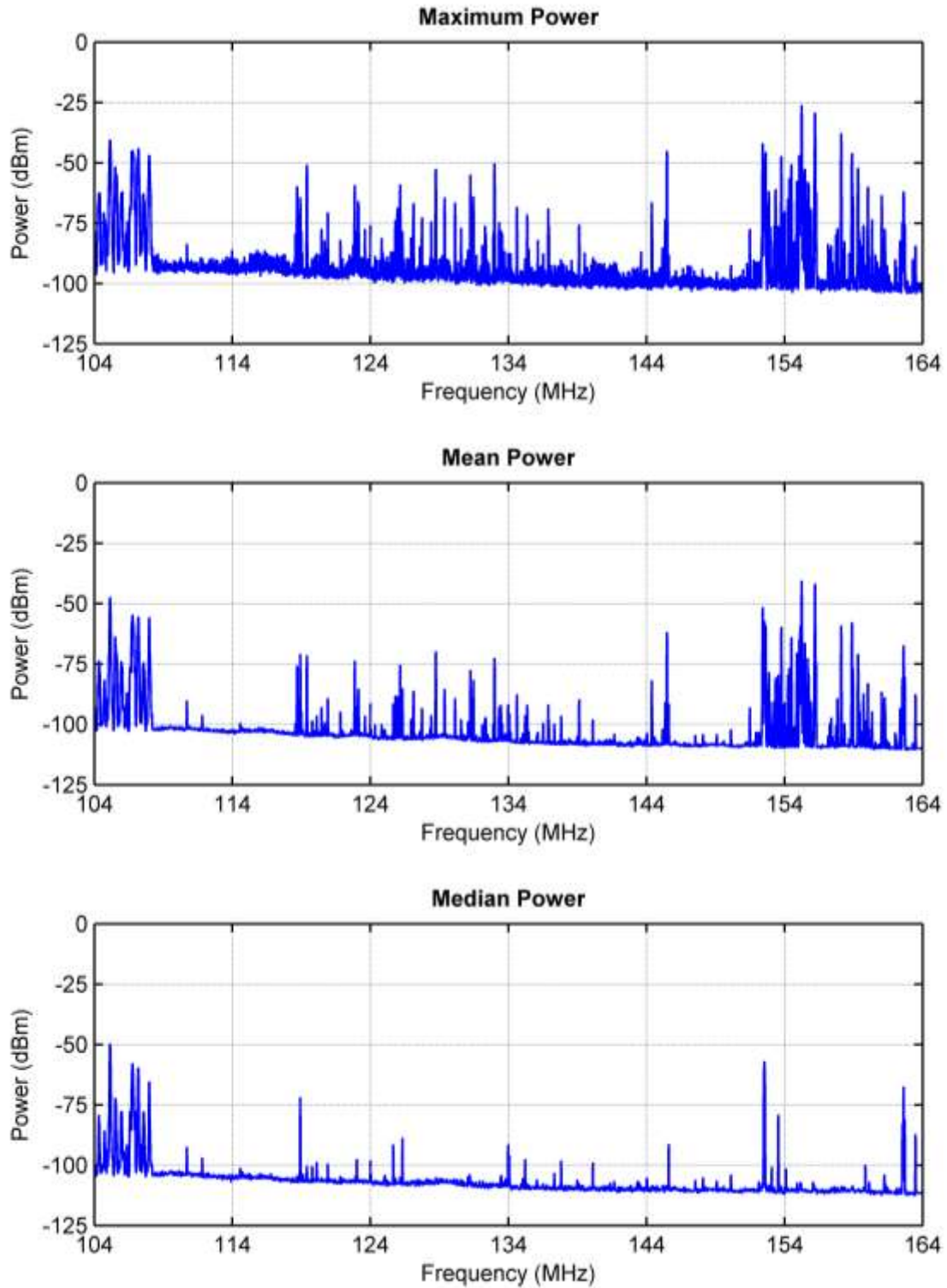


Figure A-4. Maximum, mean, and median received signal power at the Boulder business location for Event 1 (104–164 MHz, RBW = 10 kHz, 100 sweeps, sweep time = 300 ms).

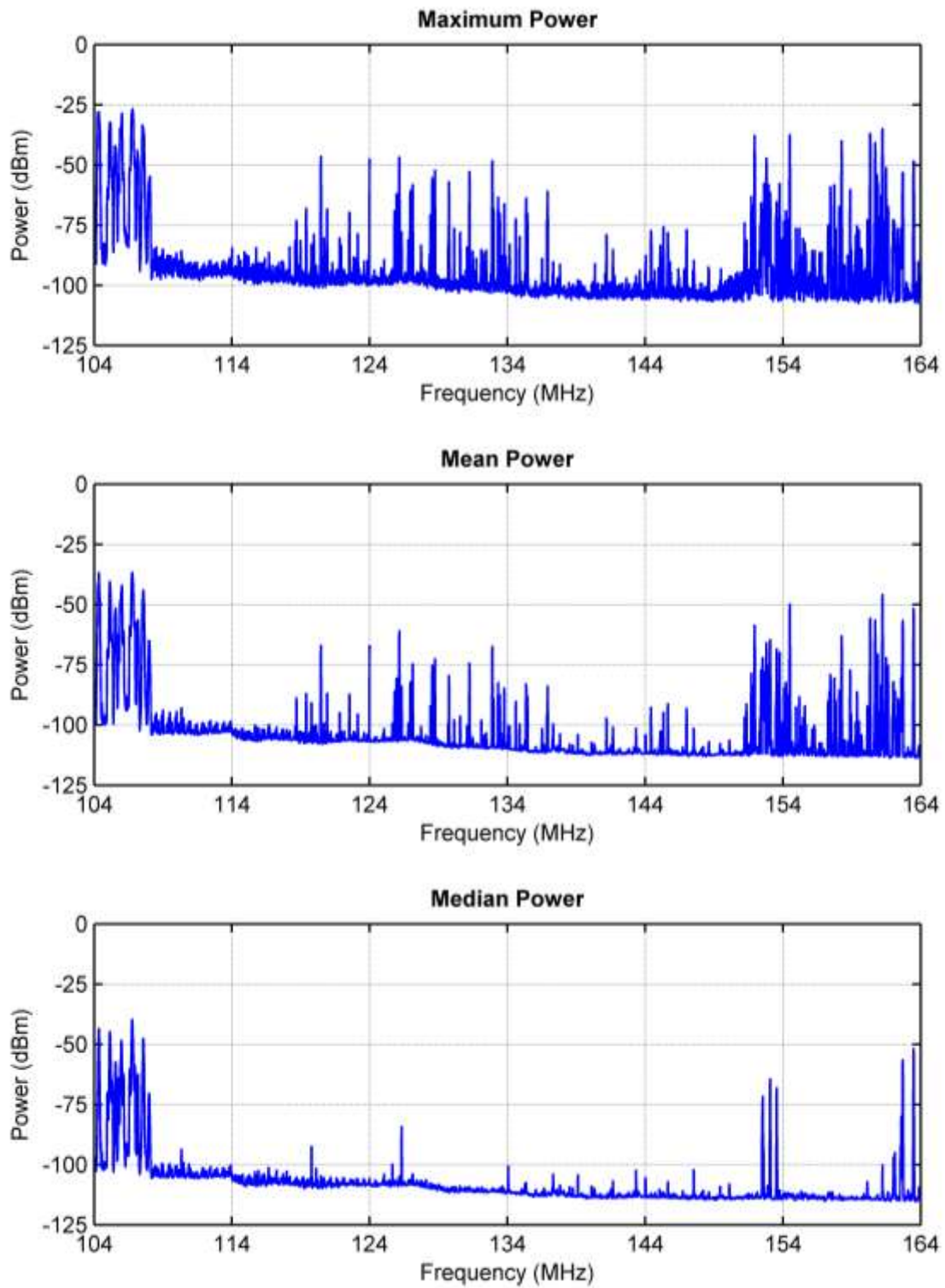


Figure A-5. Maximum, mean, and median received signal power at the Denver business location for Event 1 (104–164 MHz, RBW = 10 kHz, 100 sweeps, sweep time = 300 ms).

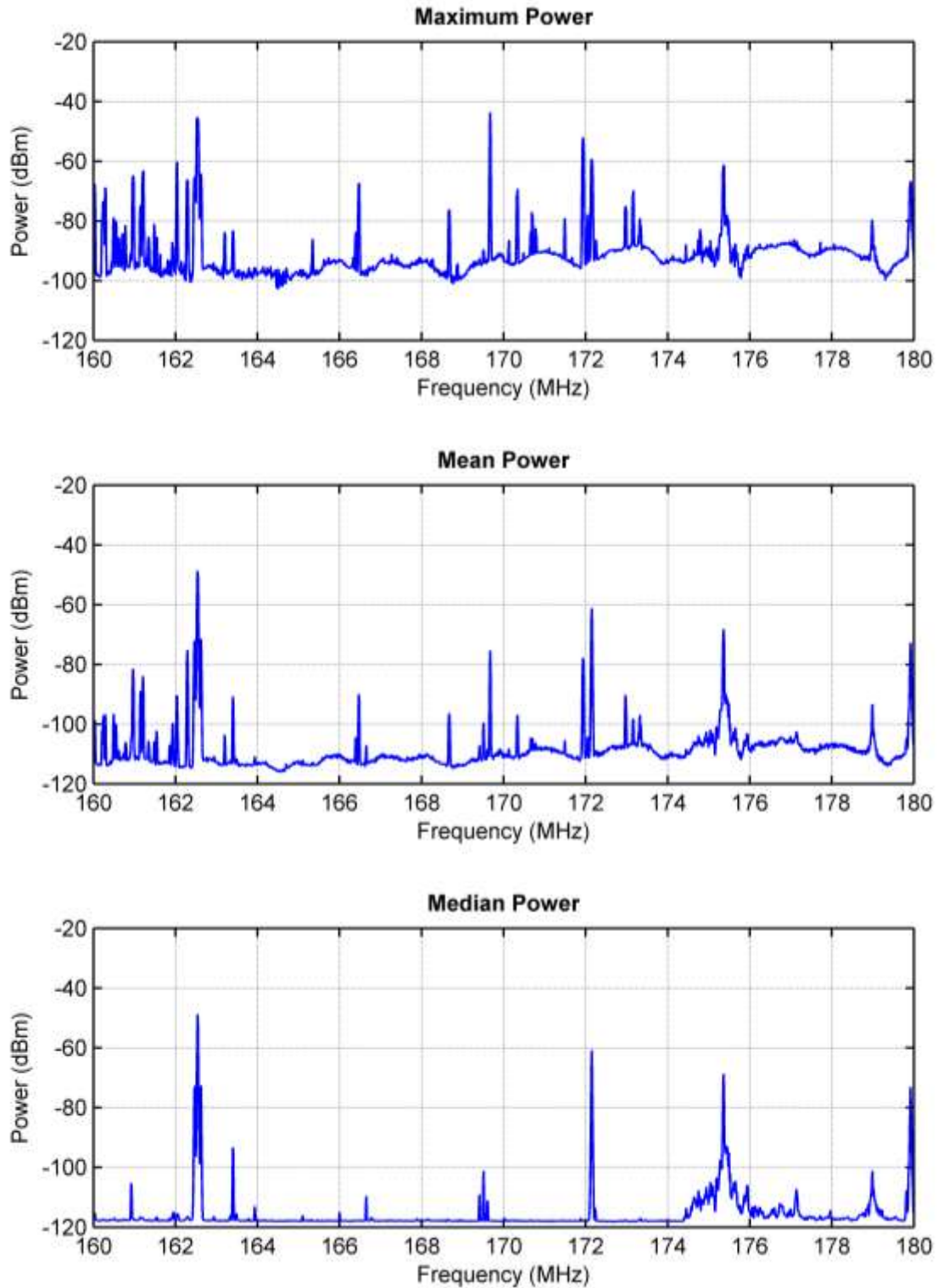


Figure A-6. Maximum, mean, and median received signal power at the Boulder residential location for Event 2 (160–180 MHz, RBW = 10 kHz, 500 sweeps, sweep time = 300 ms).

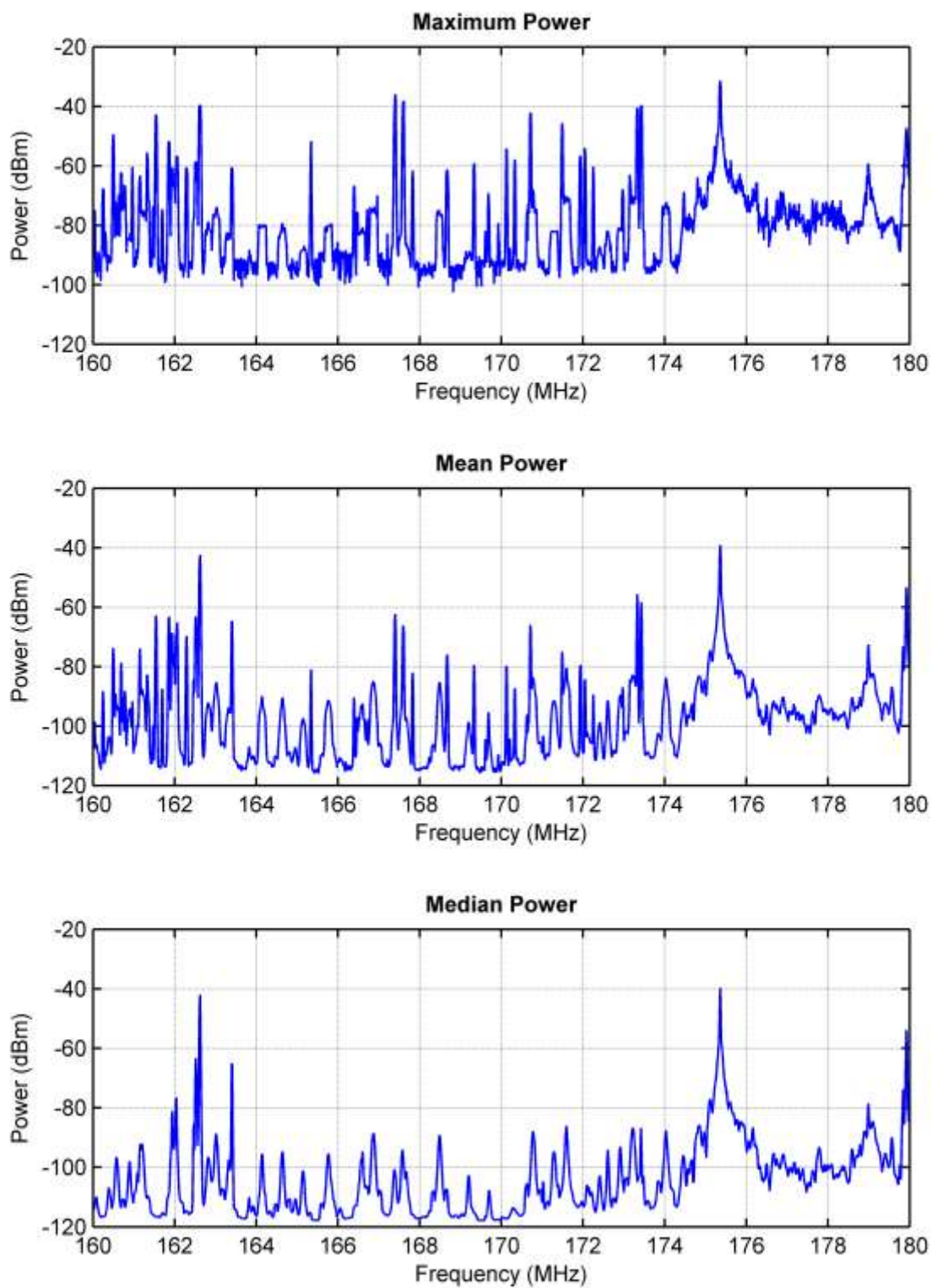


Figure A-7. Maximum, mean, and median received signal power at the Denver residential location for Event 2 (160–180 MHz, RBW = 10 kHz, 500 sweeps, sweep time = 300 ms).

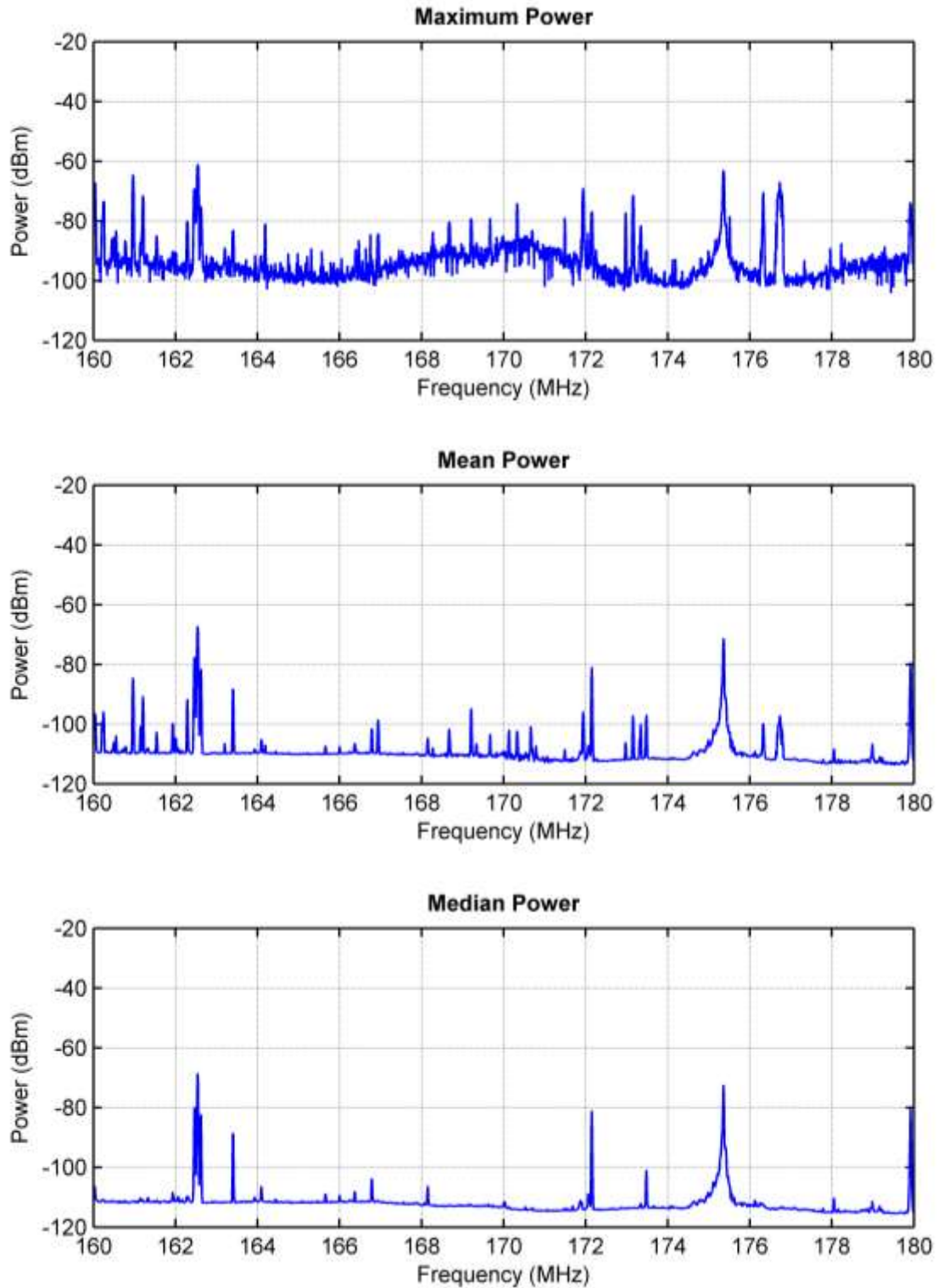


Figure A-8. Maximum, mean, and median received signal power at the Boulder business location for Event 2 (160–180 MHz, RBW = 10 kHz, 500 sweeps, sweep time = 300 ms).

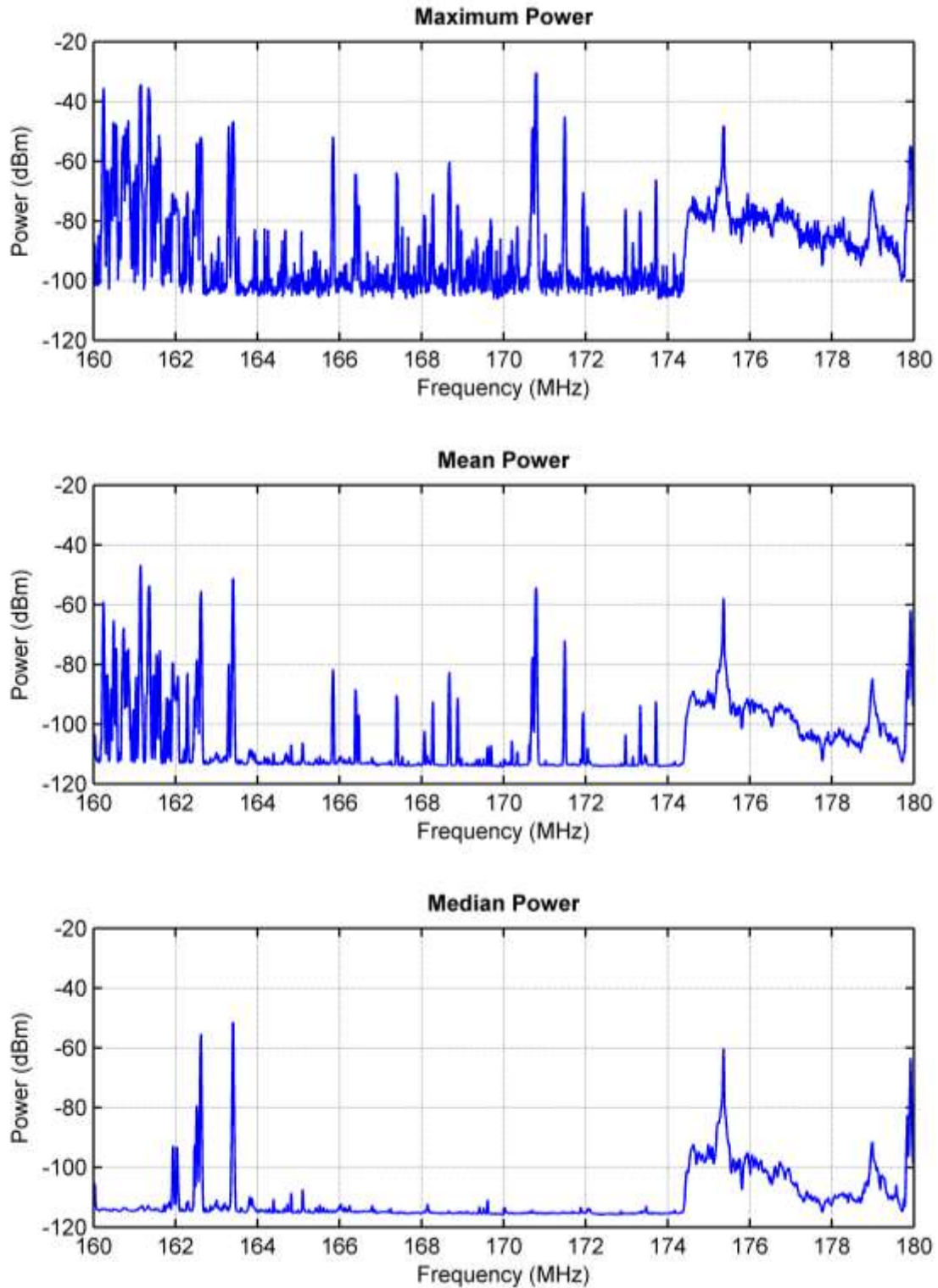


Figure A-9. Maximum, mean, and median received signal power at the Denver business location for Event 2 (160–180 MHz, RBW = 10 kHz, 500 sweeps, sweep time = 300 ms).

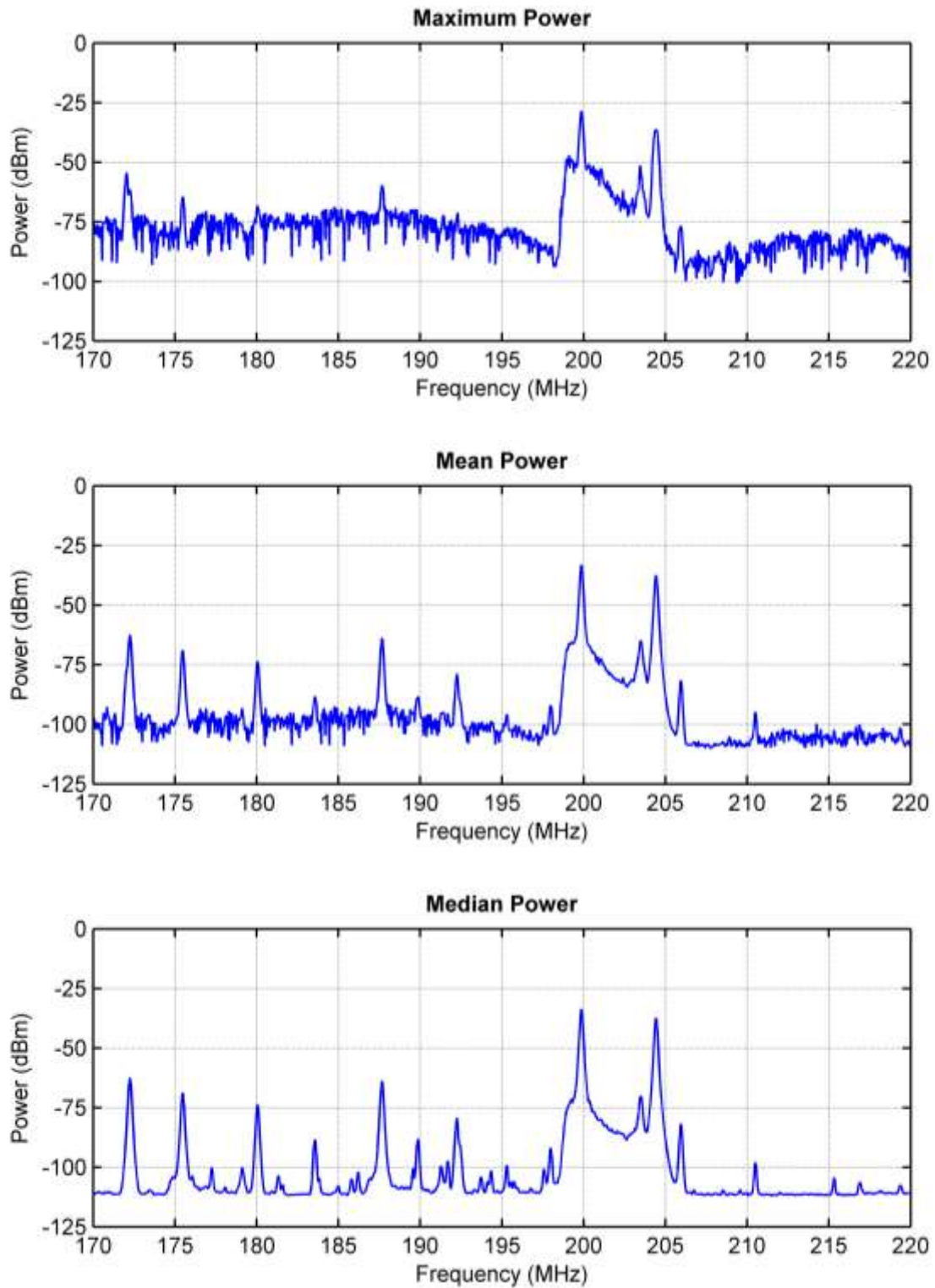


Figure A-10. Maximum, mean, and median received signal power at the Boulder residential location for Event 3 (170–220 MHz, RBW = 100 kHz, 500 sweeps, sweep time = 100 ms).

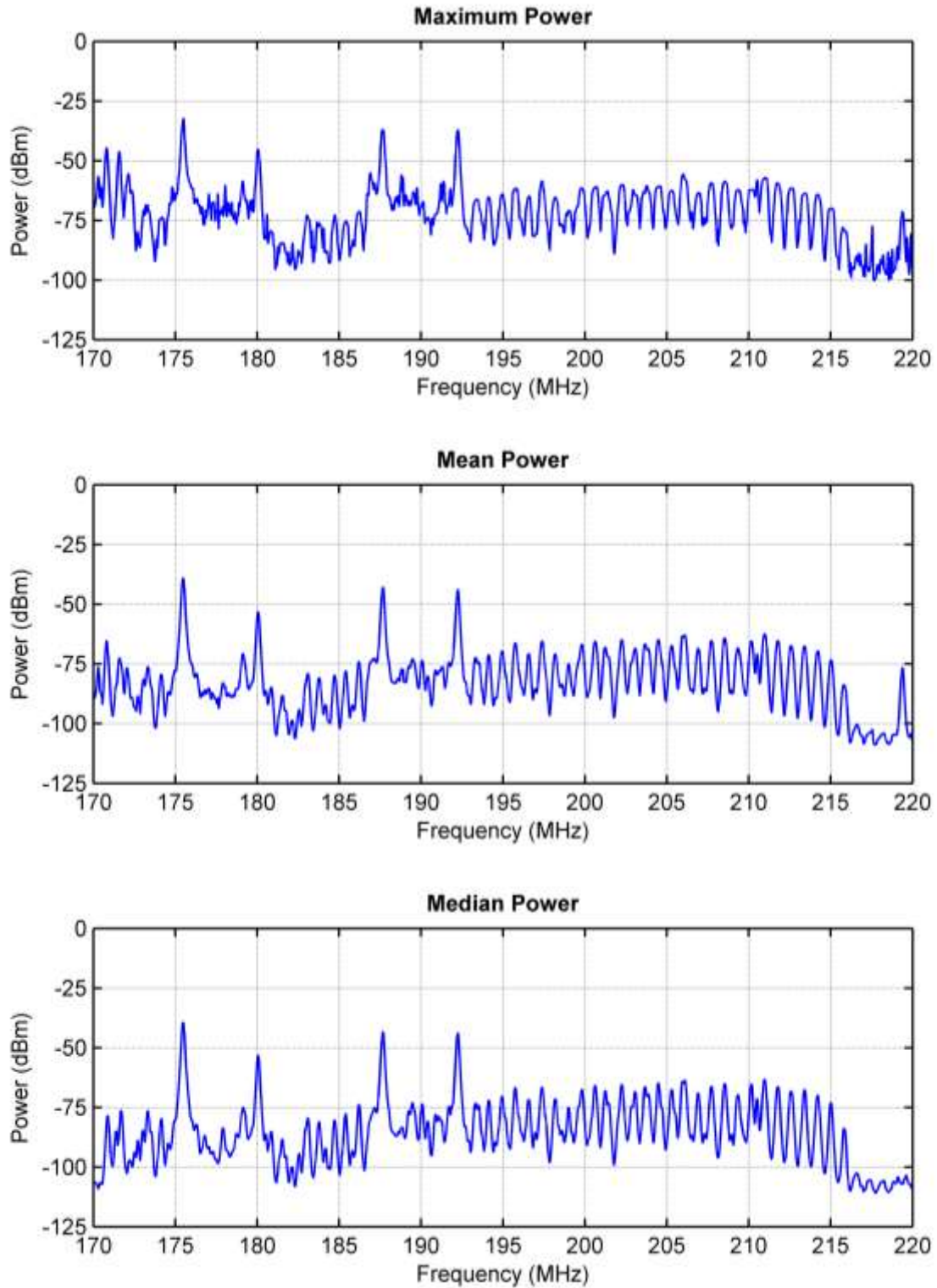


Figure A-11. Maximum, mean, and median received signal power at the Denver residential location for Event 3 (170–220 MHz, RBW = 100 kHz, 500 sweeps, sweep time = 100 ms).

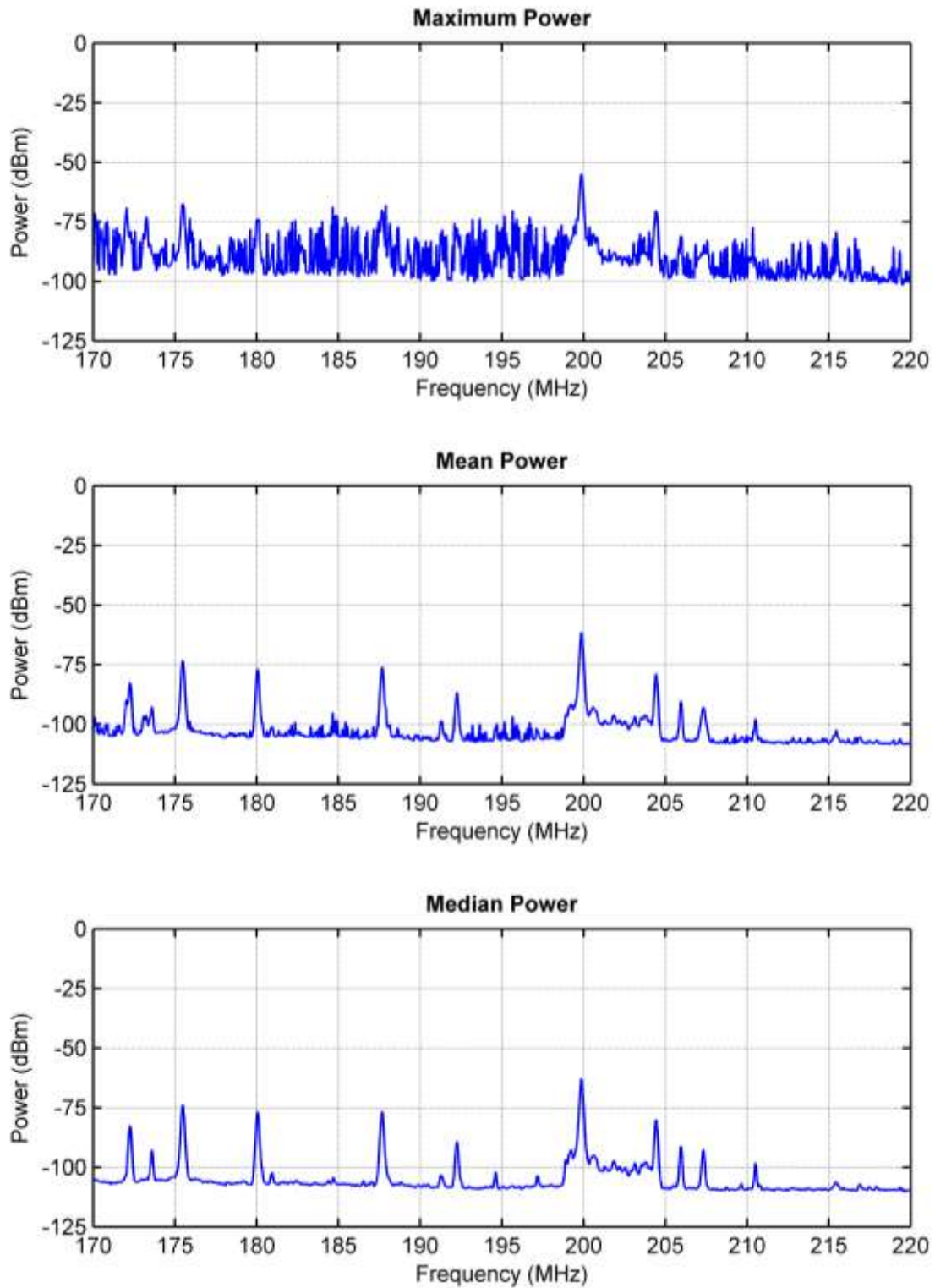


Figure A-12. Maximum, mean, and median received signal power at the Boulder business location for Event 3 (170–220 MHz, RBW = 100 kHz, 500 sweeps, sweep time = 100 ms).

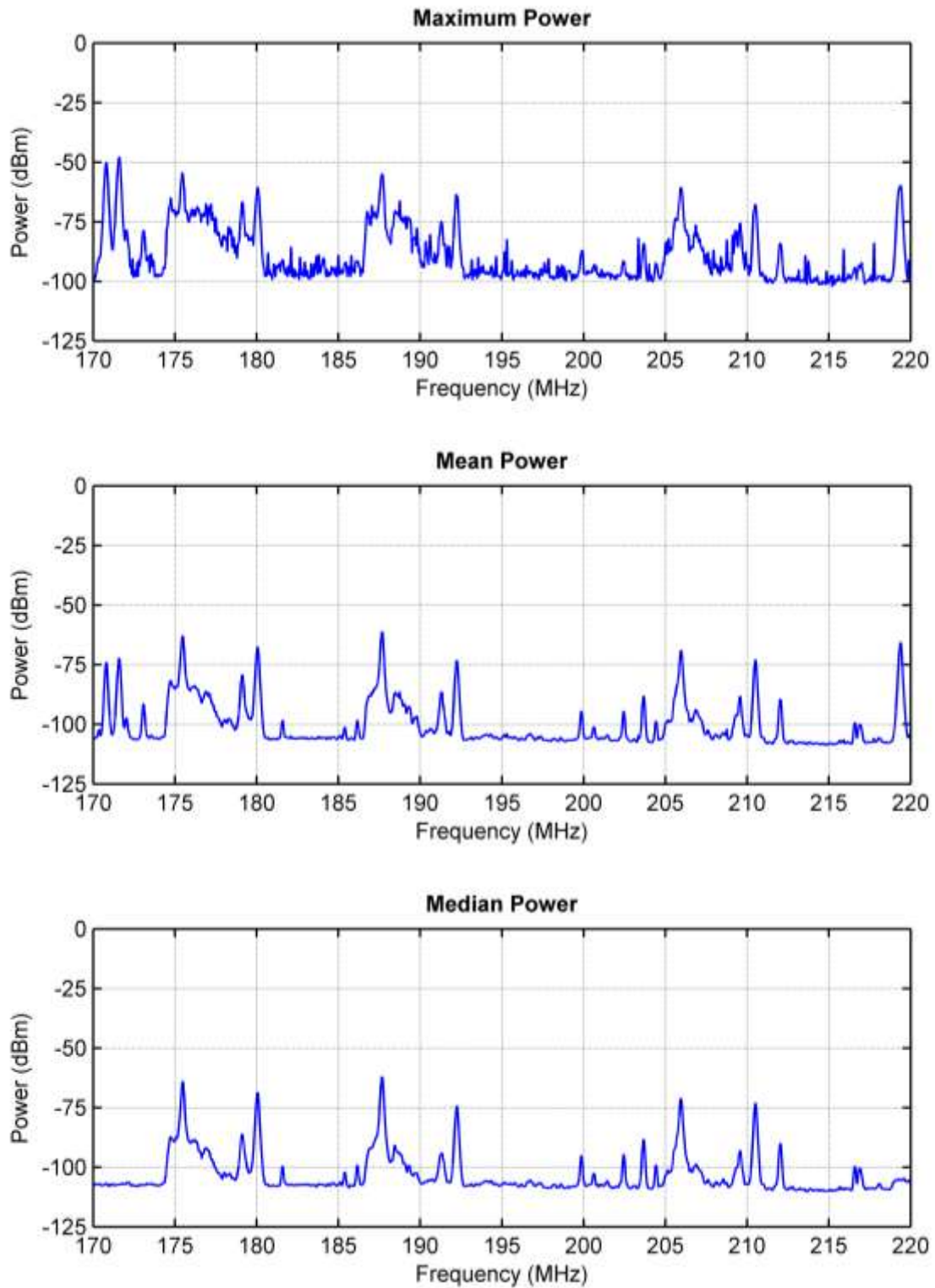


Figure A-13. Maximum, mean, and median received signal power at the Denver business location for Event 3 (170–220 MHz, RBW = 100 kHz, 500 sweeps, sweep time = 100 ms).

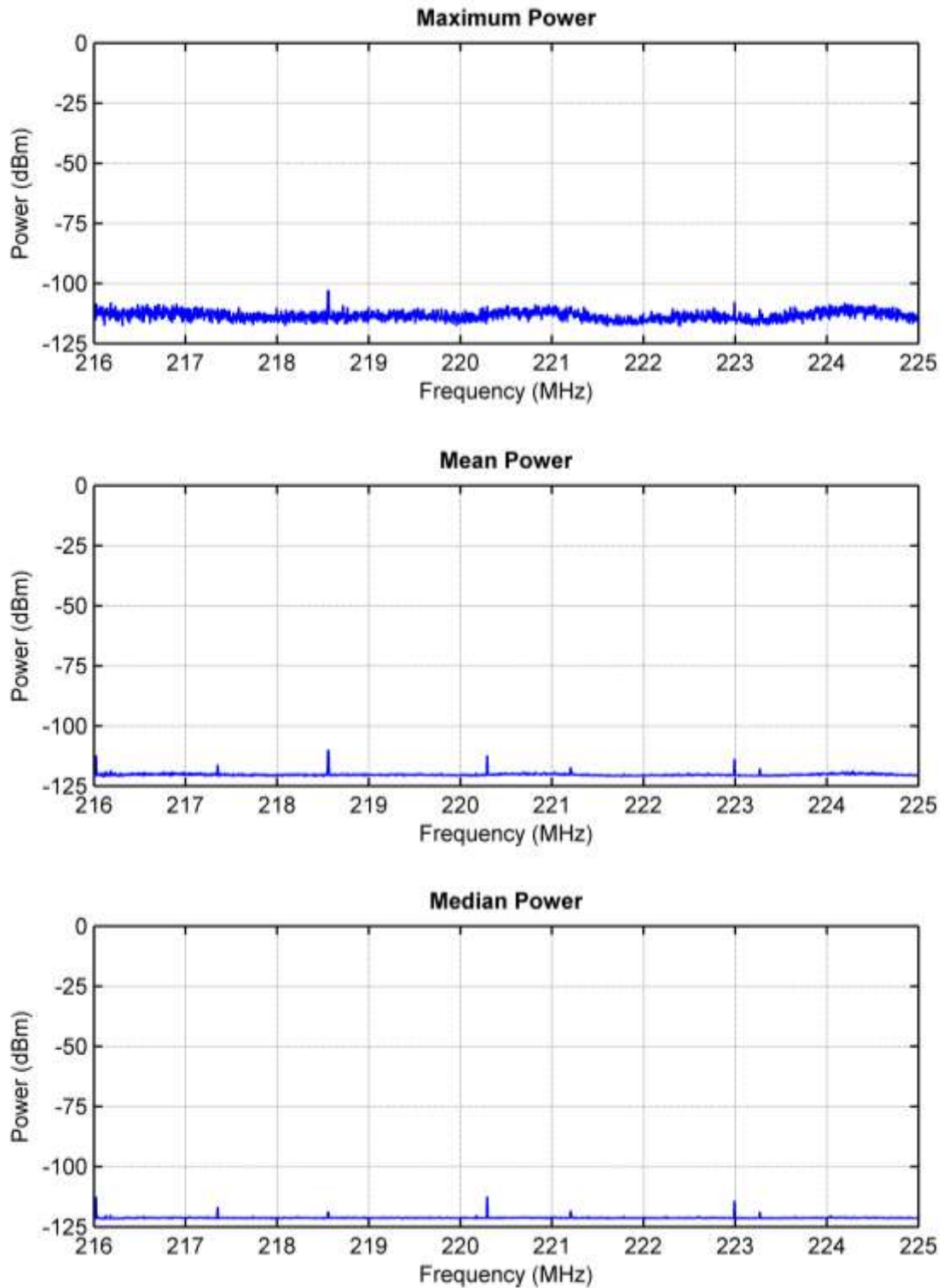


Figure A-14. Maximum, mean, and median received signal power at the Boulder residential location for Event 4 (216–225 MHz, RBW = 3 kHz, 60 sweeps, sweep time = 900 ms).

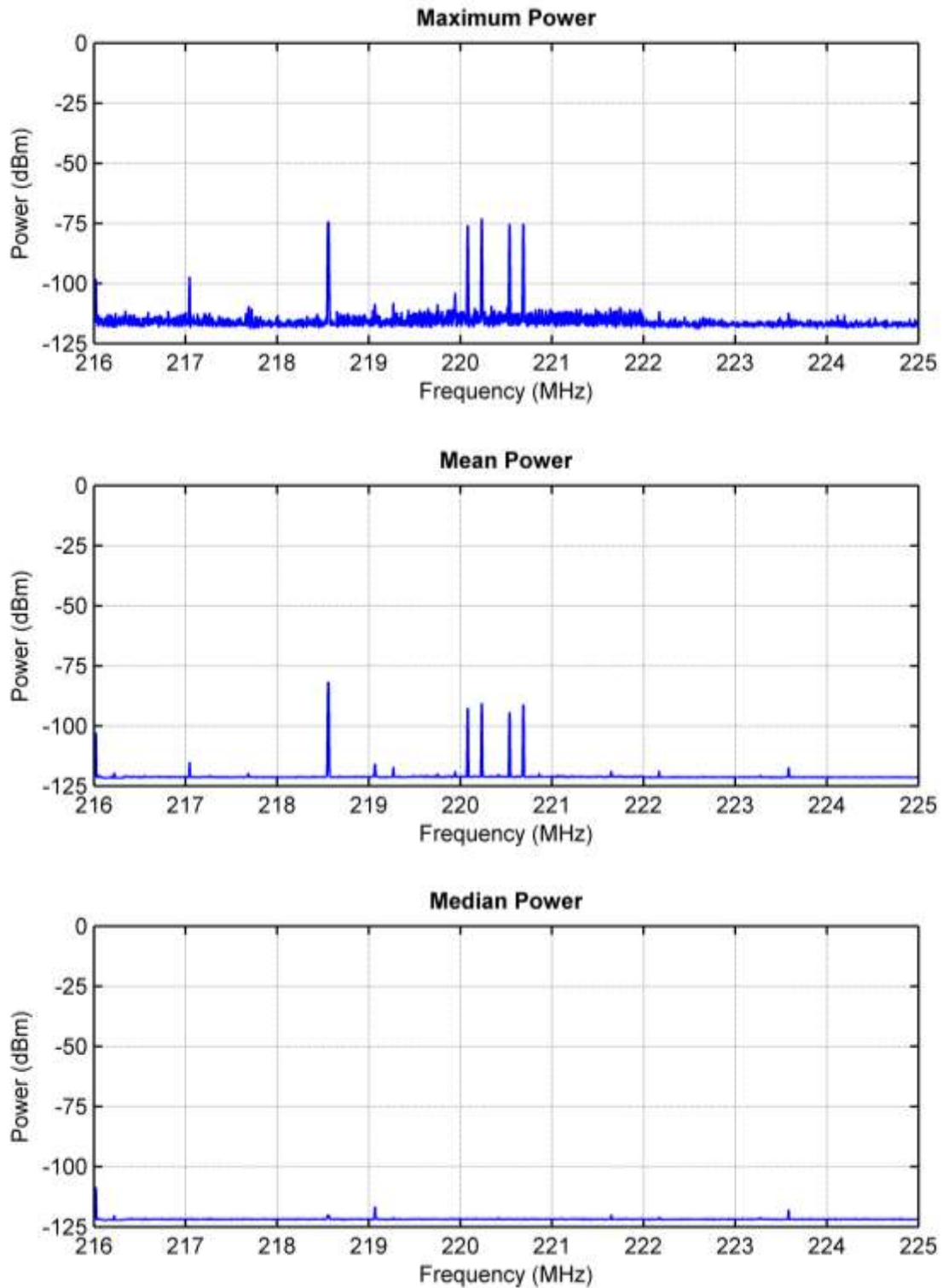


Figure A-15. Maximum, mean, and median received signal power at the Denver residential location for Event 4 (216–225 MHz, RBW = 3 kHz, 60 sweeps, sweep time = 900 ms).

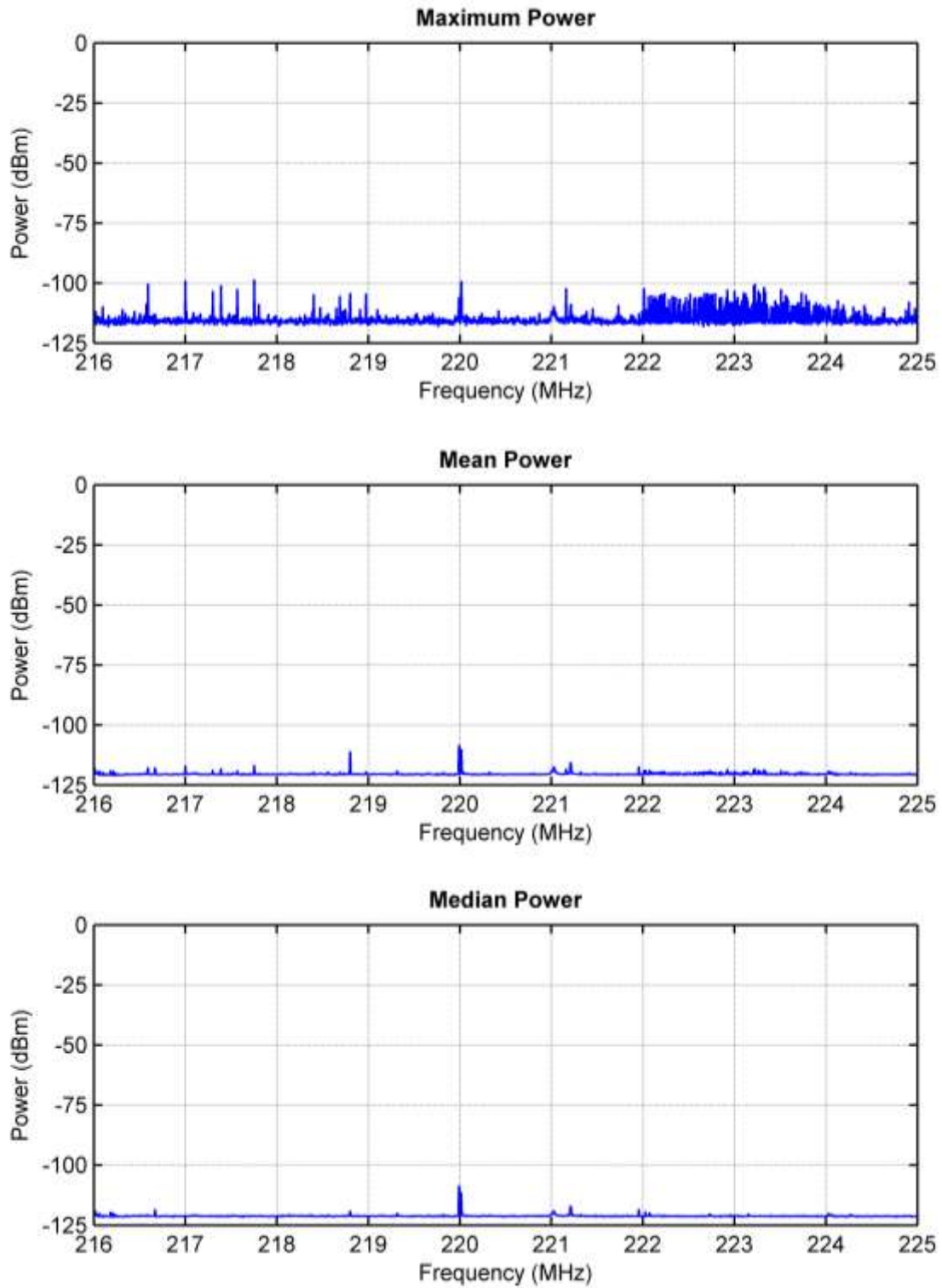


Figure A-16. Maximum, mean, and median received signal power at the Boulder business location for Event 4 (216–225 MHz, RBW = 3 kHz, 60 sweeps, sweep time = 900 ms).

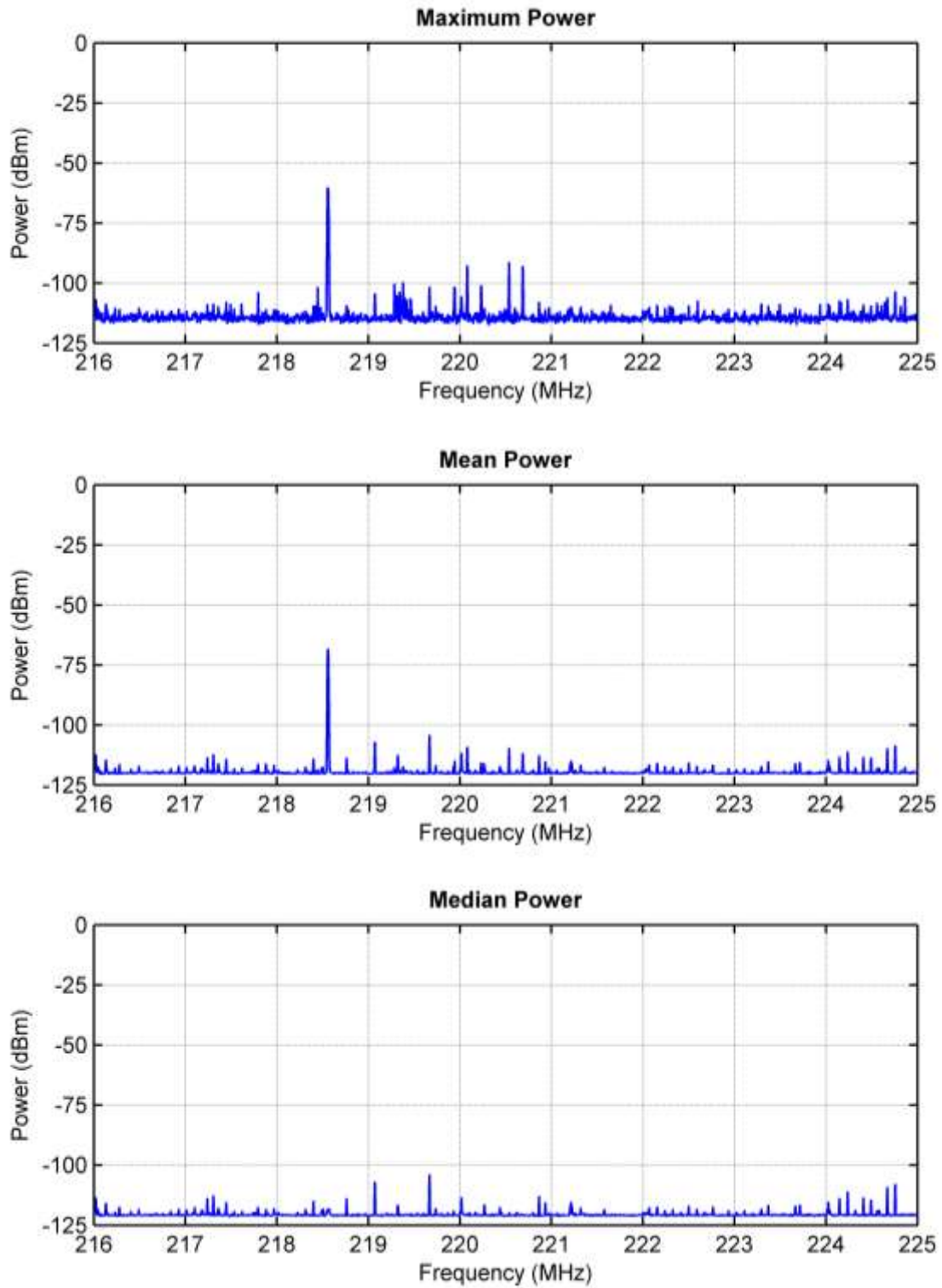


Figure A-17. Maximum, mean, and median received signal power at the Denver business location for Event 4 (216–225 MHz, RBW = 3 kHz, 60 sweeps, sweep time = 900 ms).

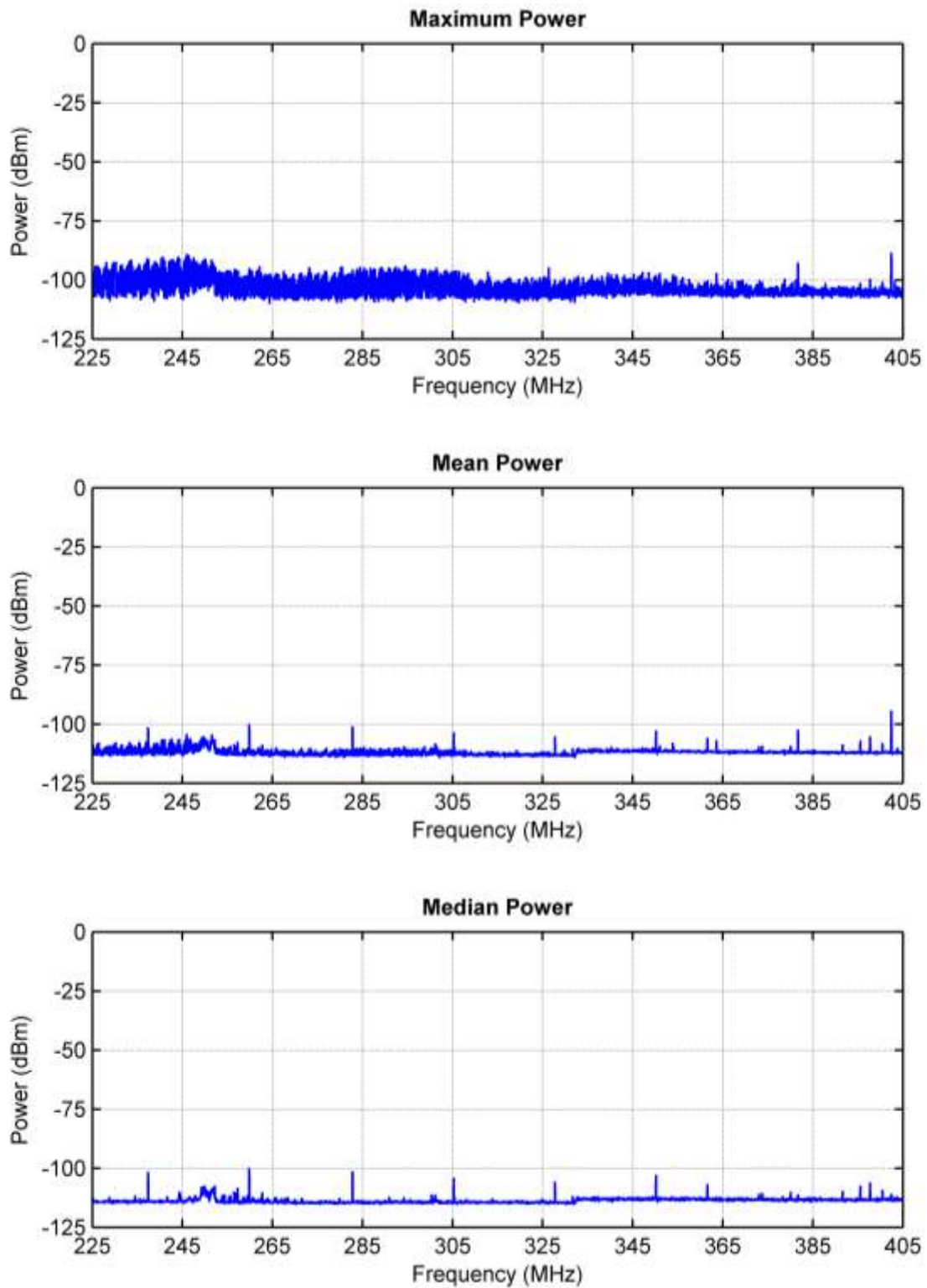


Figure A-18. Maximum, mean, and median received signal power at the Boulder residential location for Event 5 (225–405 MHz, RBW = 30 kHz, 100 sweeps, sweep time = 100 ms).

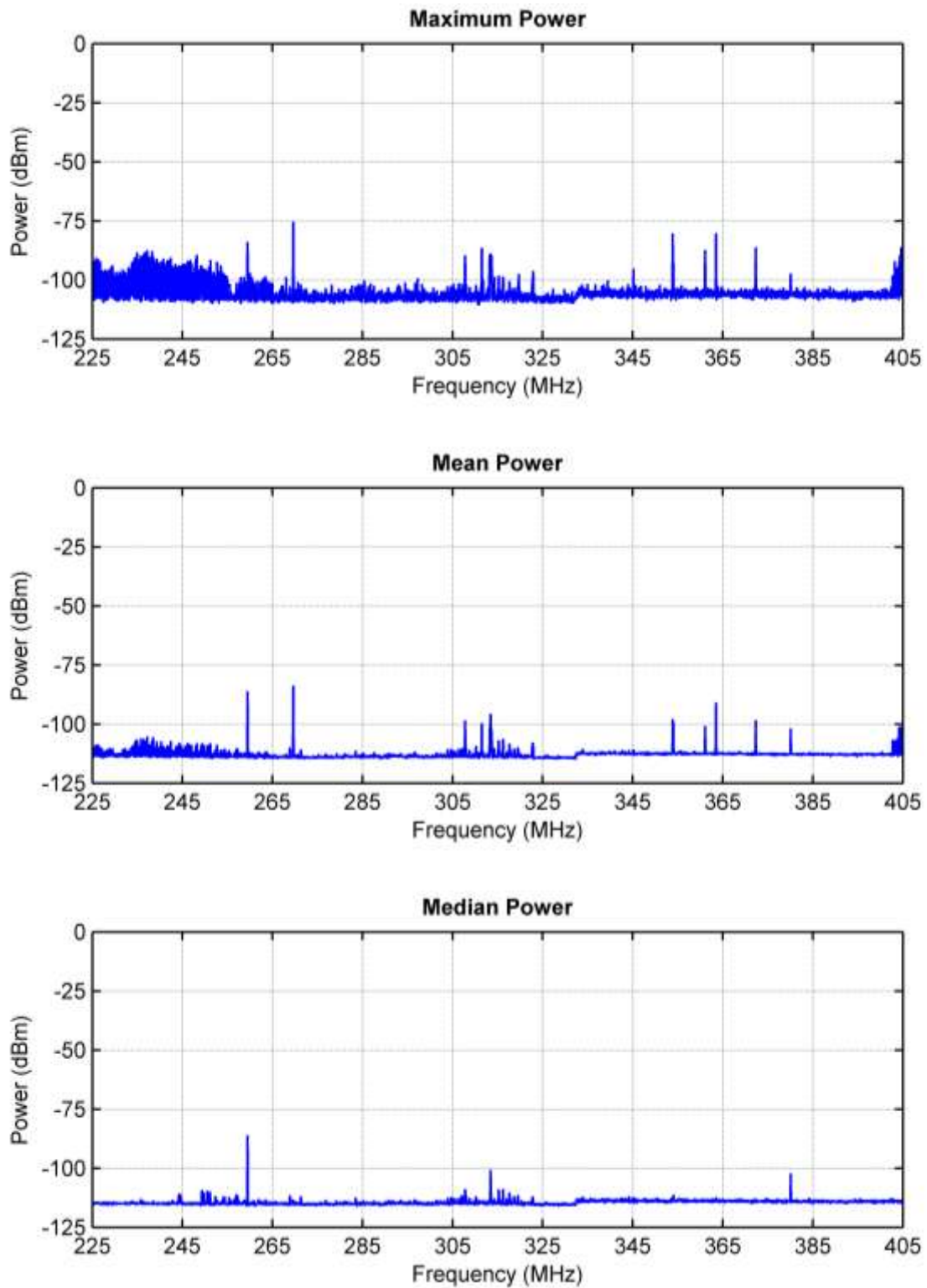


Figure A-19. Maximum, mean, and median received signal power at the Denver residential location for Event 5 (225–405 MHz, RBW = 30 kHz, 100 sweeps, sweep time = 100 ms).

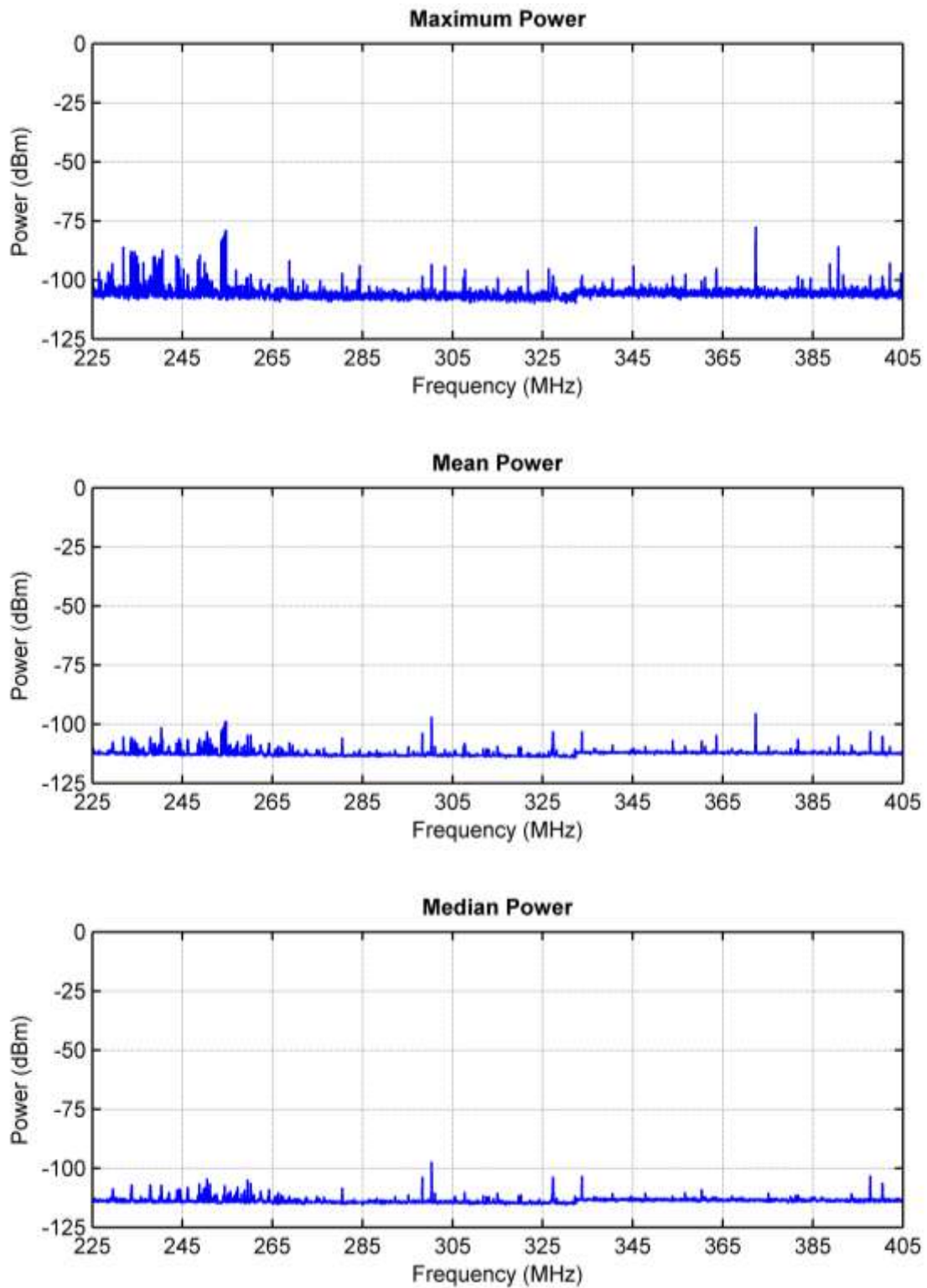


Figure A-20. Maximum, mean, and median received signal power at the Boulder business location for Event 5 (225–405 MHz, RBW = 30 kHz, 100 sweeps, sweep time = 100 ms).

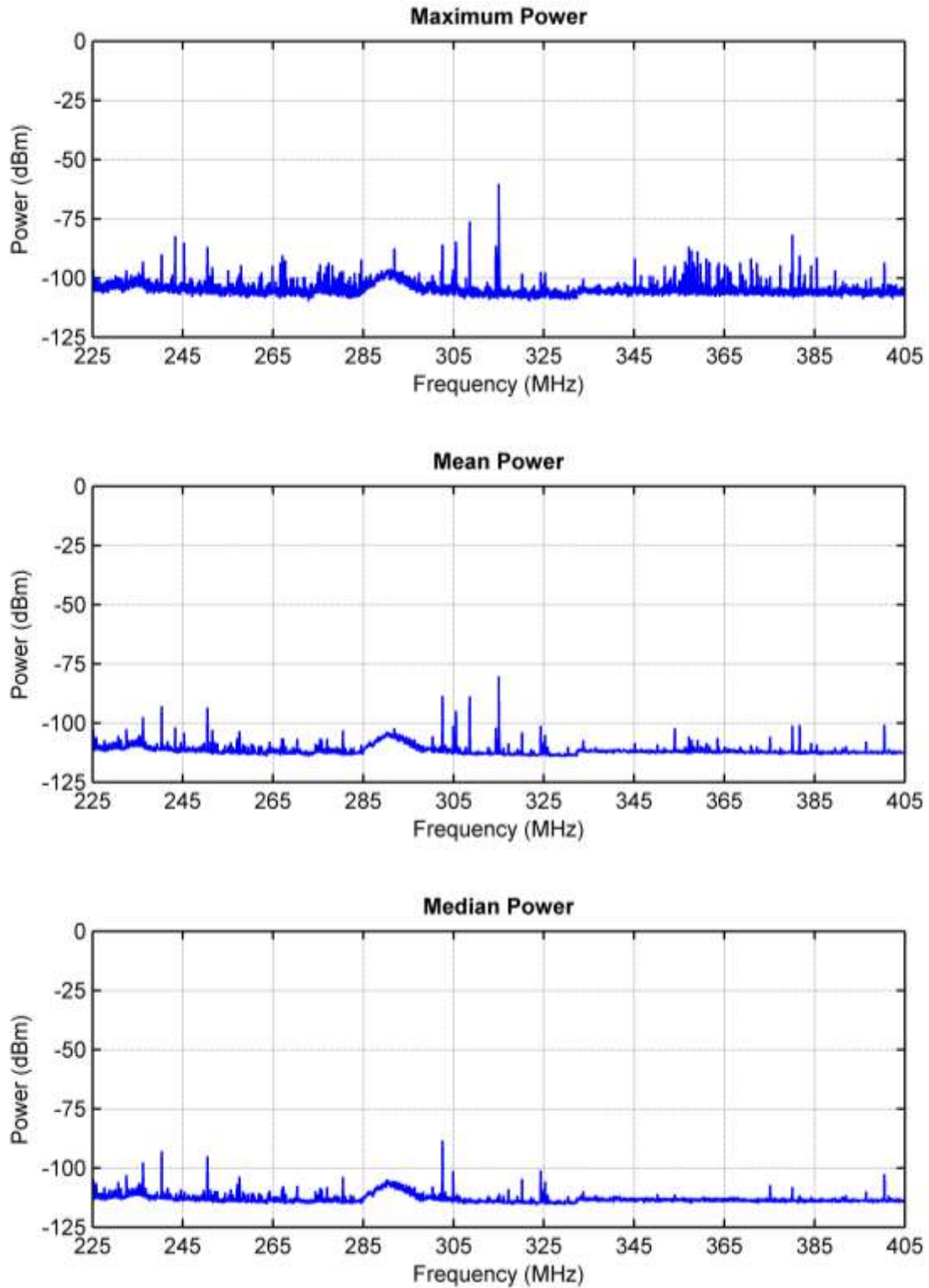


Figure A-21. Maximum, mean, and median received signal power at the Denver business location for Event 5 (225–405 MHz, RBW = 30 kHz, 100 sweeps, sweep time = 100 ms).

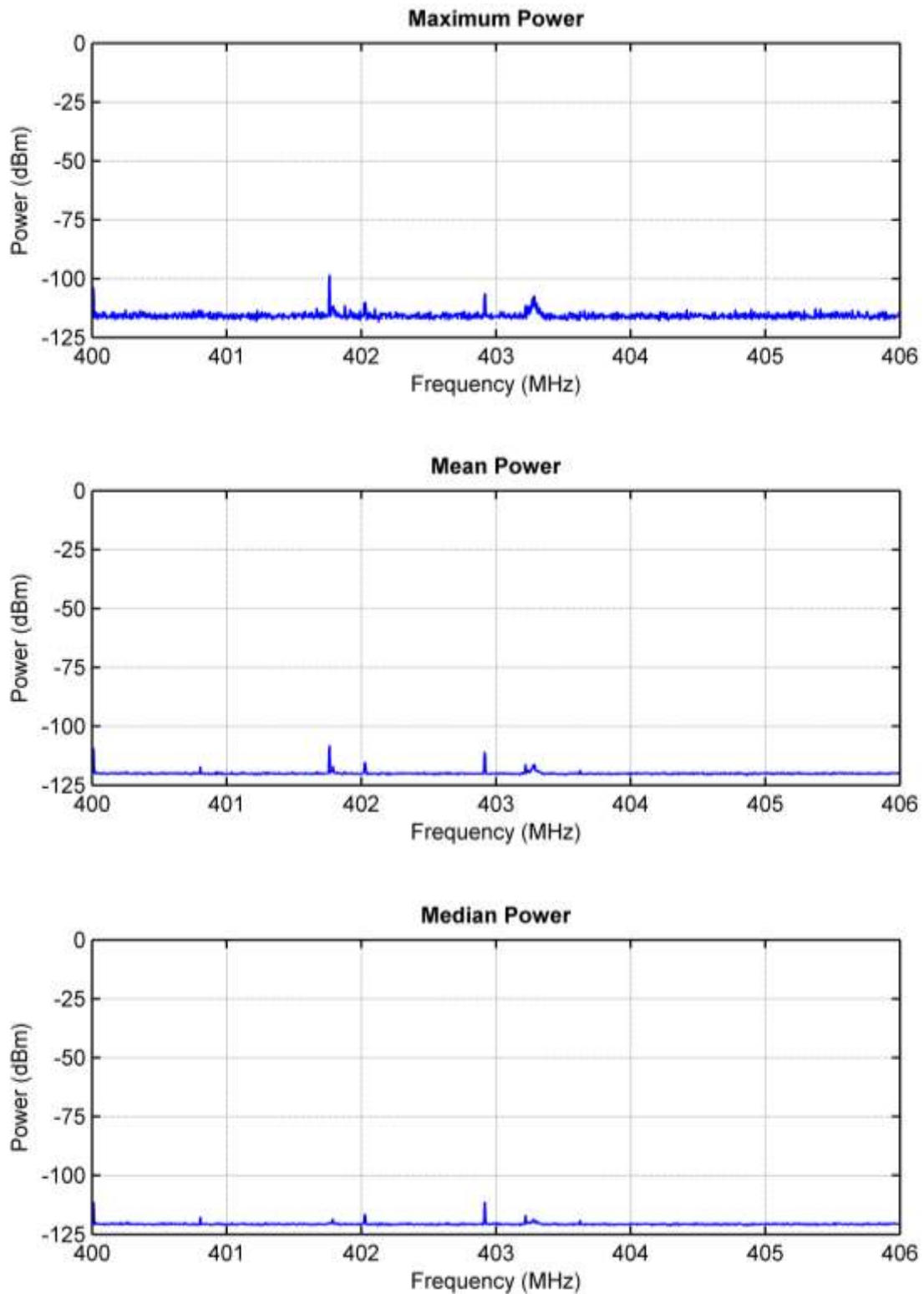


Figure A-22. Maximum, mean, and median received signal power at the Boulder residential location for Event 6 (400–406 MHz, RBW = 3 kHz, 60 sweeps, sweep time = 900 ms).

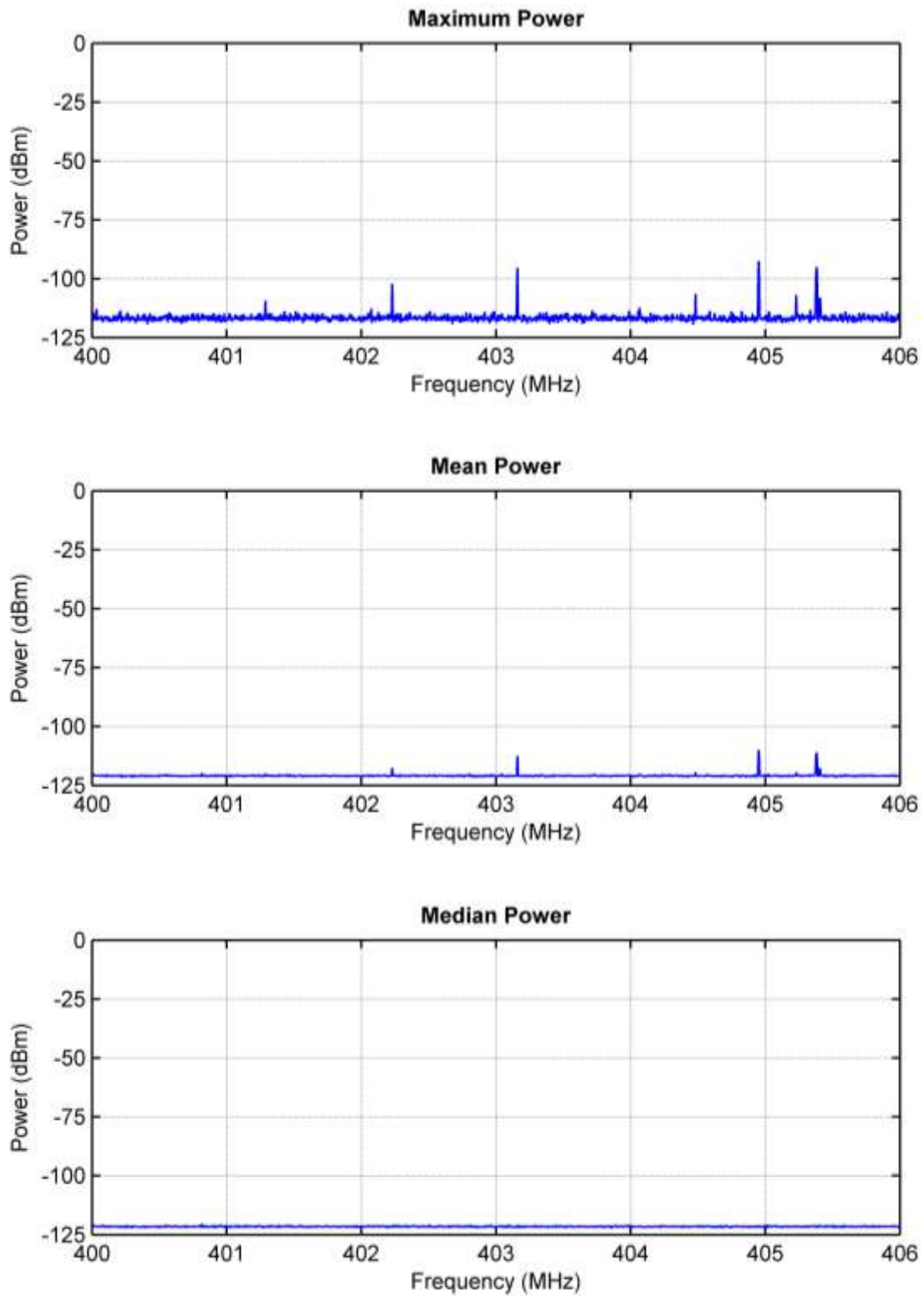


Figure A-23. Maximum, mean, and median received signal power at the Denver residential location for Event 6 (400–406 MHz, RBW = 3 kHz, 60 sweeps, sweep time = 900 ms).

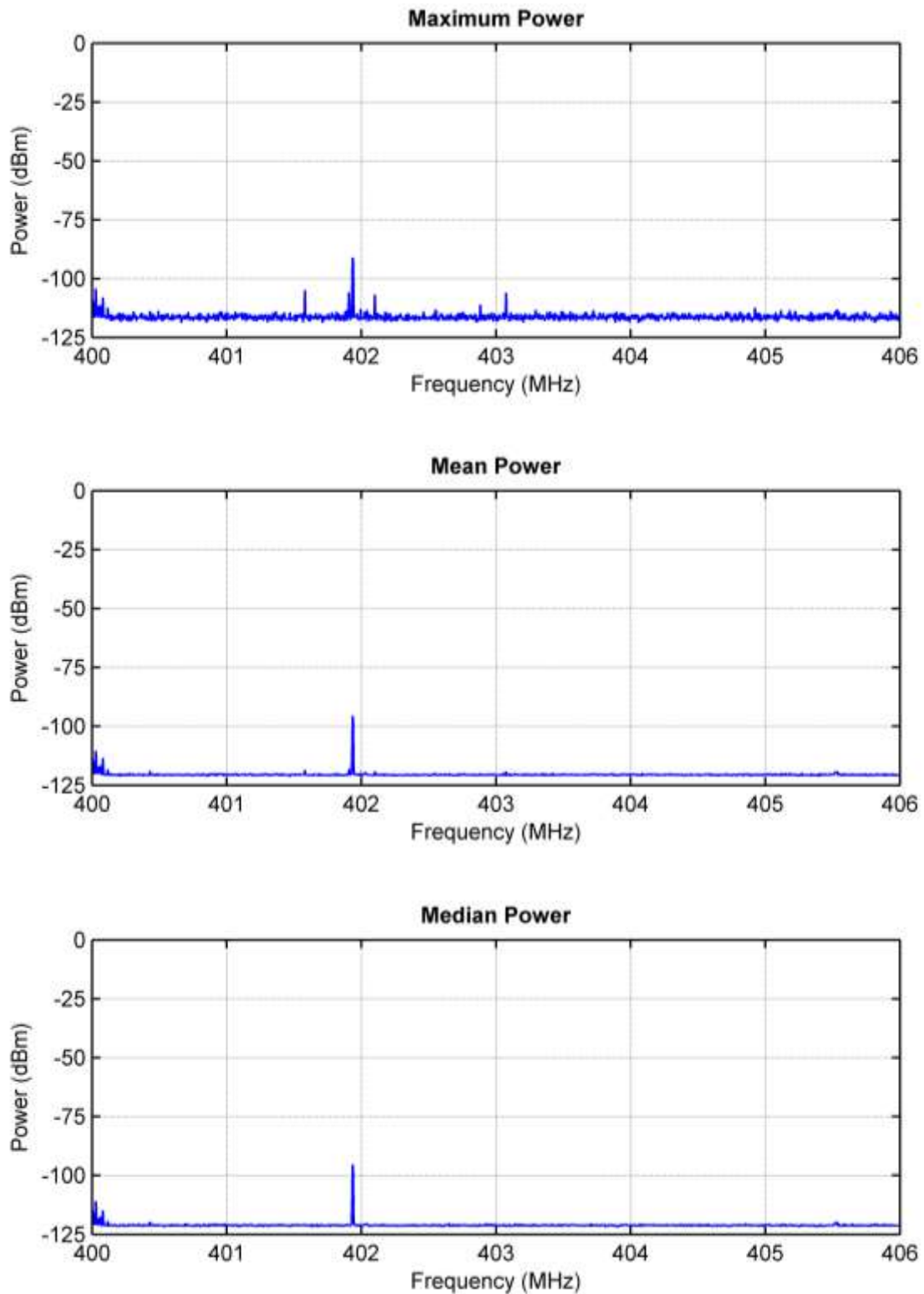


Figure A-24. Maximum, mean, and median received signal power at the Boulder business location for Event 6 (400–406 MHz, RBW = 3 kHz, 60 sweeps, sweep time = 900 ms).

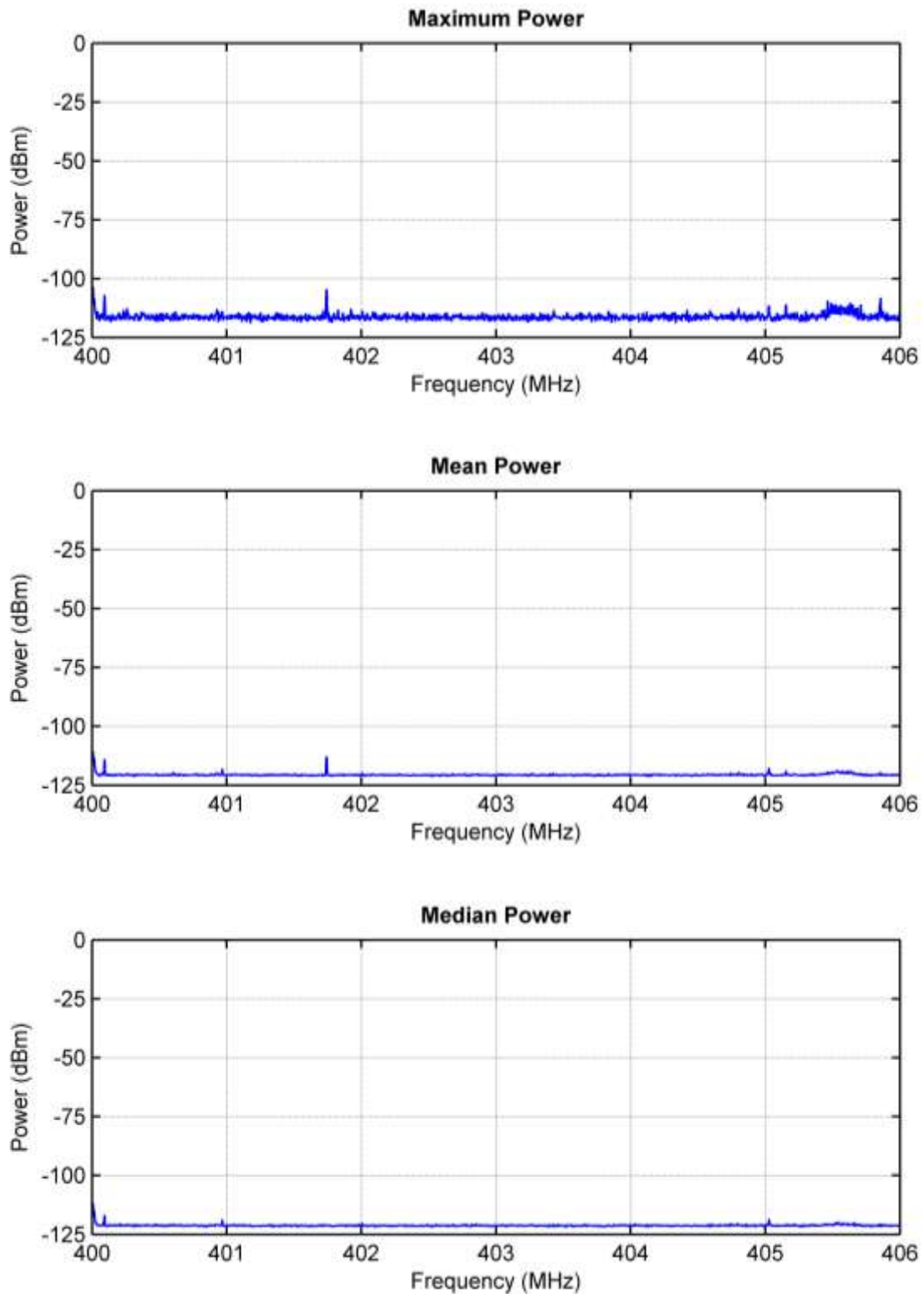


Figure A-25. Maximum, mean, and median received signal power at the Denver business location for Event 6 (400–406 MHz, RBW = 3 kHz, 60 sweeps, sweep time = 900 ms).

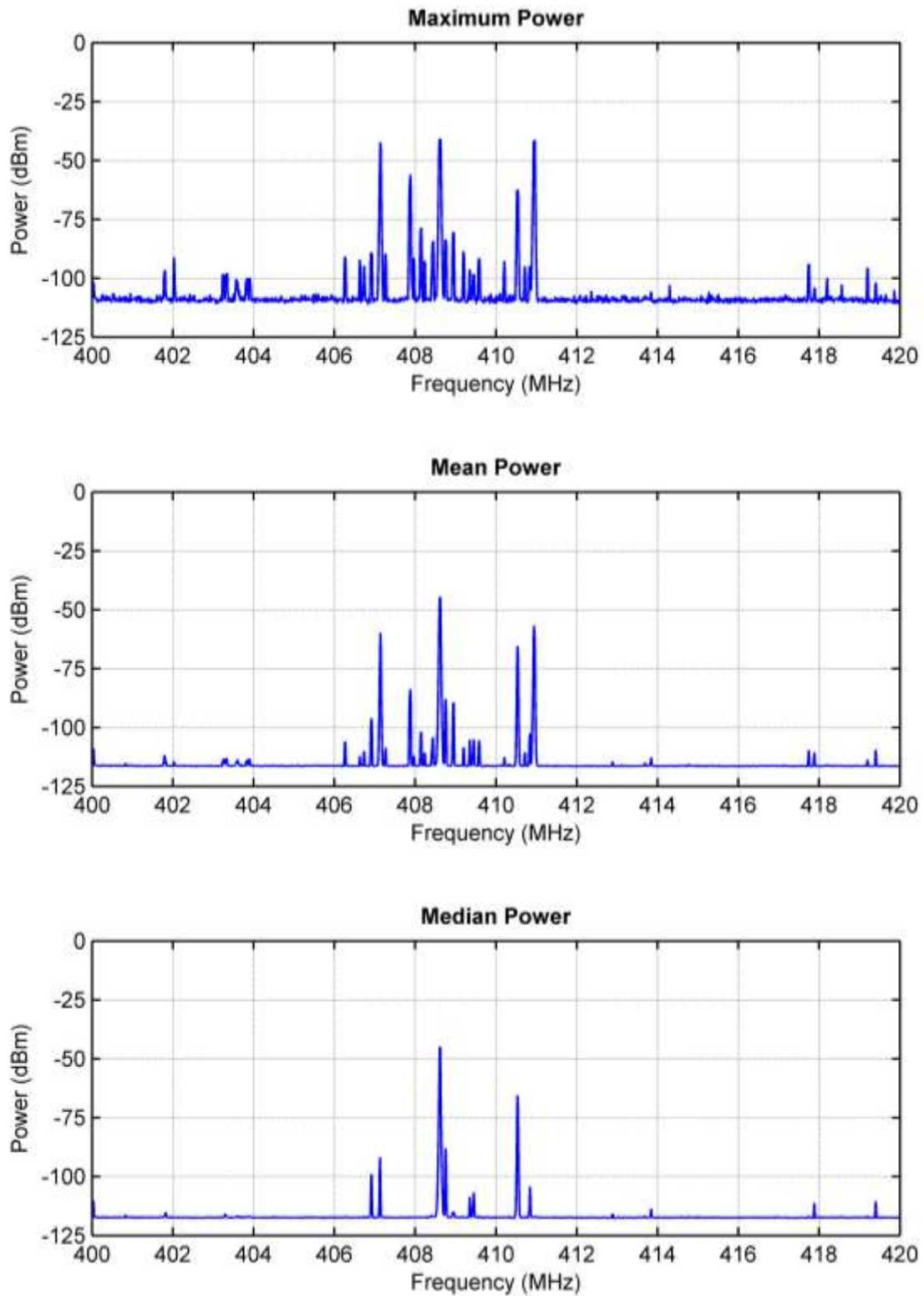


Figure A-26. Maximum, mean, and median received signal power at the Boulder residential location for Event 7 (400–420 MHz, RBW = 10 kHz, 200 sweeps, sweep time = 300 ms).

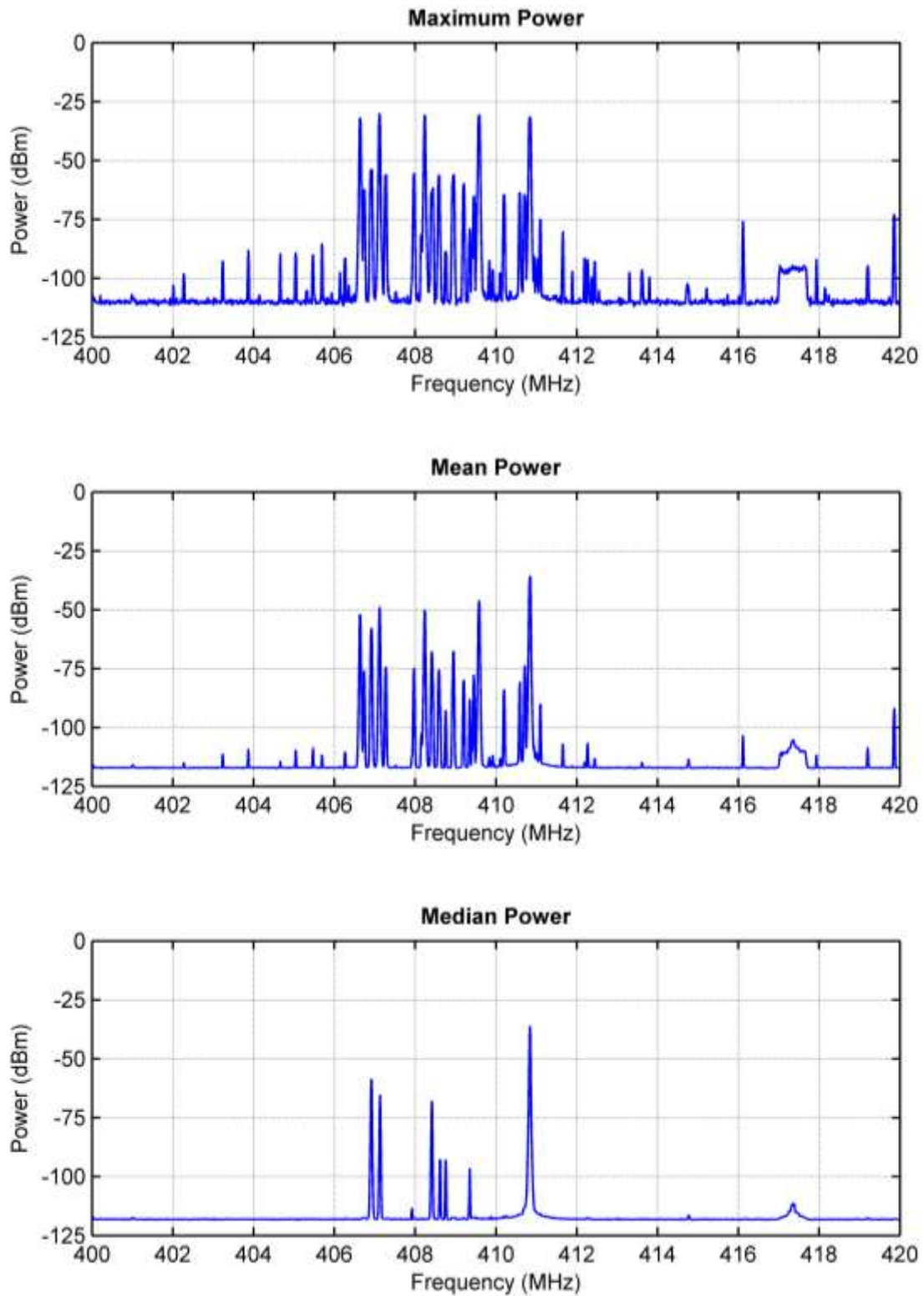


Figure A-27. Maximum, mean, and median received signal power at the Denver residential location for Event 7 (400–420 MHz, RBW = 10 kHz, 200 sweeps, sweep time = 300 ms).

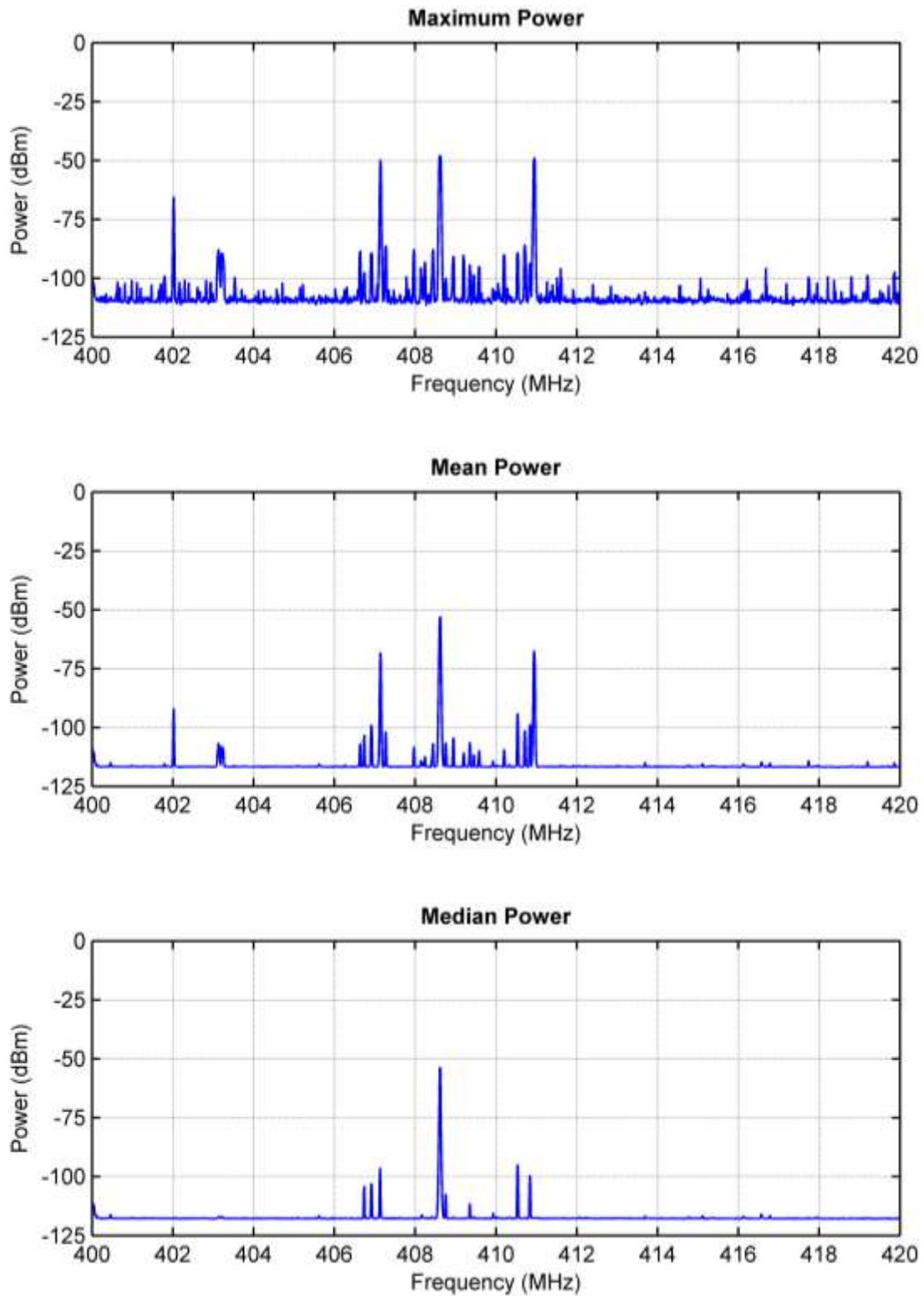


Figure A-28. Maximum, mean, and median received signal power at the Boulder business location for Event 7 (400–420 MHz, RBW = 10 kHz, 200 sweeps, sweep time = 300 ms).

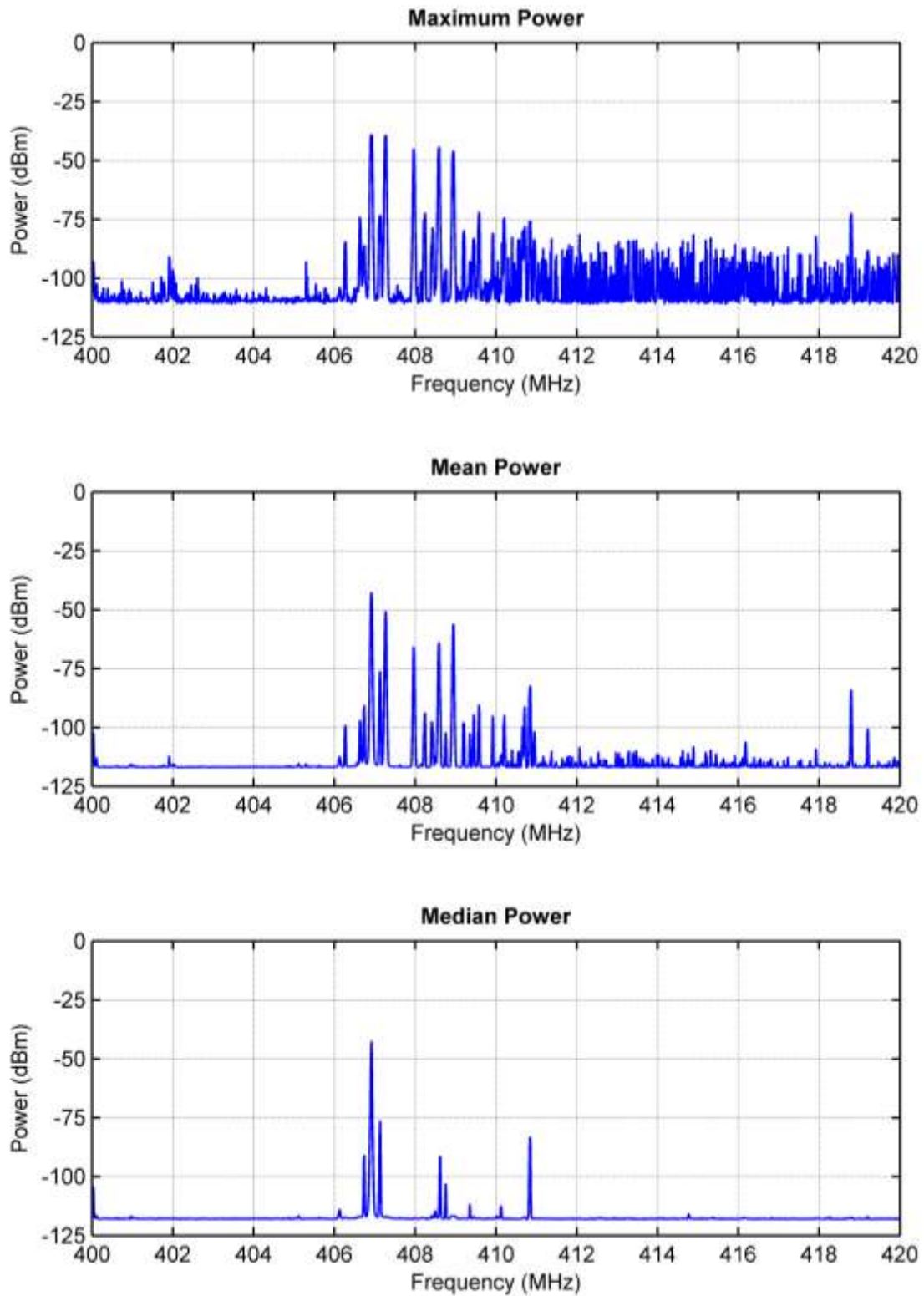


Figure A-29. Maximum, mean, and median received signal power at the Denver business location for Event 7 (400–420 MHz, RBW = 10 kHz, 200 sweeps, sweep time = 300 ms).

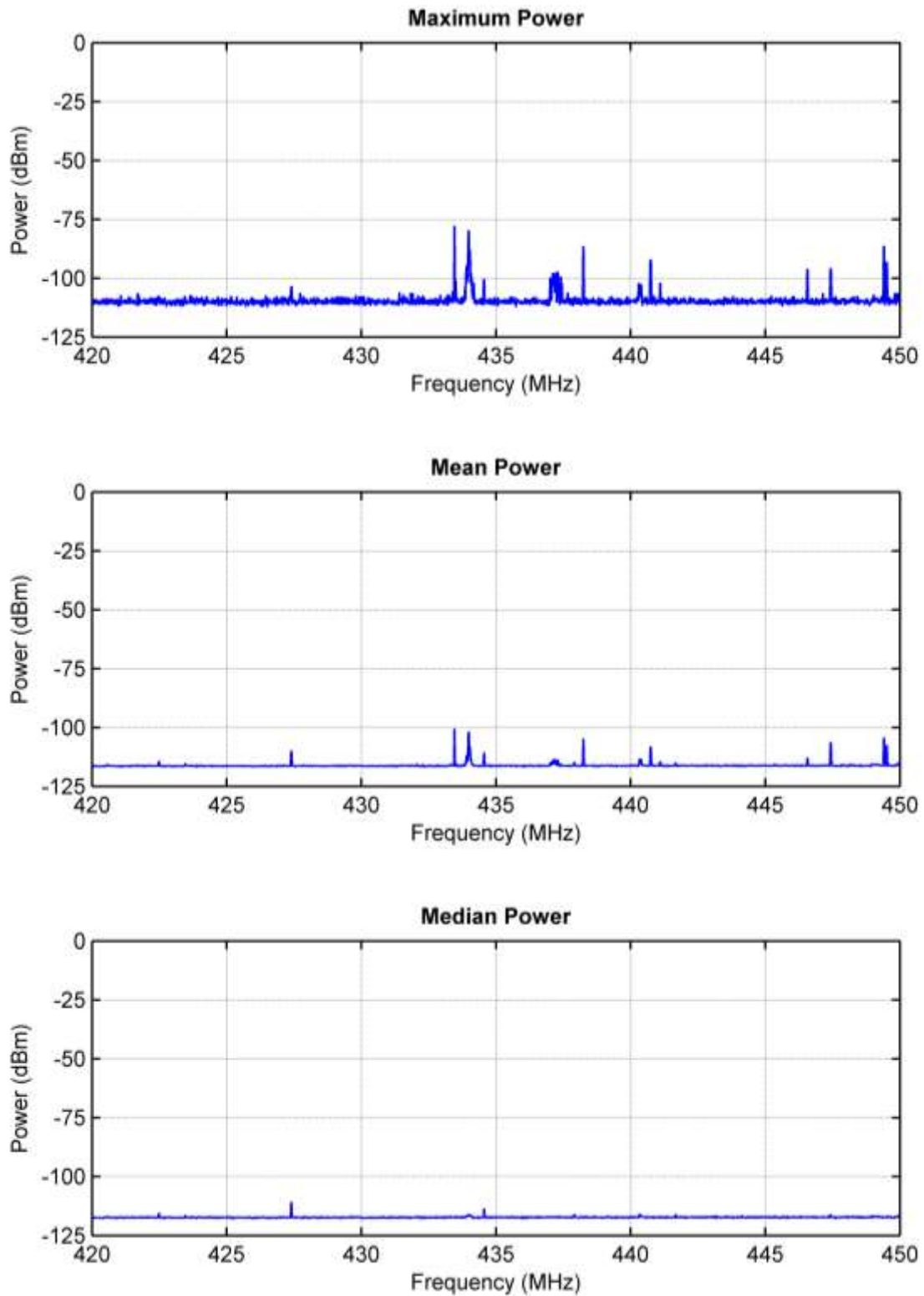


Figure A-30. Maximum, mean, and median received signal power at the Boulder residential location for Event 8 (420–450 MHz, RBW = 10 kHz, 100 sweeps, sweep time = 300 ms).

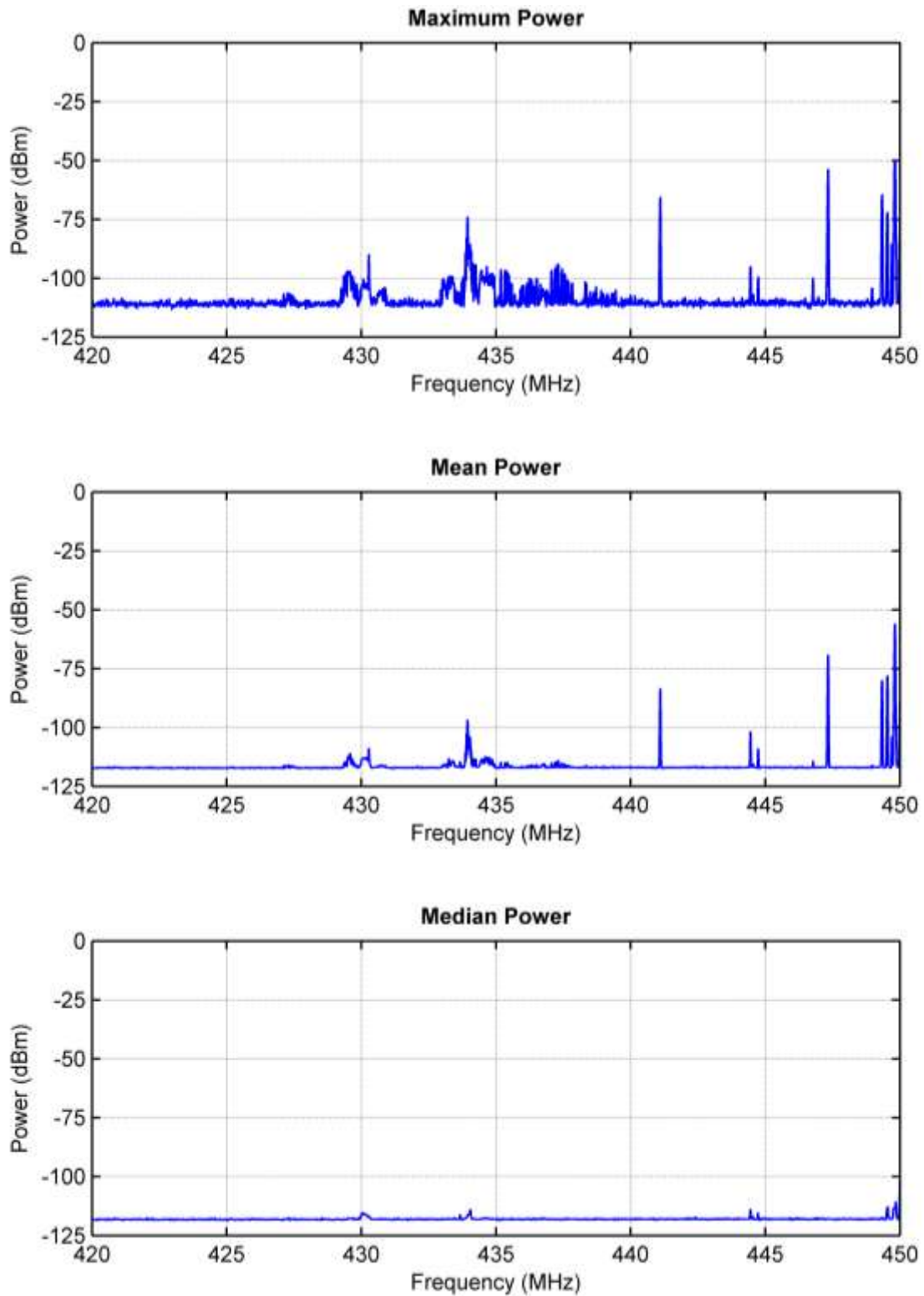


Figure A-31. Maximum, mean, and median received signal power at the Denver residential location for Event 8 (420–450 MHz, RBW = 10 kHz, 100 sweeps, sweep time = 300 ms).

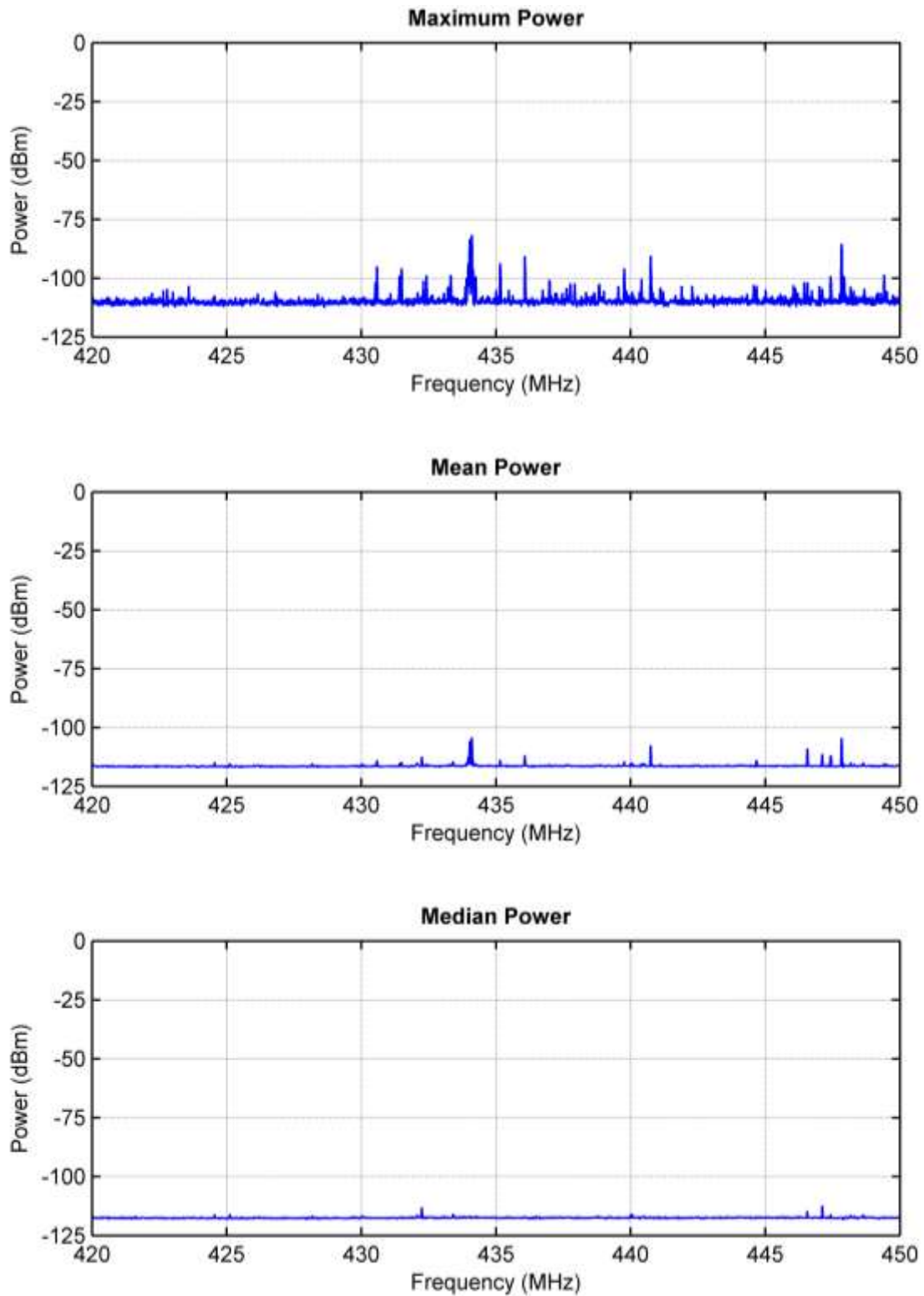


Figure A-32. Maximum, mean, and median received signal power at the Boulder business location for Event 8 (420–450 MHz, RBW = 10 kHz, 100 sweeps, sweep time = 300 ms).

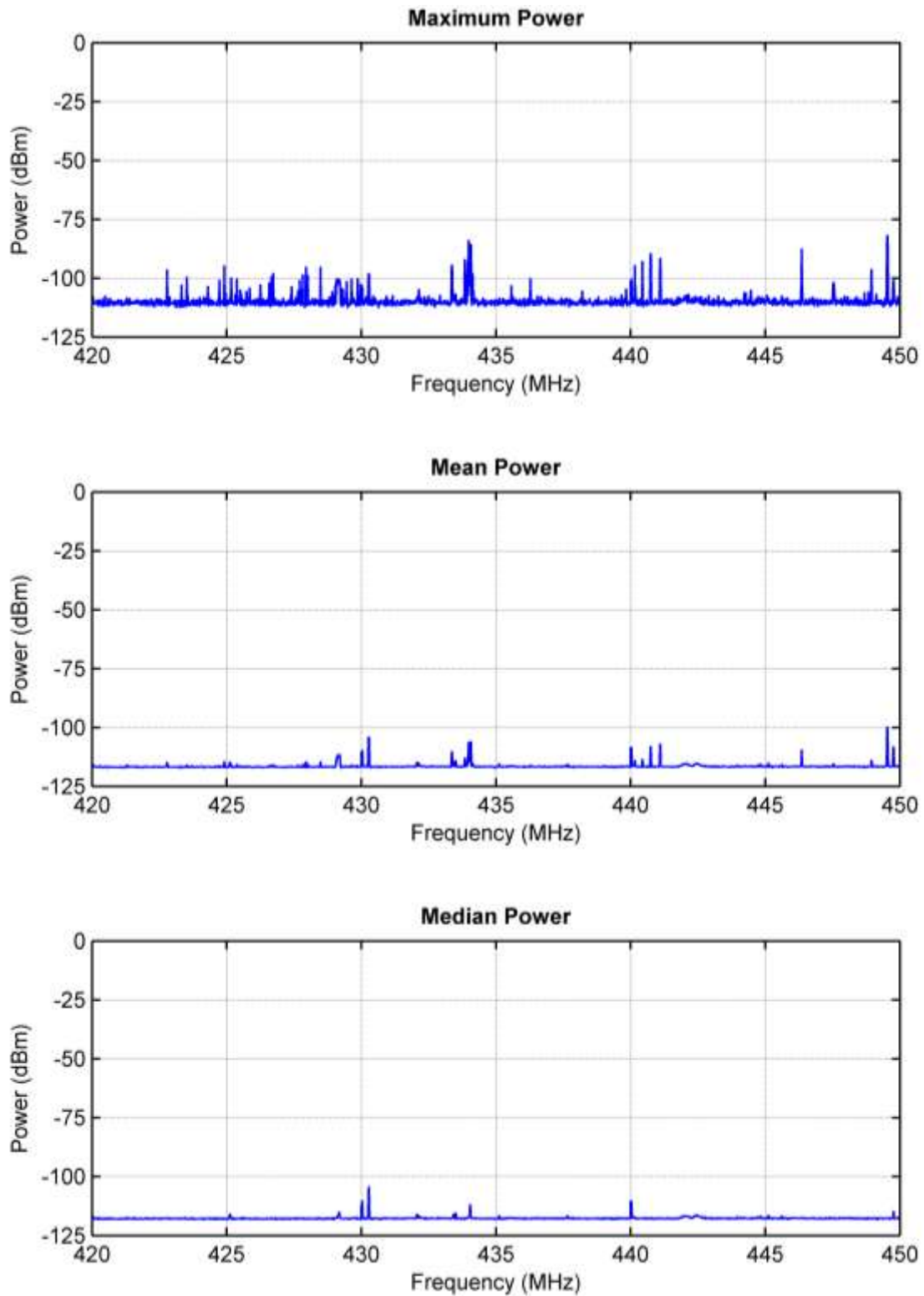


Figure A-33. Maximum, mean, and median received signal power at the Denver business location for Event 8 (420–450 MHz, RBW = 10 kHz, 100 sweeps, sweep time = 300 ms).

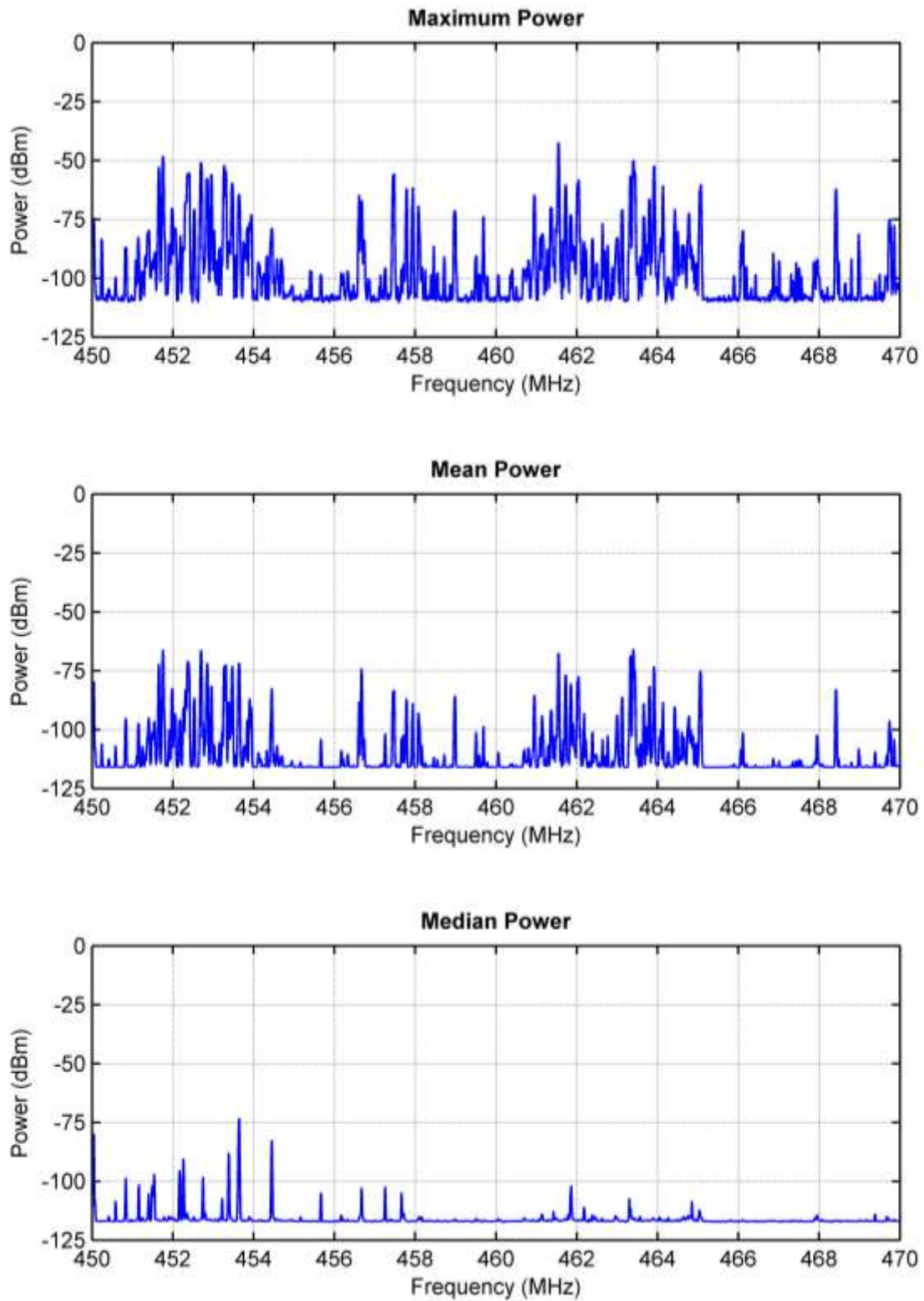


Figure A-34. Maximum, mean, and median received signal power at the Boulder residential location for Event 9 (450–470 MHz, RBW = 10 kHz, 200 sweeps, sweep time = 300 ms).

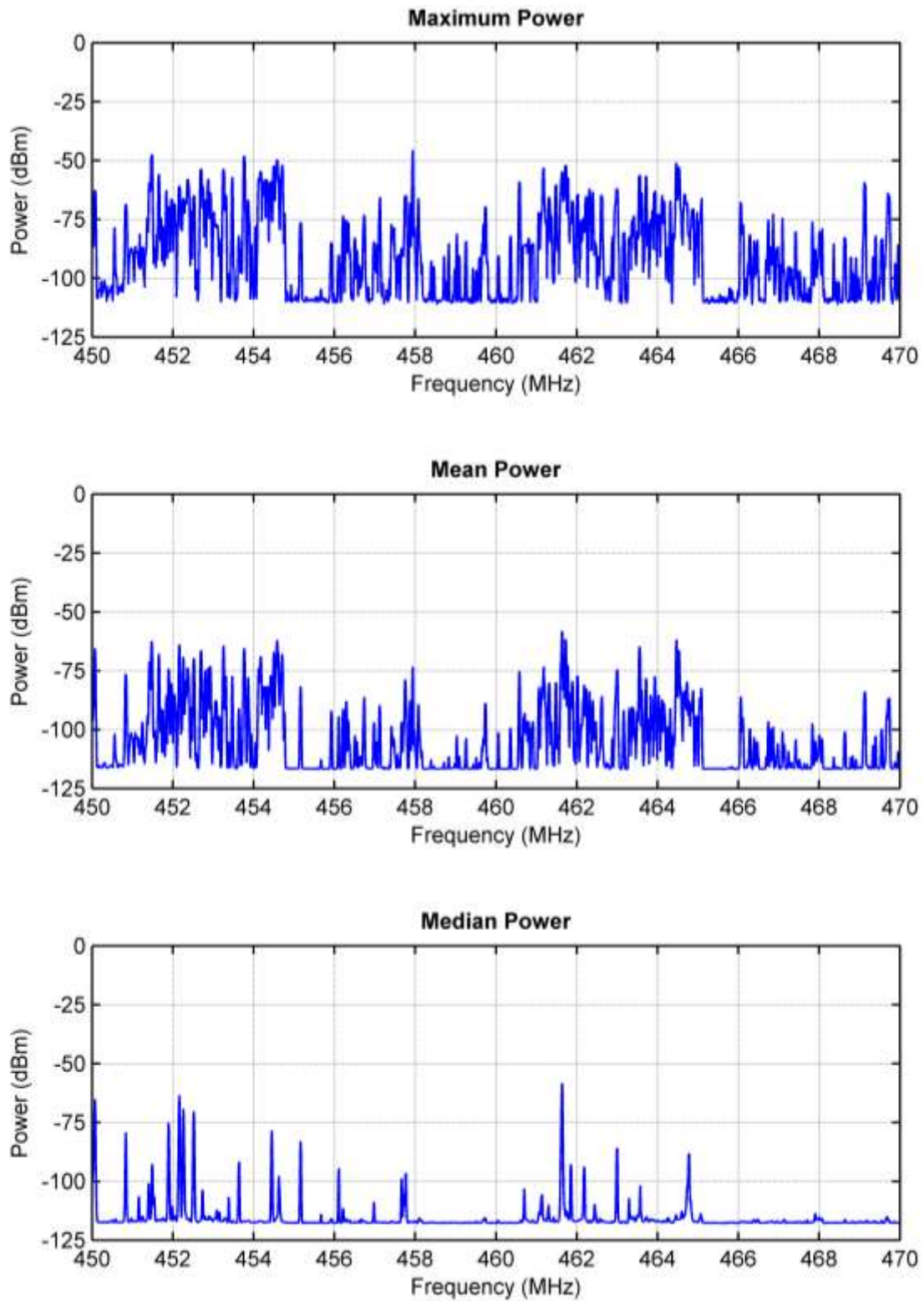


Figure A-35. Maximum, mean, and median received signal power at the Denver residential location for Event 9 (450–470 MHz, RBW = 10 kHz, 200 sweeps, sweep time = 300 ms).

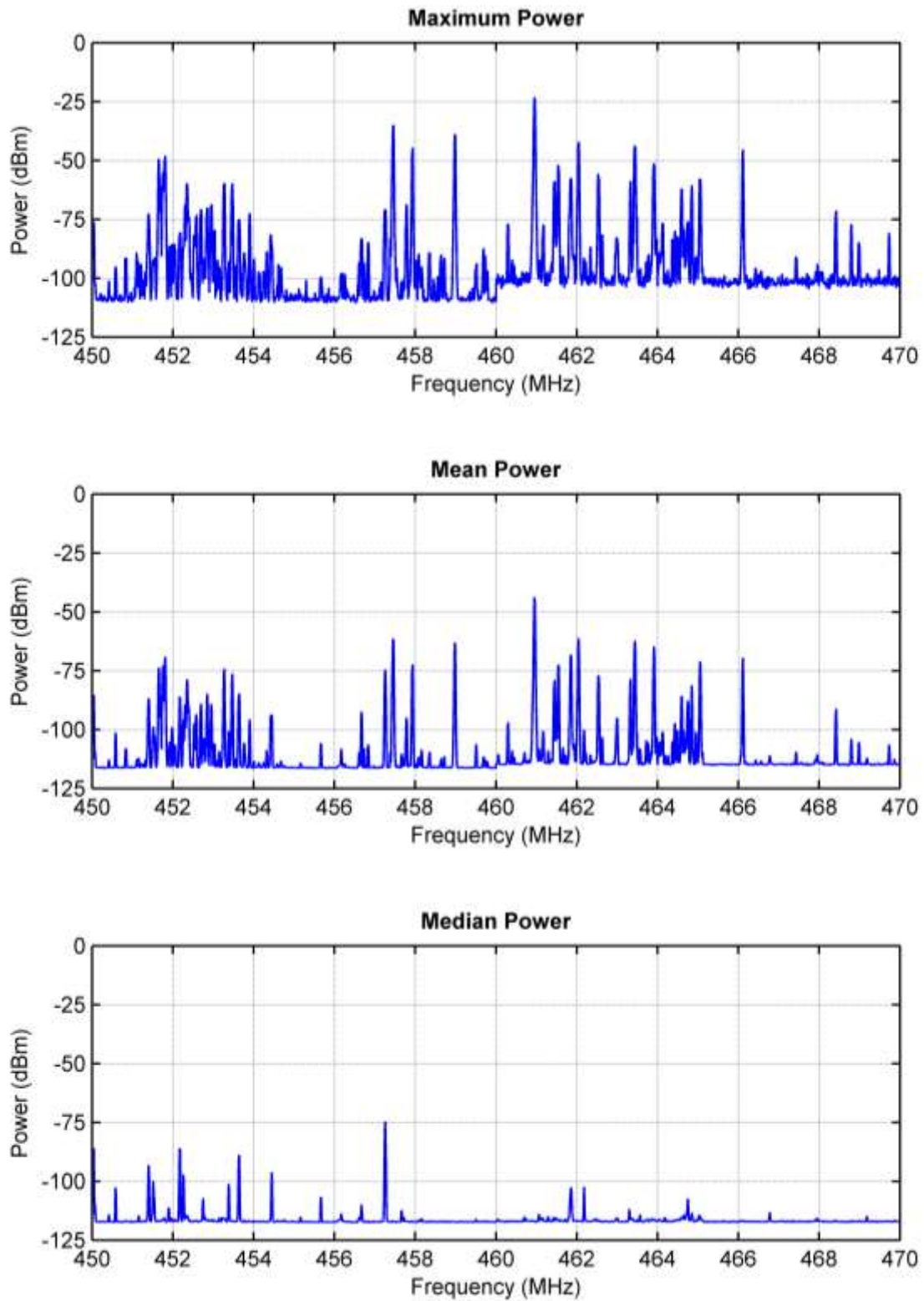


Figure A-36. Maximum, mean, and median received signal power at the Boulder business location for Event 9 (450–470 MHz, RBW = 10 kHz, 200 sweeps, sweep time = 300 ms).

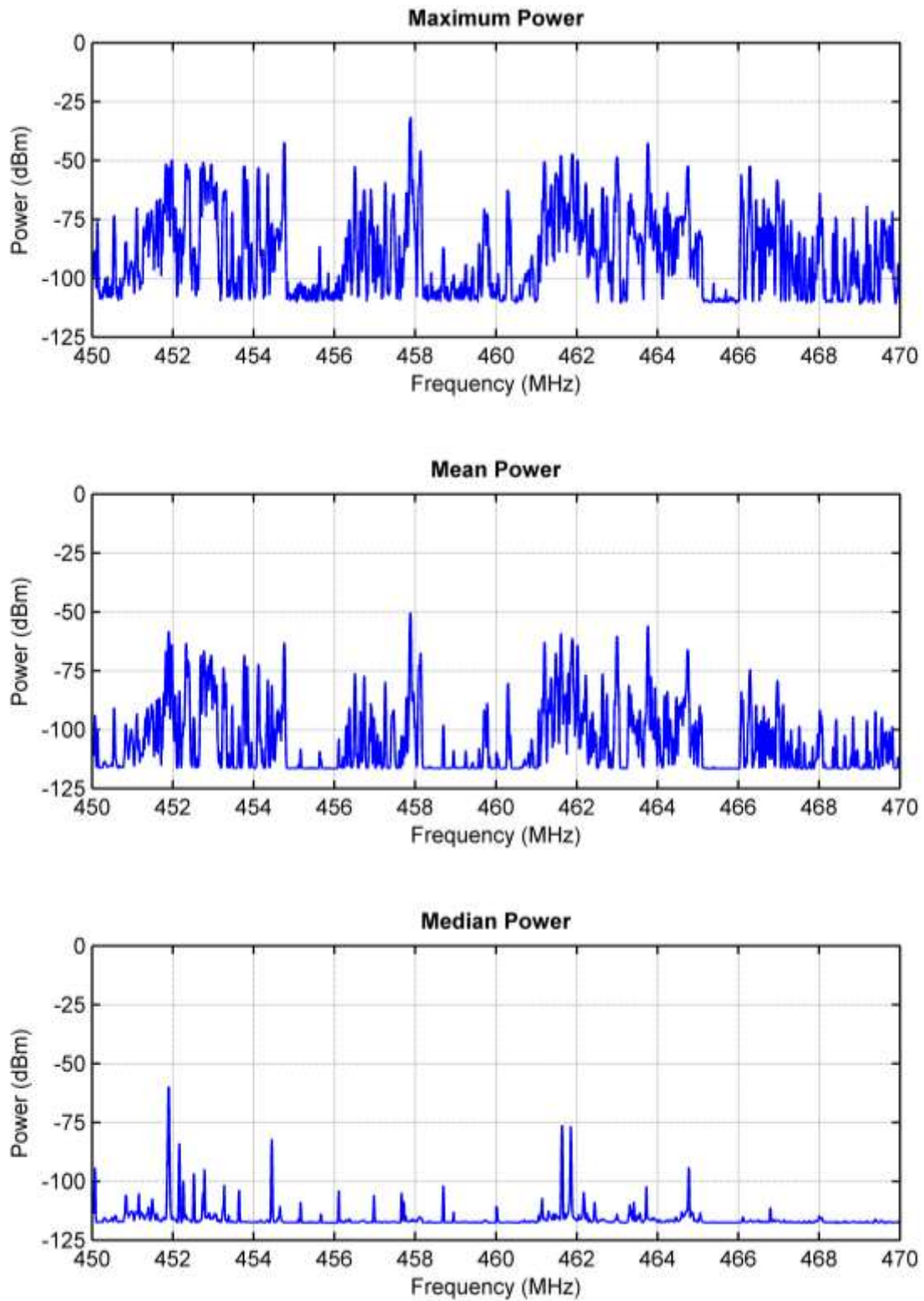


Figure A-37. Maximum, mean, and median received signal power at the Denver business location for Event 9 (450–470 MHz, RBW = 10 kHz, 200 sweeps, sweep time = 300 ms).

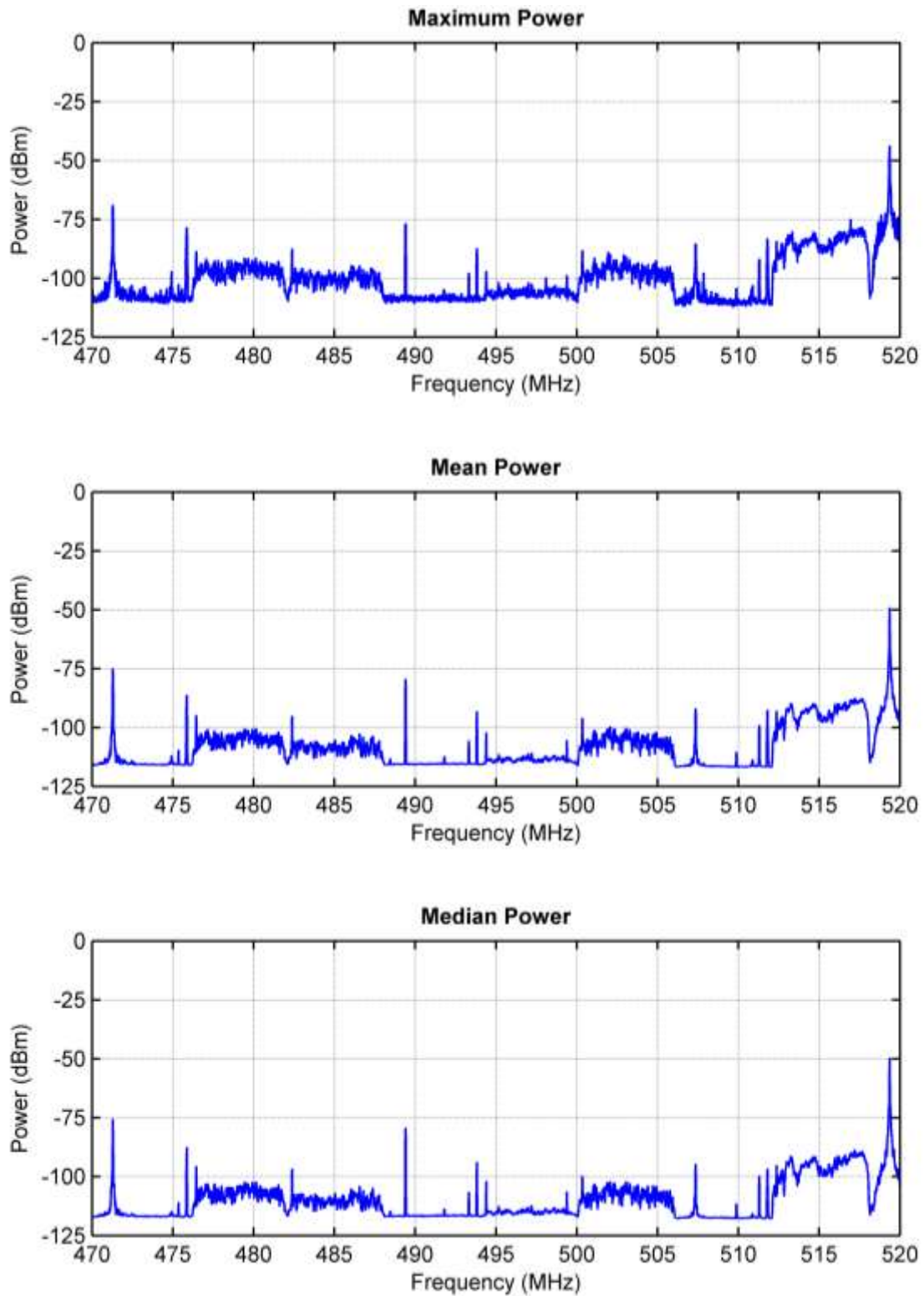


Figure A-38. Maximum, mean, and median received signal power at the Boulder residential location for Event 10 (470–520 MHz, RBW = 10 kHz, 100 sweeps, sweep time = 300 ms).

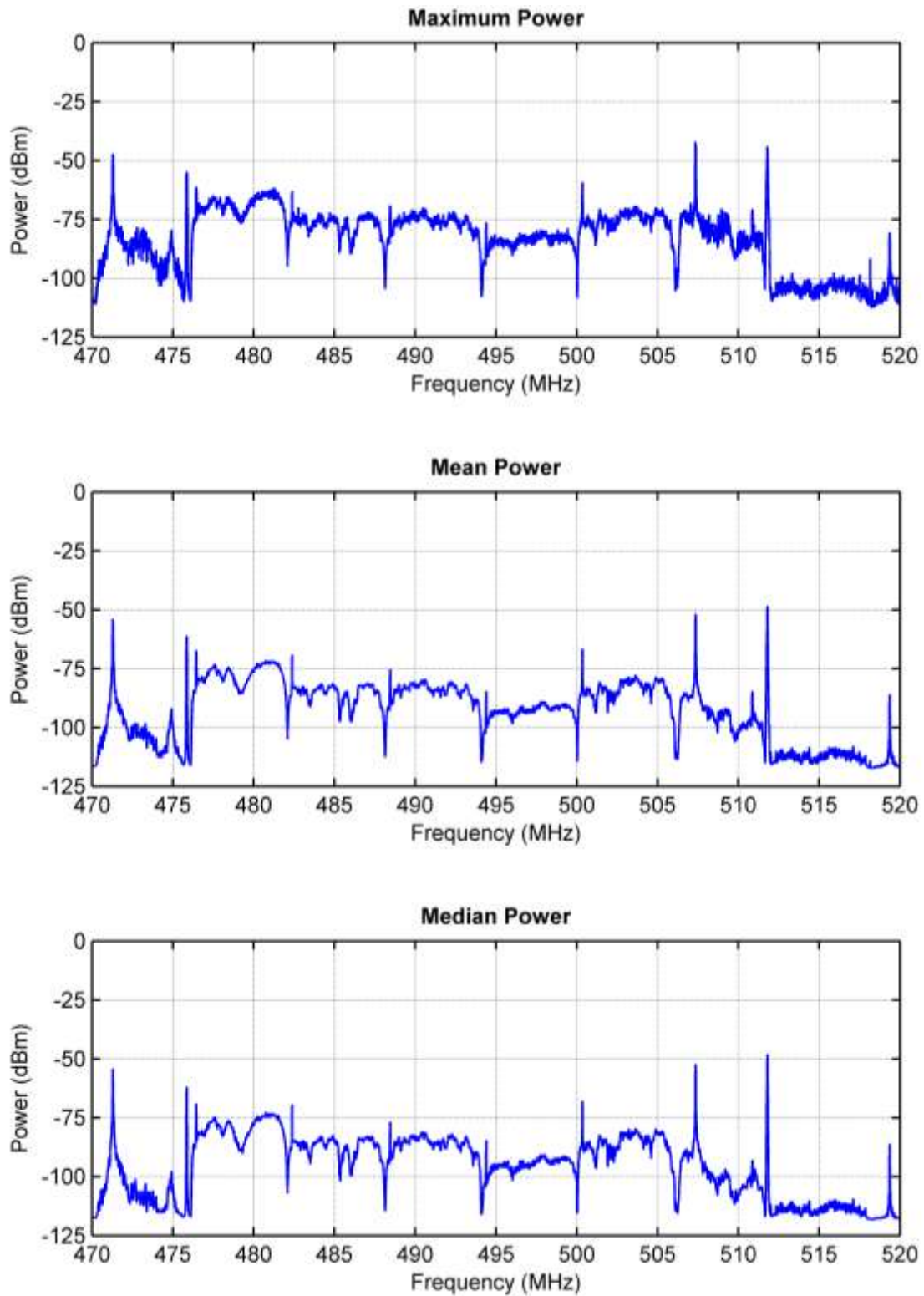


Figure A-39. Maximum, mean, and median received signal power at the Denver residential location for Event 10 (470–520 MHz, RBW = 10 kHz, 100 sweeps, sweep time = 300 ms).

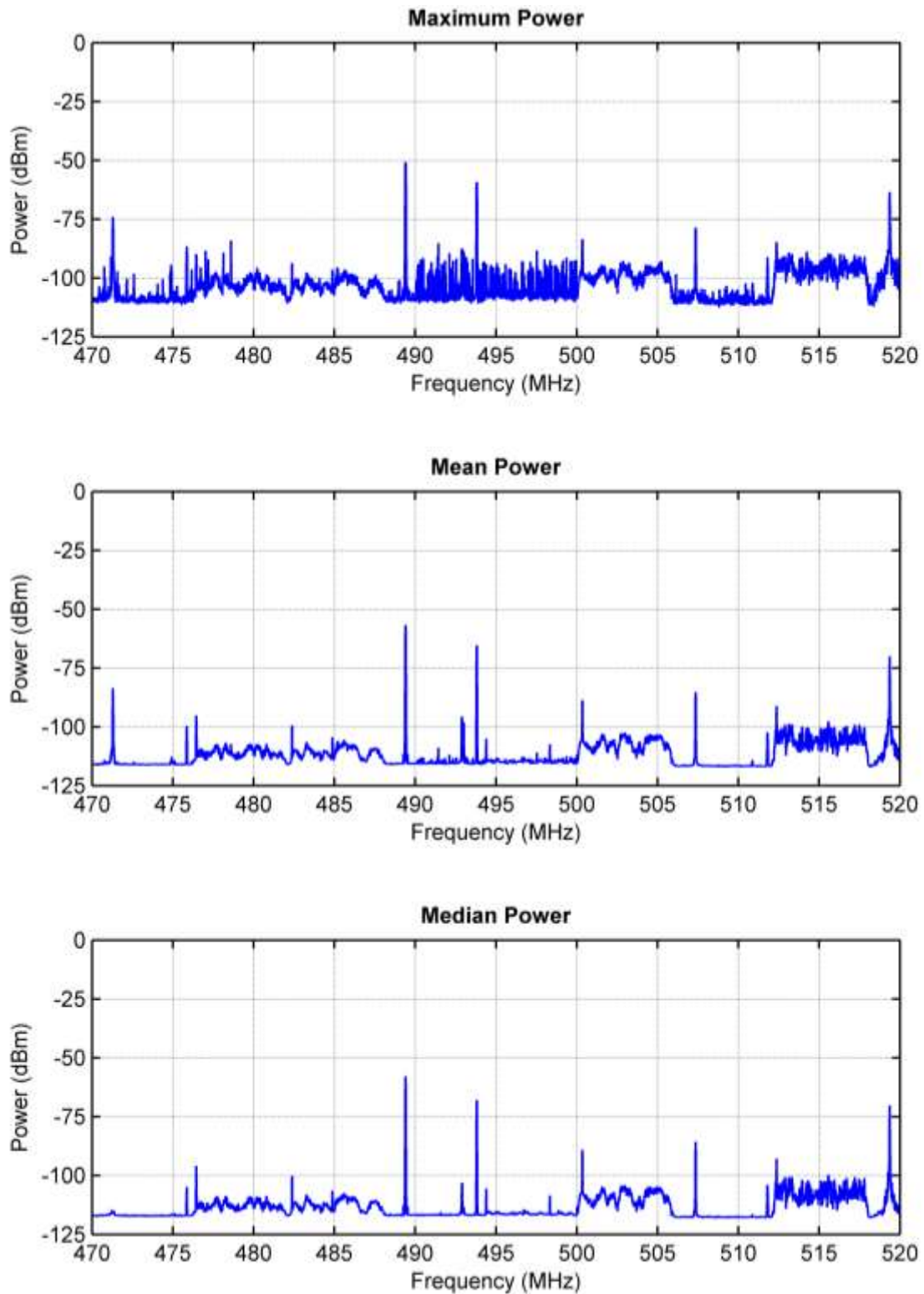


Figure A-40. Maximum, mean, and median received signal power at the Boulder business location for Event 10 (470–520 MHz, RBW = 10 kHz, 100 sweeps, sweep time = 300 ms).

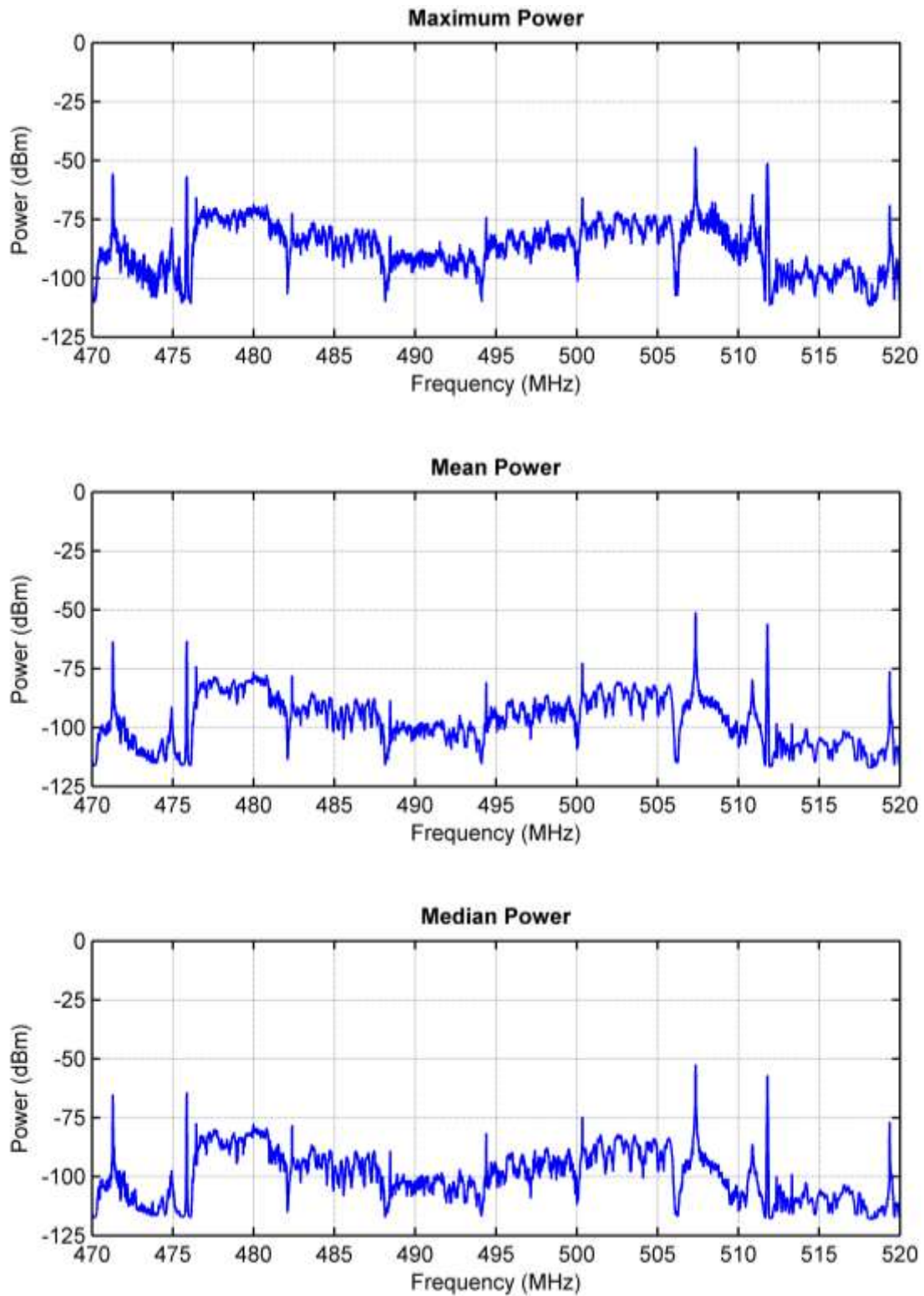


Figure A-41. Maximum, mean, and median received signal power at the Denver business location for Event 10 (470–520 MHz, RBW = 10 kHz, 100 sweeps, sweep time = 300 ms).

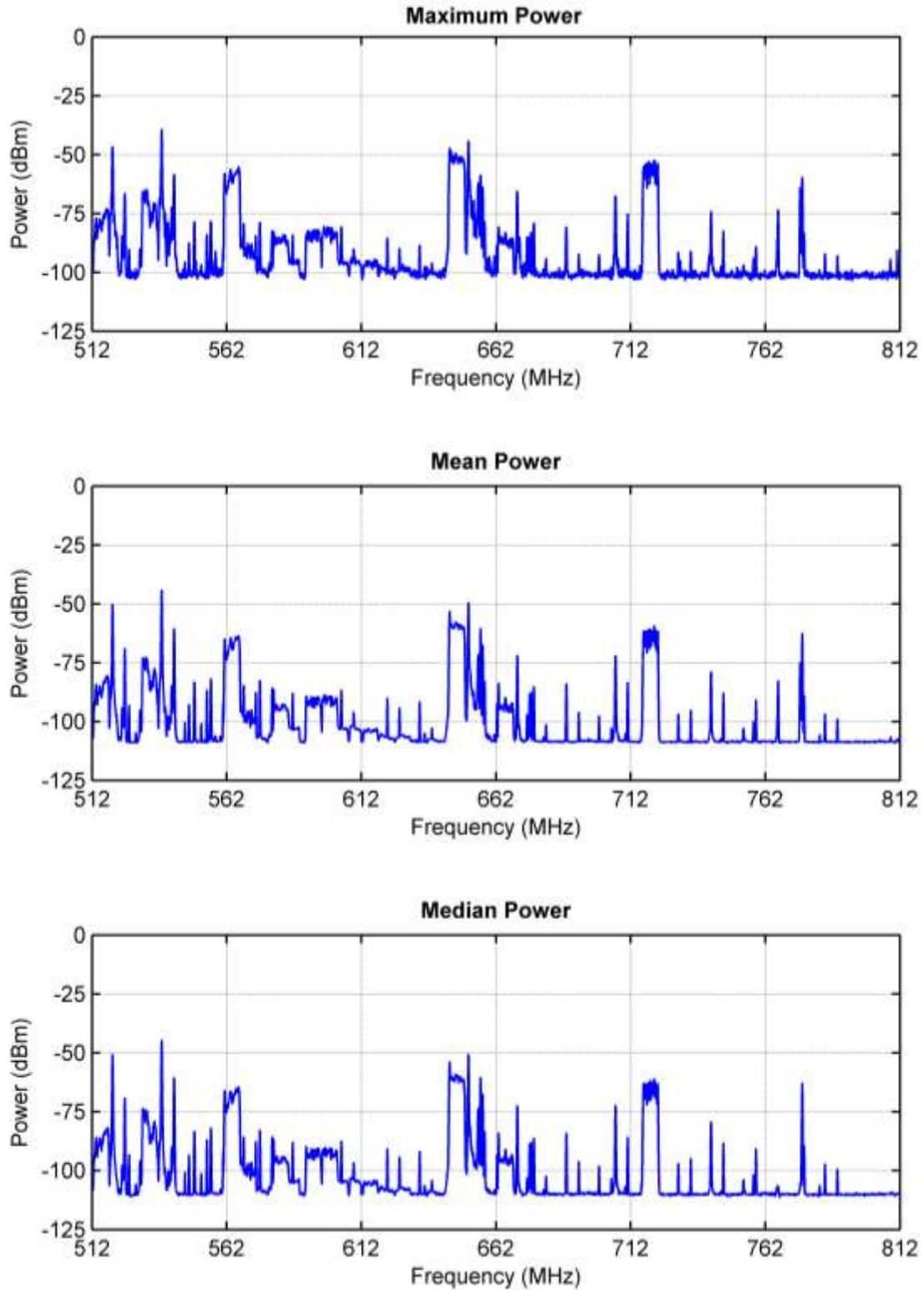


Figure A-42. Maximum, mean, and median received signal power at the Boulder residential location for Event 11 (512–812 MHz, RBW = 100 kHz, 200 sweeps, sweep time = 100 ms).

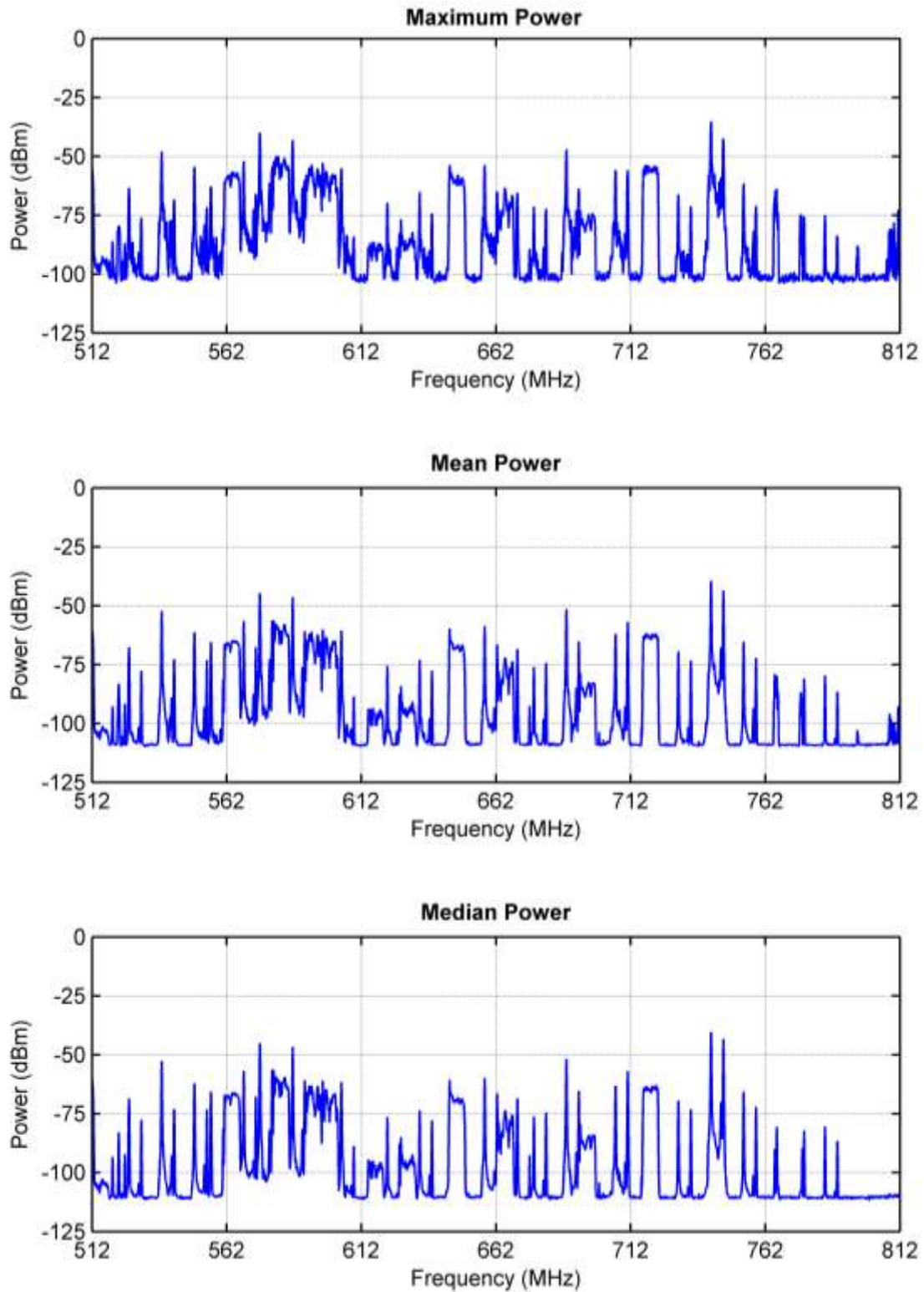


Figure A-43. Maximum, mean, and median received signal power at the Denver residential location for Event 11 (512–812 MHz, RBW = 100 kHz, 200 sweeps, sweep time = 100 ms).

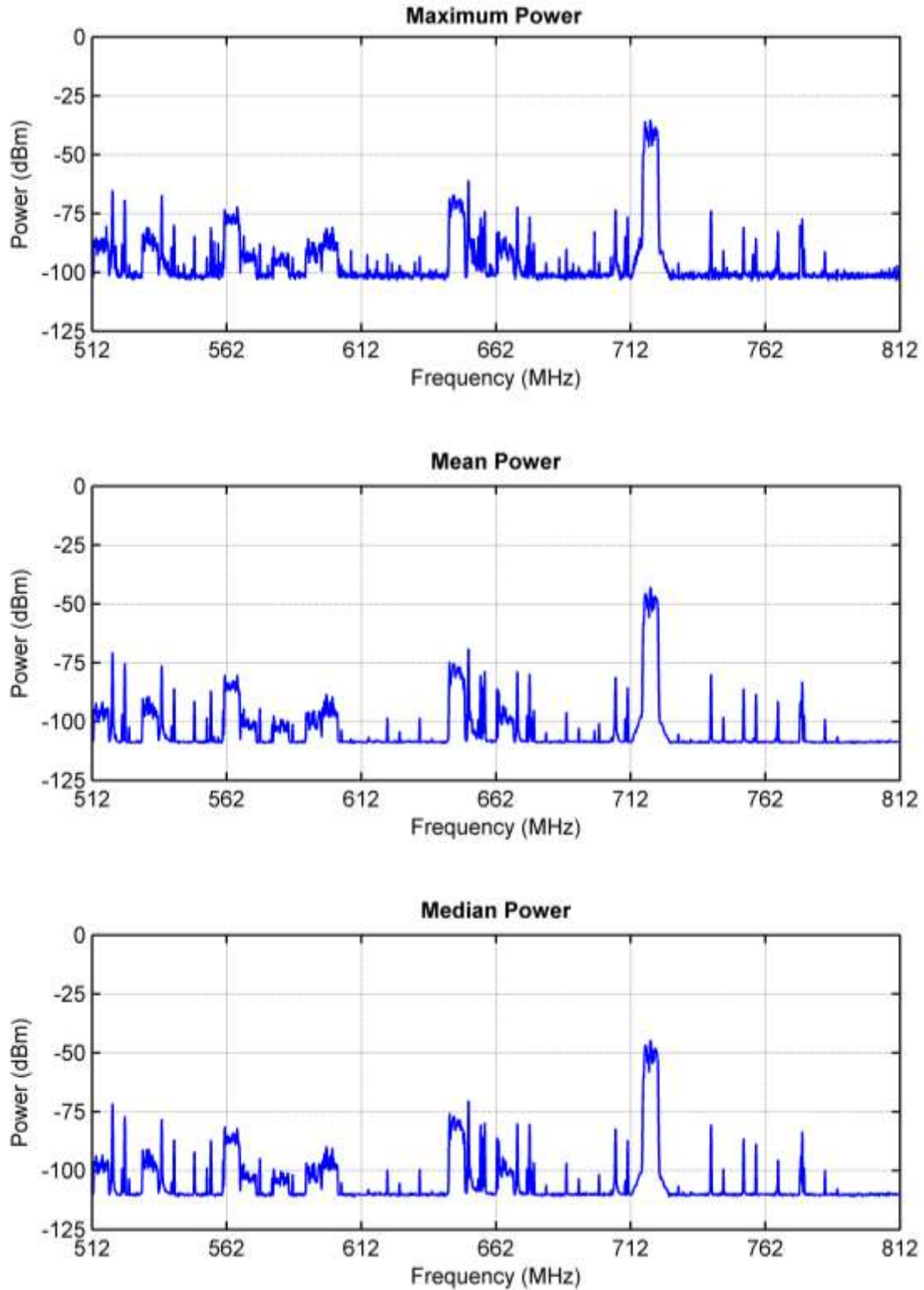


Figure A-44. Maximum, mean, and median received signal power at the Boulder business location for Event 11 (512–812 MHz, RBW = 100 kHz, 200 sweeps, sweep time = 100 ms).

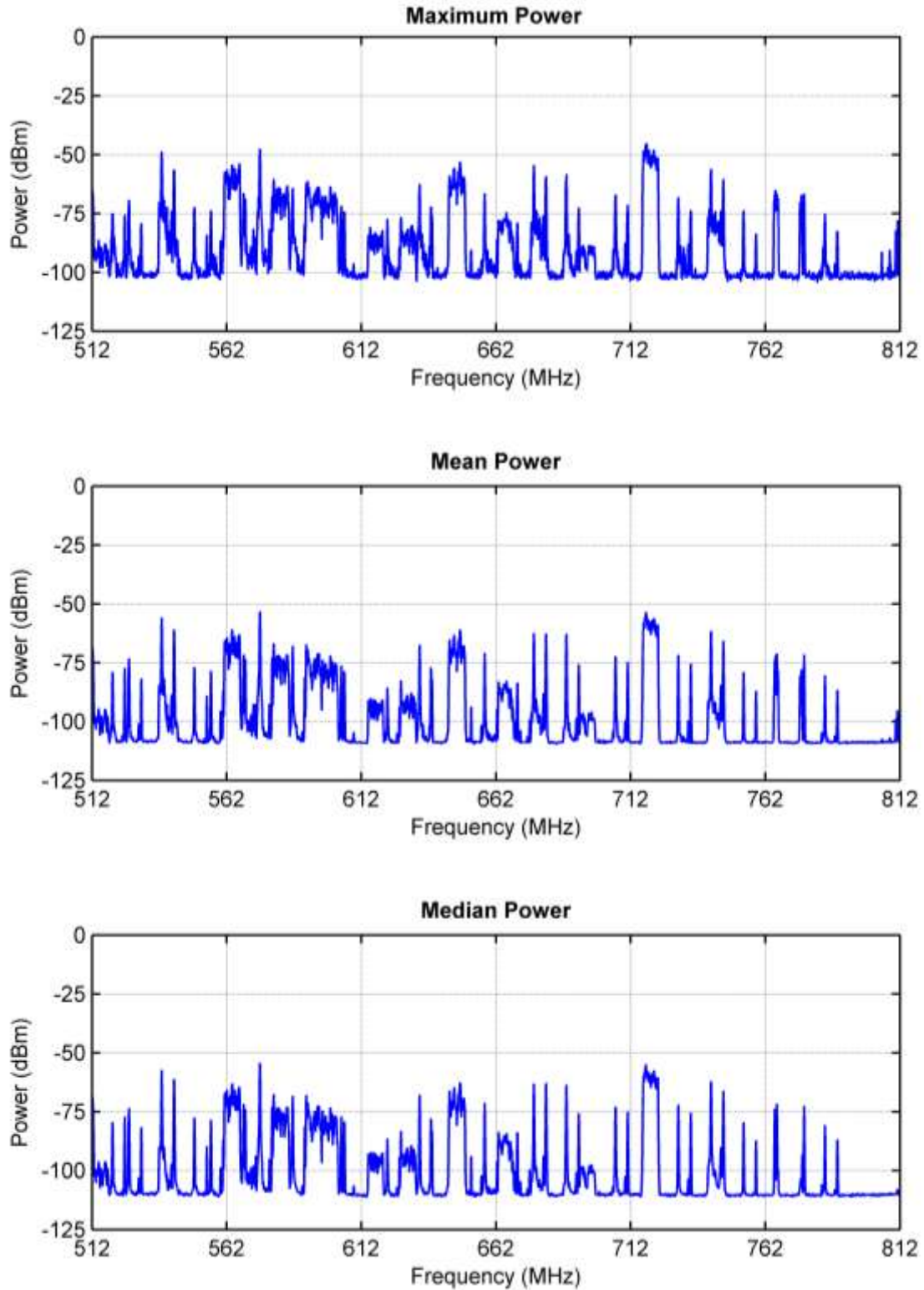


Figure A-45. Maximum, mean, and median received signal power at the Denver business location for Event 11 (512–812 MHz, RBW = 100 kHz, 200 sweeps, sweep time = 100 ms).

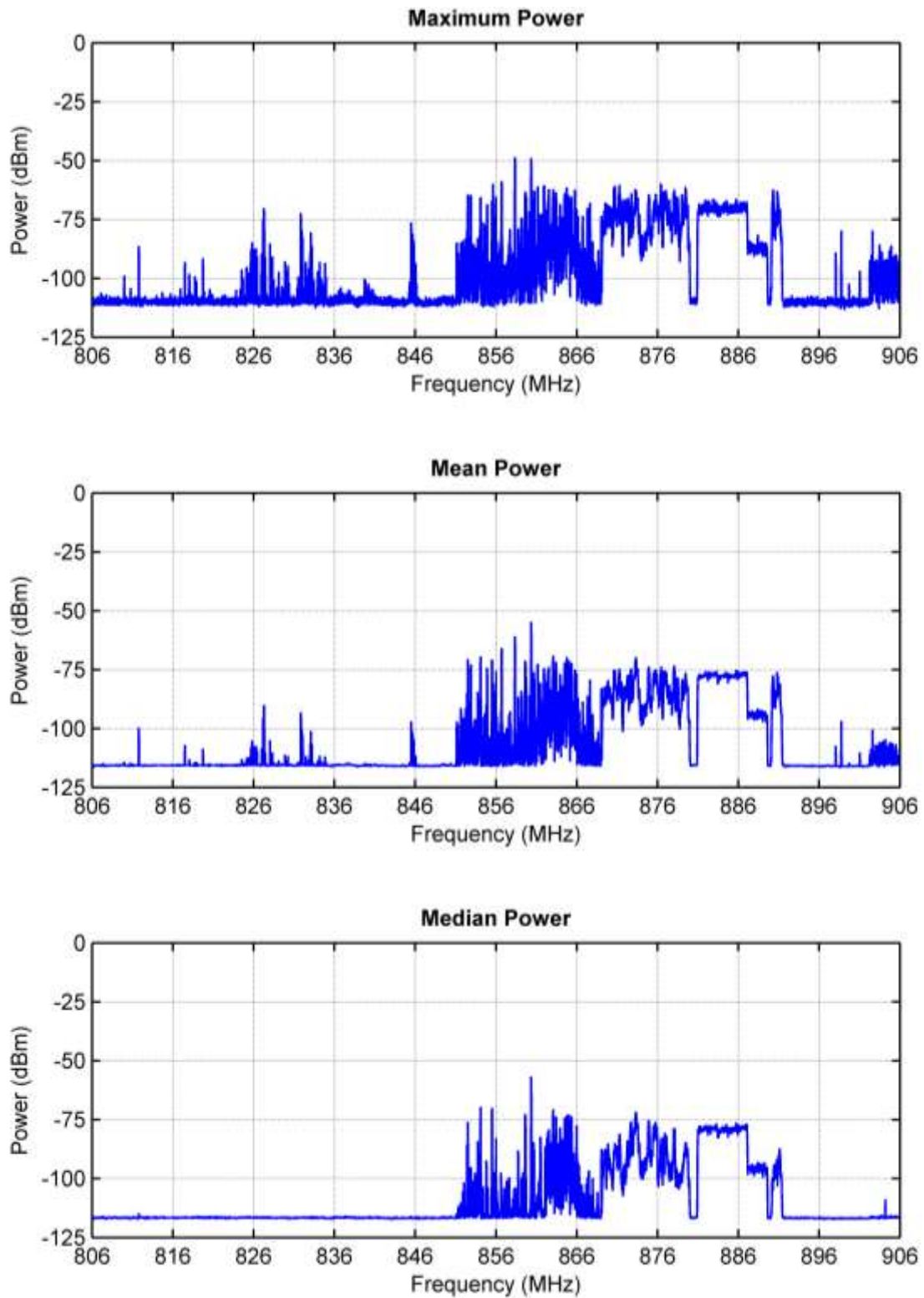


Figure A-46. Maximum, mean, and median received signal power at the Boulder residential location for Event 12 (806–906 MHz, RBW = 10 kHz, 60 sweeps, sweep time = 300 ms).

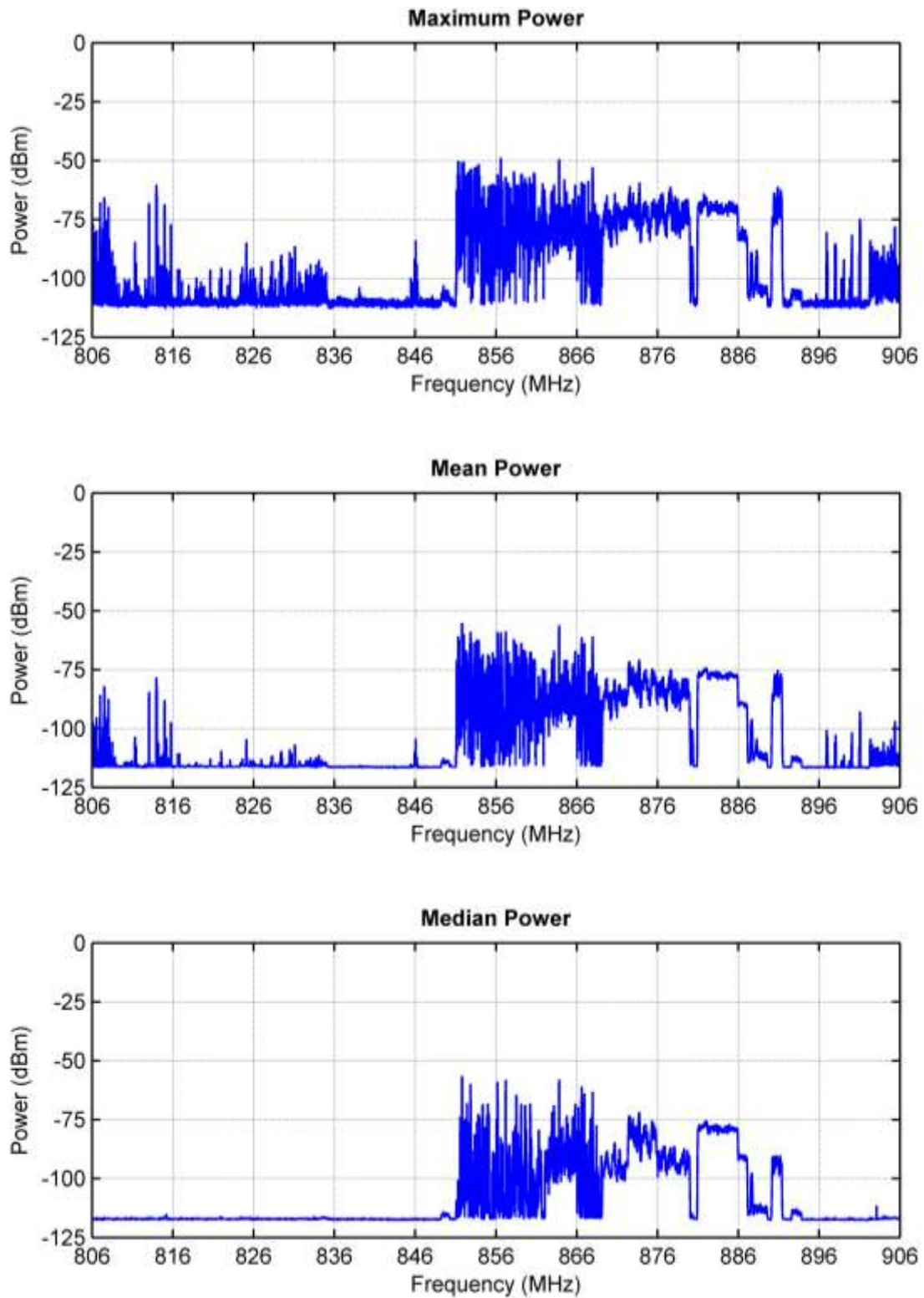


Figure A-47. Maximum, mean, and median received signal power at the Denver residential location for Event 12 (806–906 MHz, RBW = 10 kHz, 60 sweeps, sweep time = 300 ms).

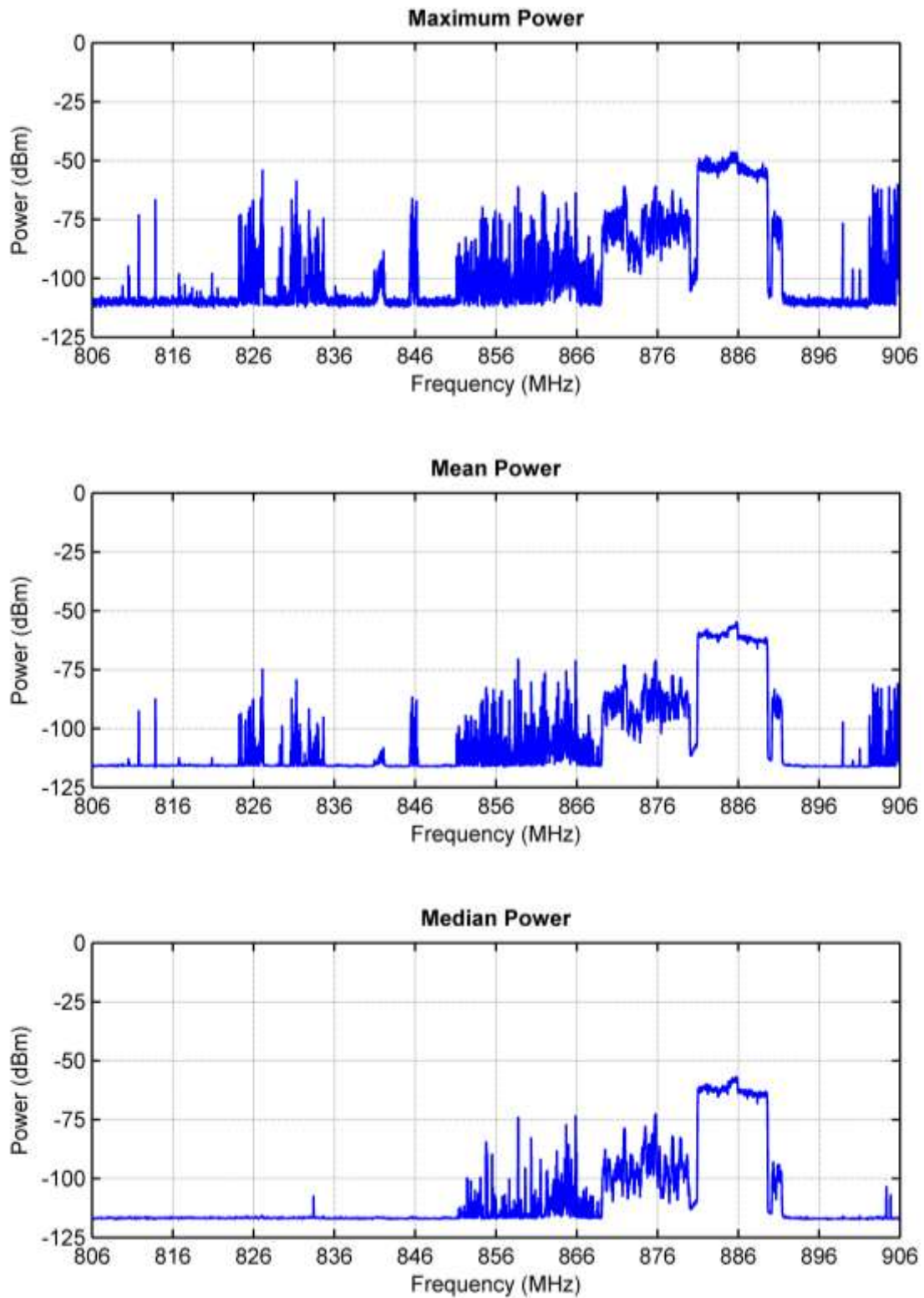


Figure A-48. Maximum, mean, and median received signal power at the Boulder business location for Event 12 (806–906 MHz, RBW = 10 kHz, 60 sweeps, sweep time = 300 ms).

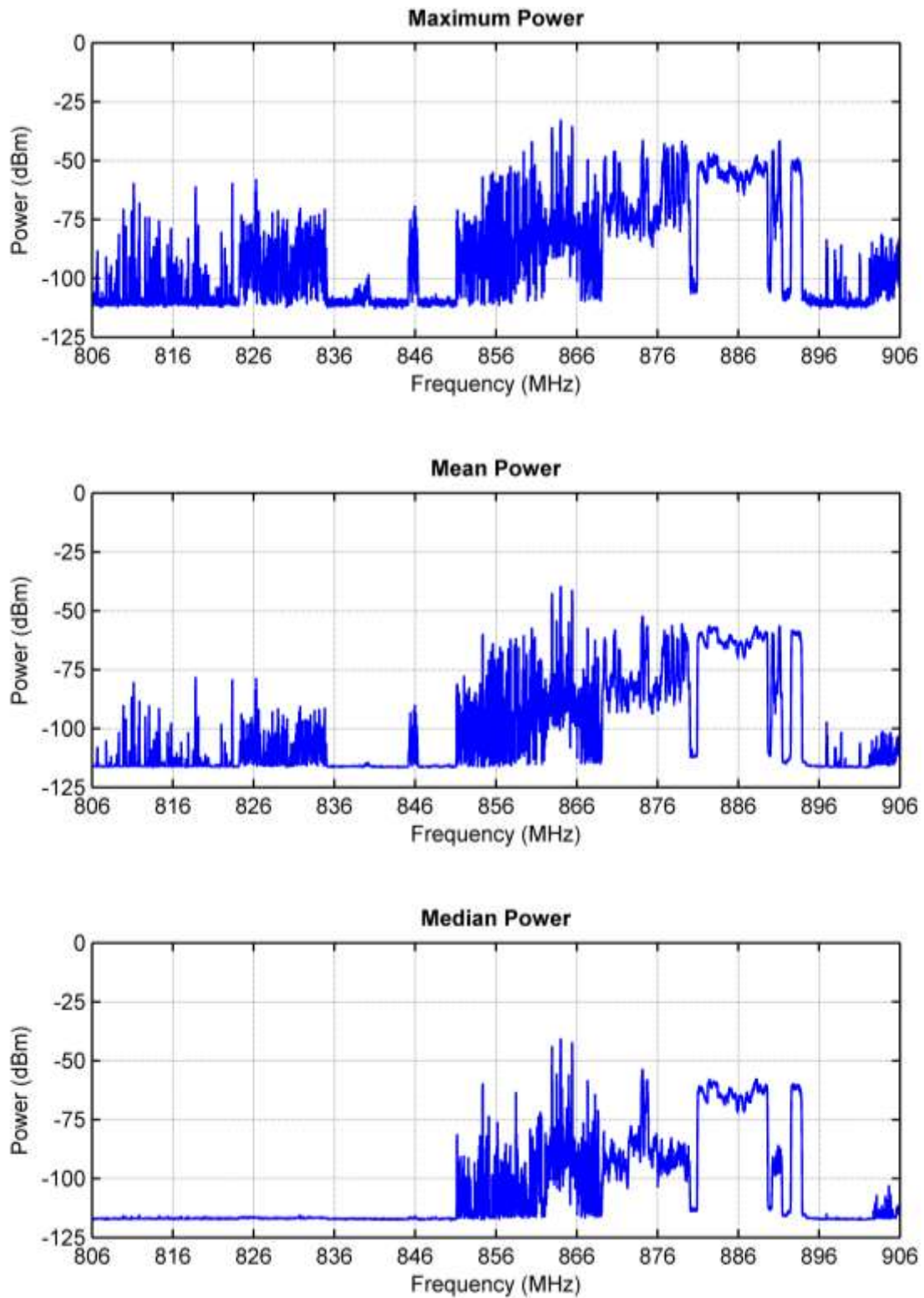


Figure A-49. Maximum, mean, and median received signal power at the Denver business location for Event 12 (806–906 MHz, RBW = 10 kHz, 60 sweeps, sweep time = 300 ms).

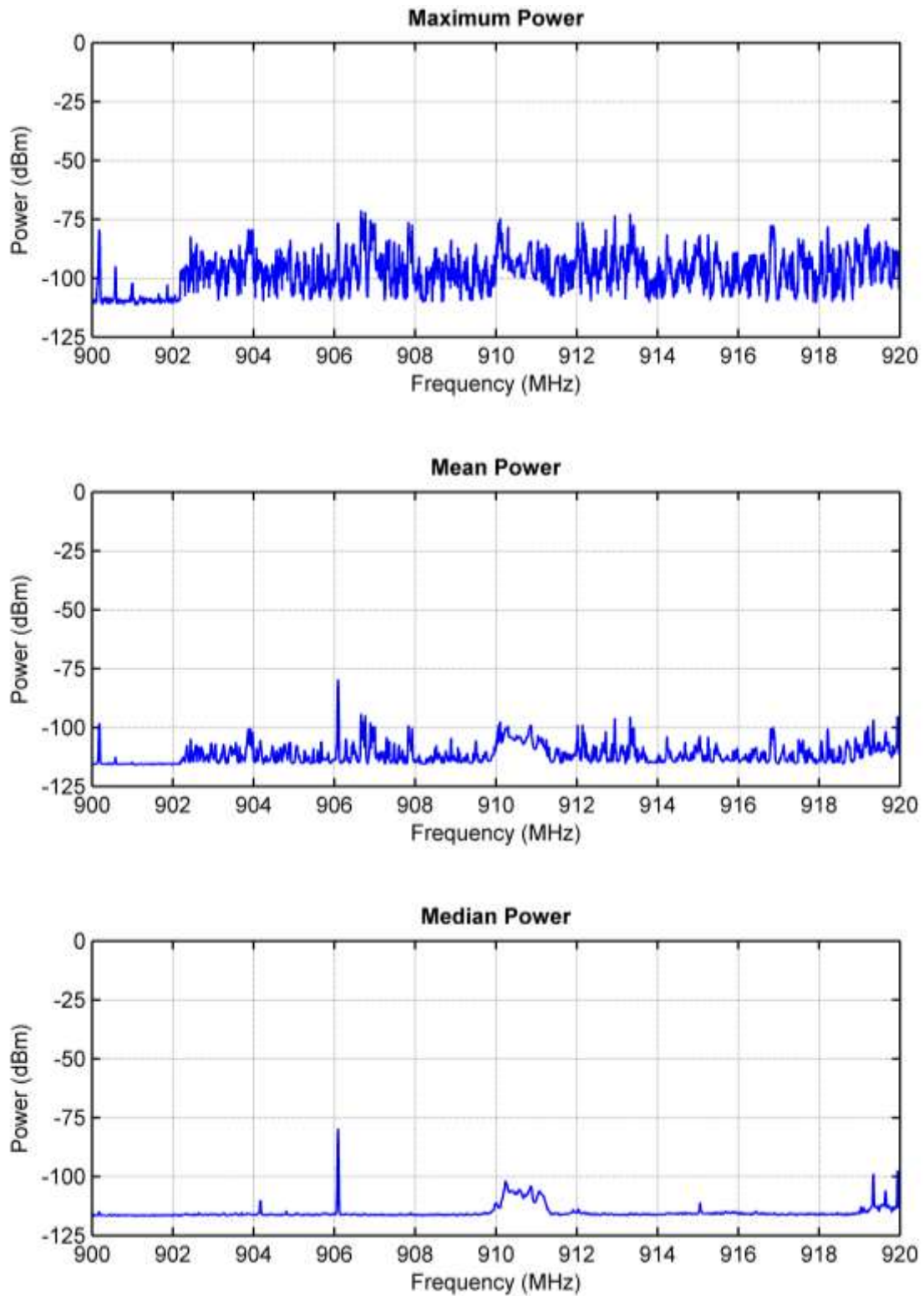


Figure A-50. Maximum, mean, and median received signal power at the Boulder residential location for Event 13 (900–920 MHz, RBW = 10 kHz, 100 sweeps, sweep time = 300 ms).

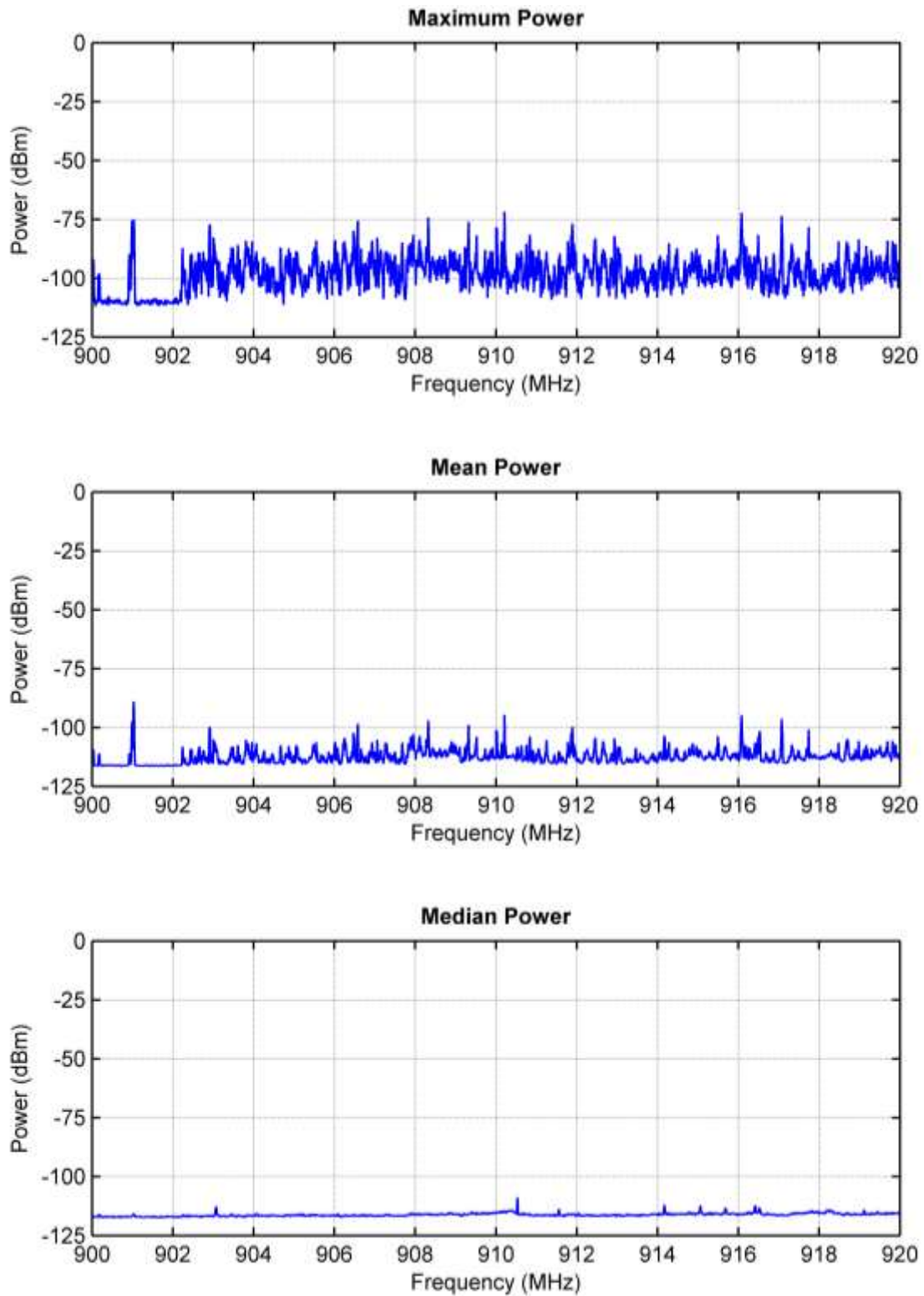


Figure A-51. Maximum, mean, and median received signal power at the Denver residential location for Event 13 (900–920 MHz, RBW = 10 kHz, 100 sweeps, sweep time = 300 ms).

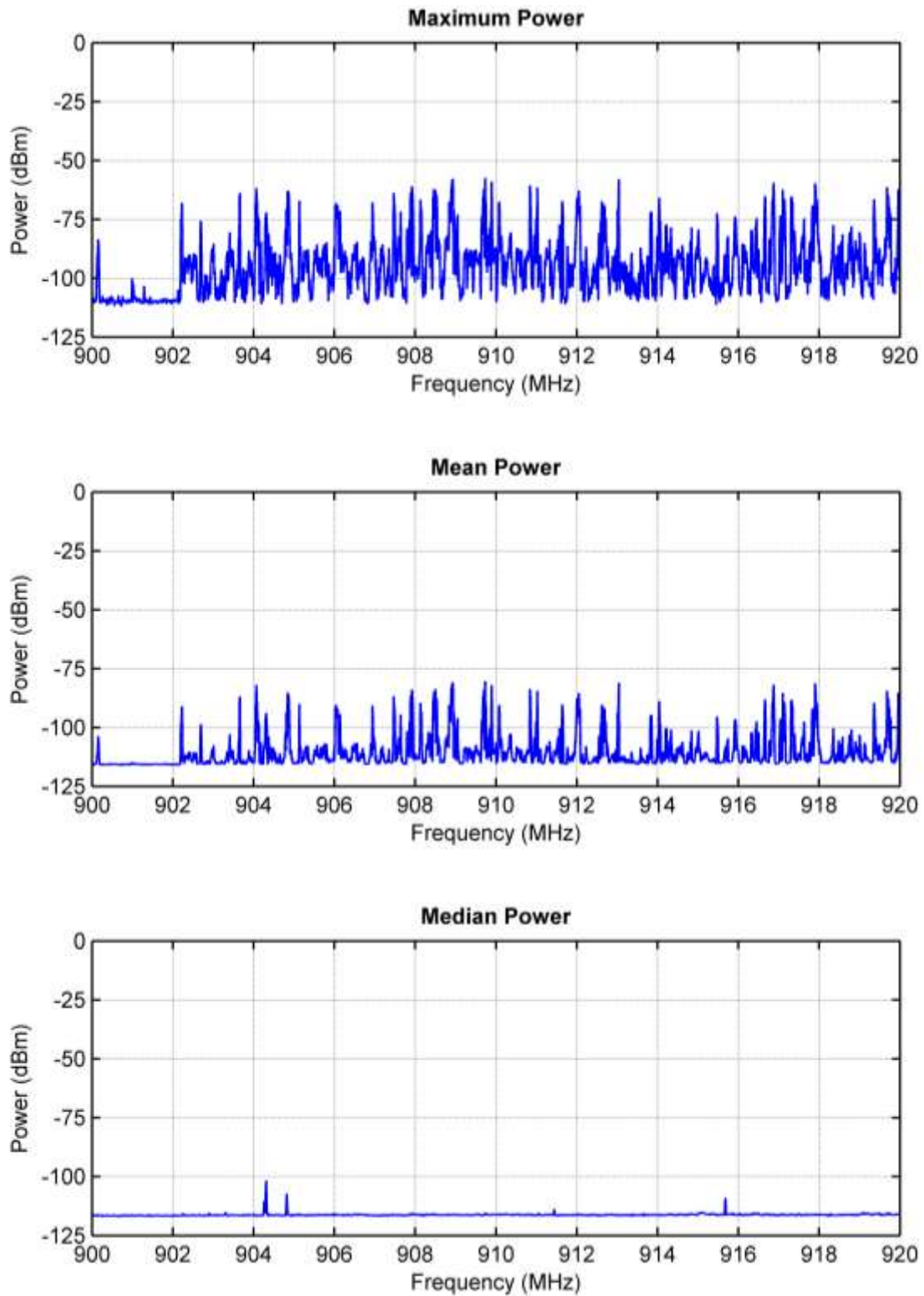


Figure A-52. Maximum, mean, and median received signal power at the Boulder business location for Event 13 (900–920 MHz, RBW = 10 kHz, 100 sweeps, sweep time = 300 ms).

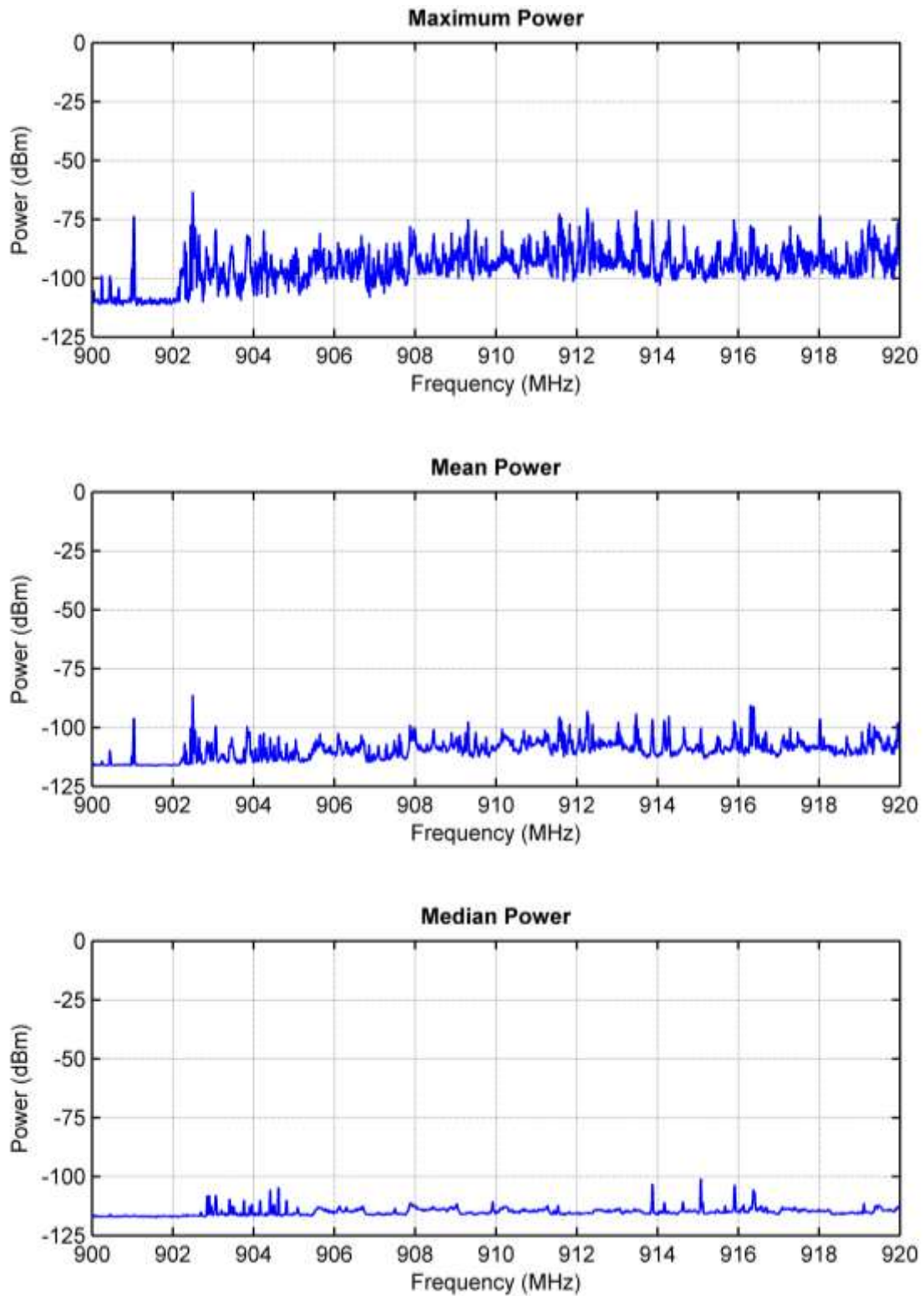


Figure A-53. Maximum, mean, and median received signal power at the Denver business location for Event 13 (900–920 MHz, RBW = 10 kHz, 100 sweeps, sweep time = 300 ms).

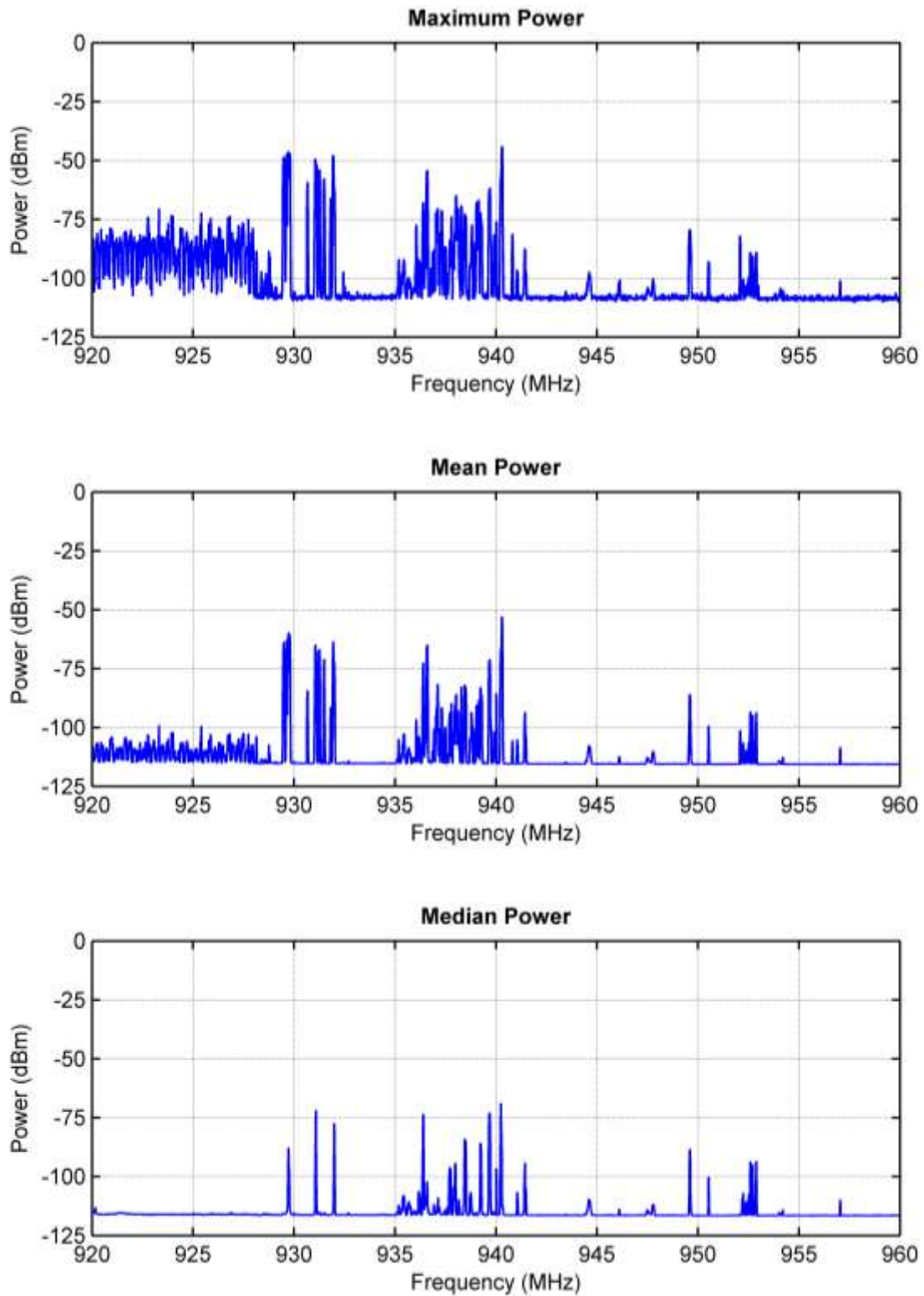


Figure A-54. Maximum, mean, and median received signal power at the Boulder residential location for Event 14 (920–960 MHz, RBW = 10 kHz, 300 sweeps, sweep time = 300 ms).

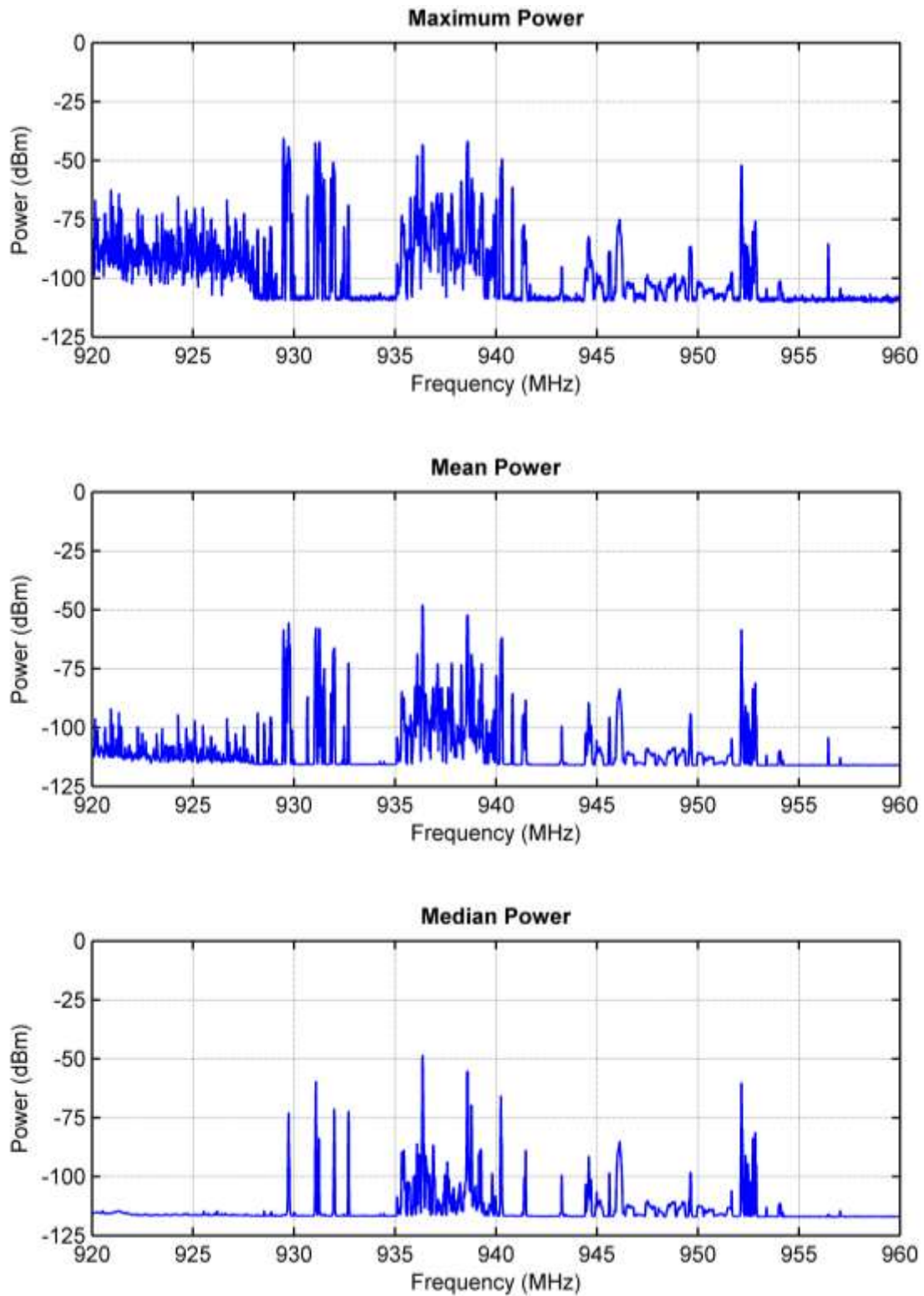


Figure A-55. Maximum, mean, and median received signal power at the Denver residential location for Event 14 (920–960 MHz, RBW = 10 kHz, 300 sweeps, sweep time = 300 ms).

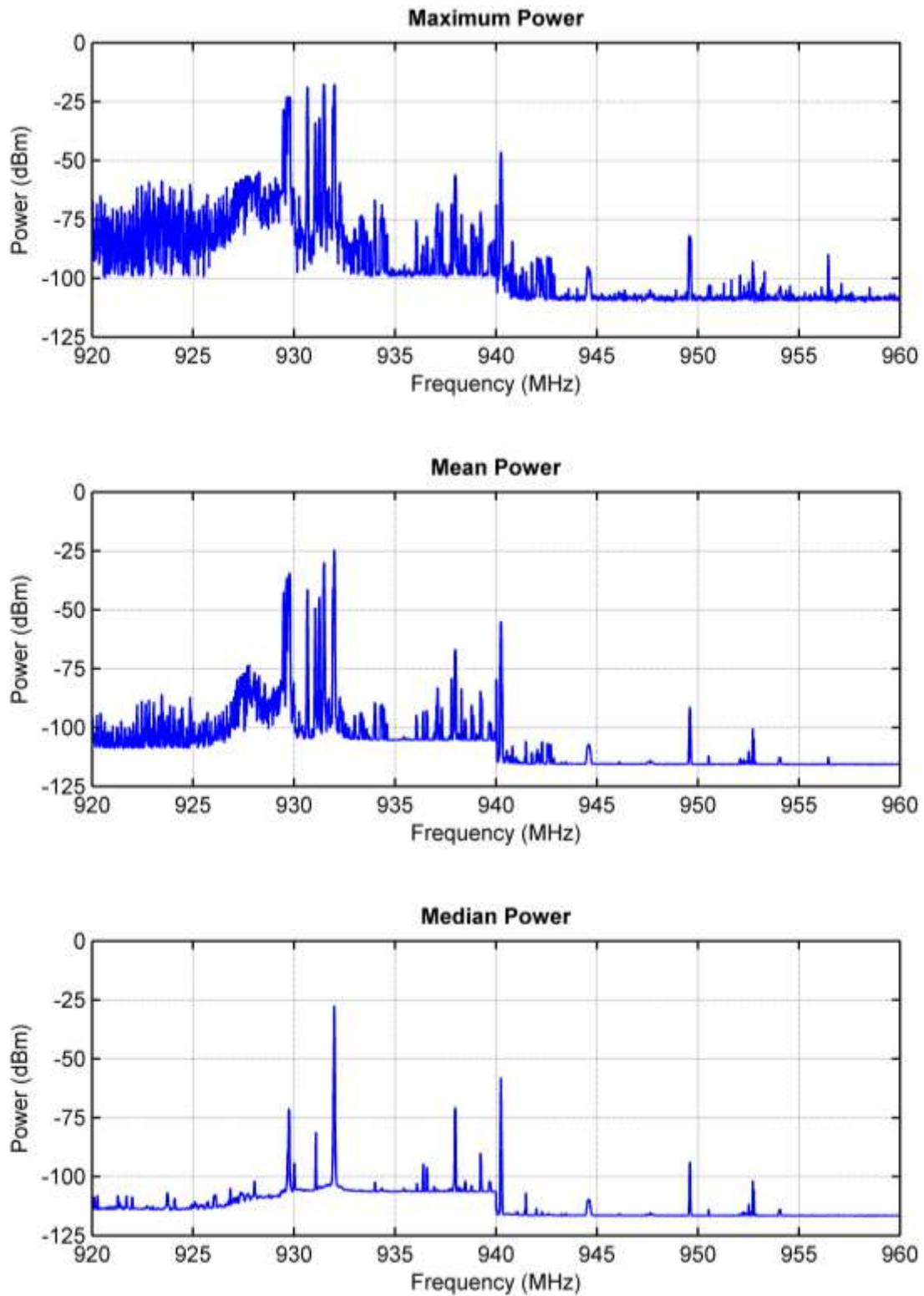


Figure A-56. Maximum, mean, and median received signal power at the Boulder business location for Event 14 (920–960 MHz, RBW = 10 kHz, 300 sweeps, sweep time = 300 ms).

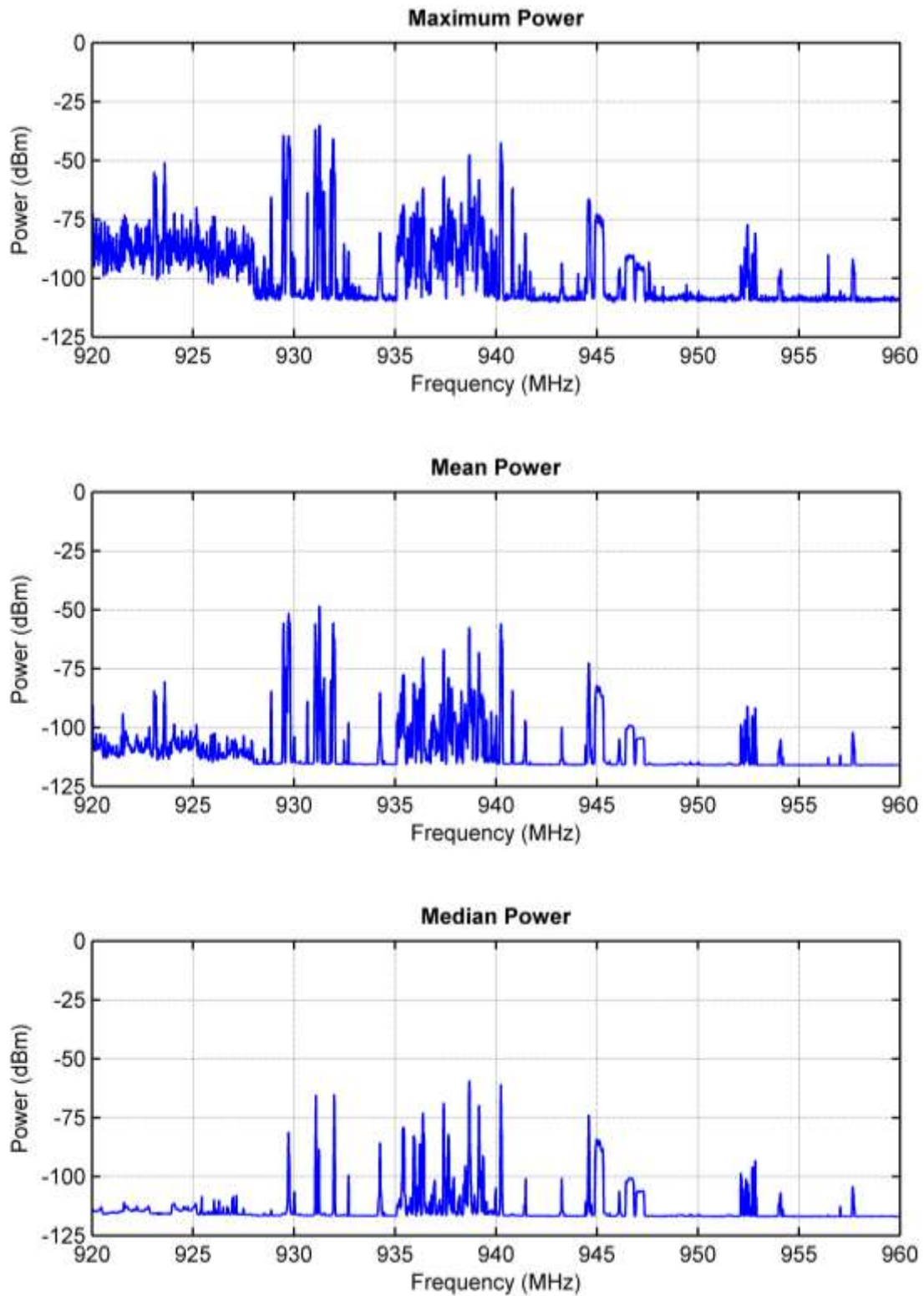


Figure A-57. Maximum, mean, and median received signal power at the Denver business location for Event 14 (920–960 MHz, RBW = 10 kHz, 300 sweeps, sweep time = 300 ms).

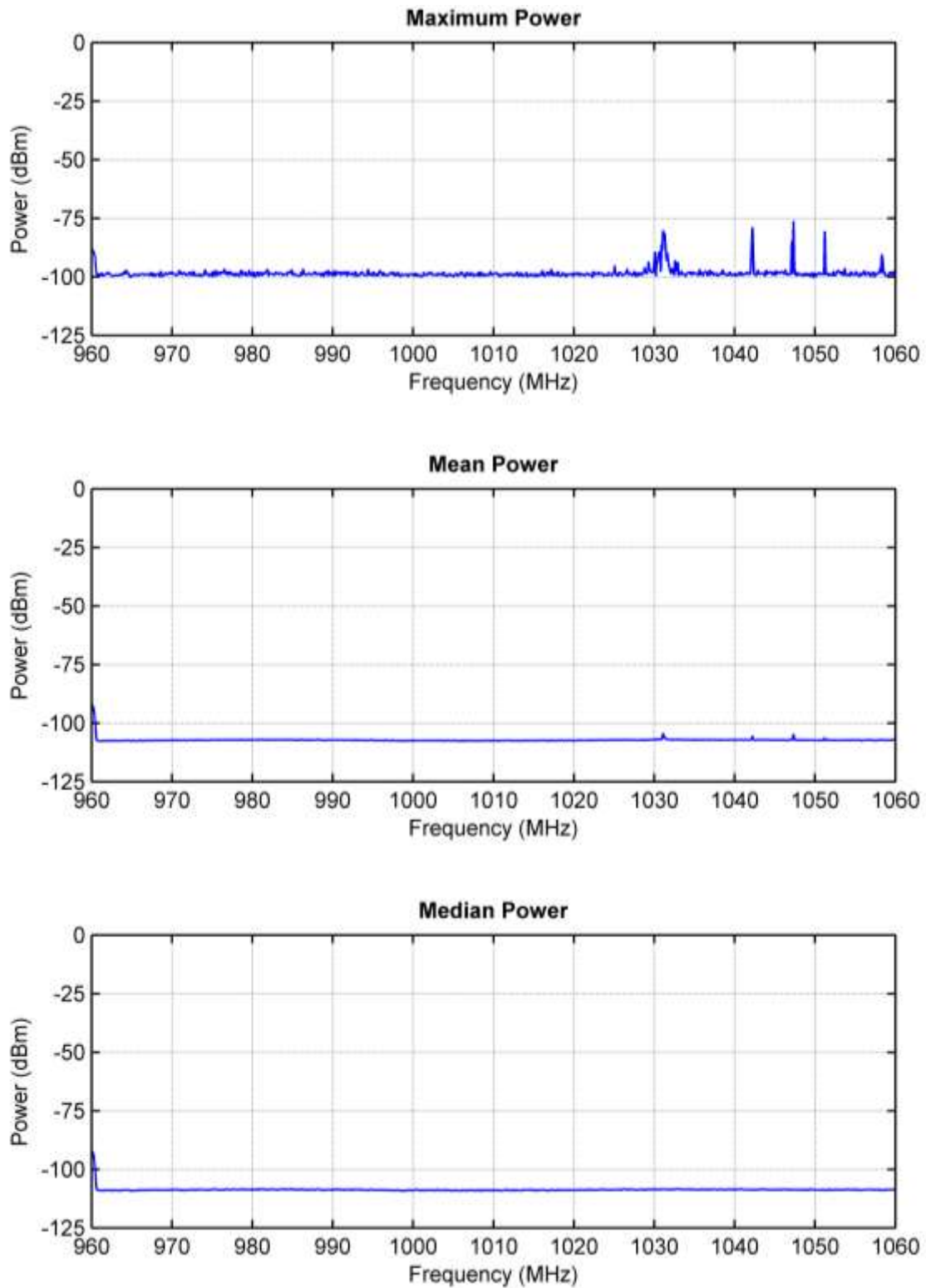


Figure A-58. Maximum, mean, and median received signal power at the Boulder residential location for Event 15 (960–1060 MHz, RBW = 100 kHz, 500 sweeps, sweep time = 100 ms).

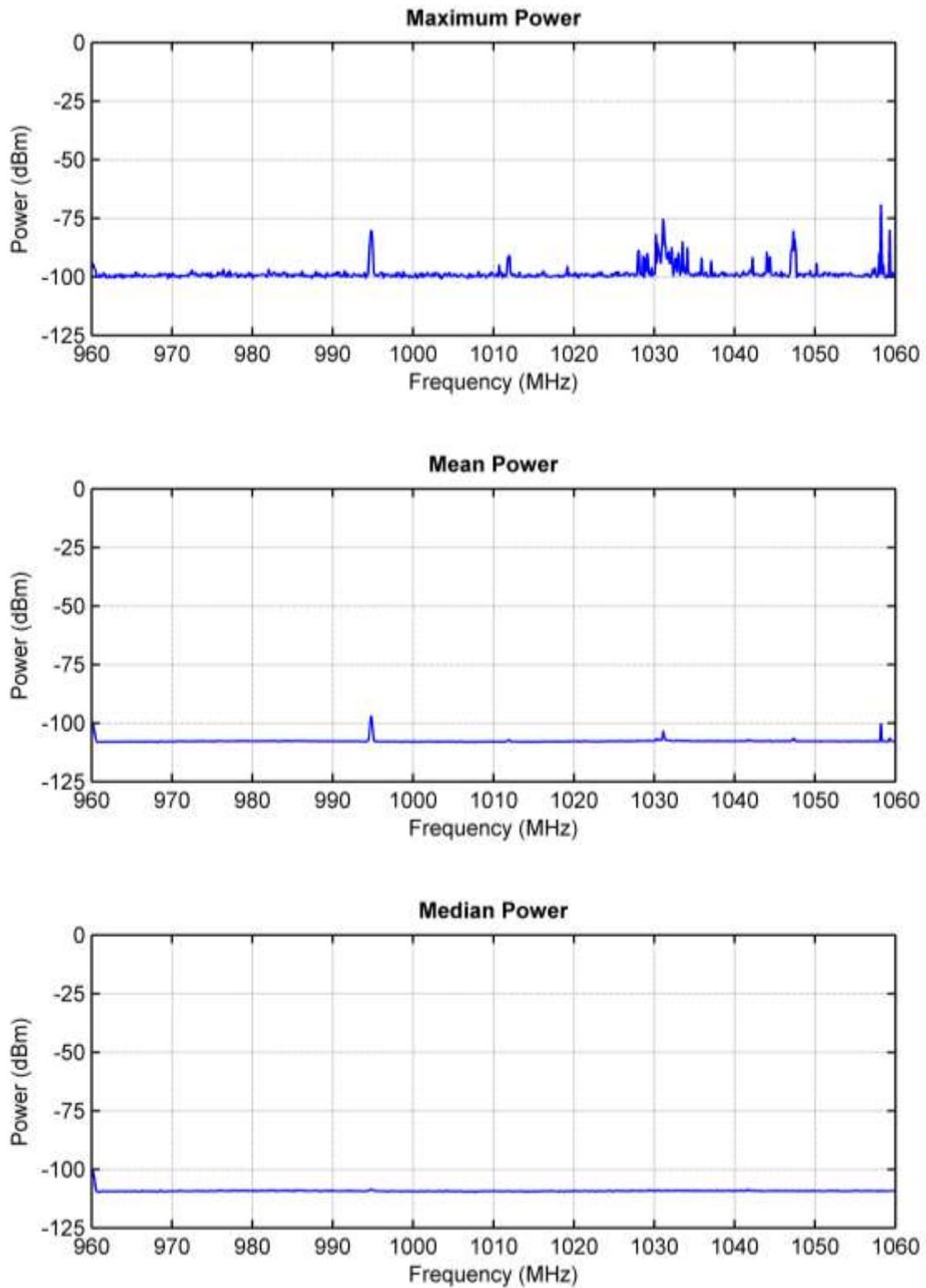


Figure A-59. Maximum, mean, and median received signal power at the Denver residential location for Event 15 (960–1060 MHz, RBW = 100 kHz, 500 sweeps, sweep time = 100 ms).

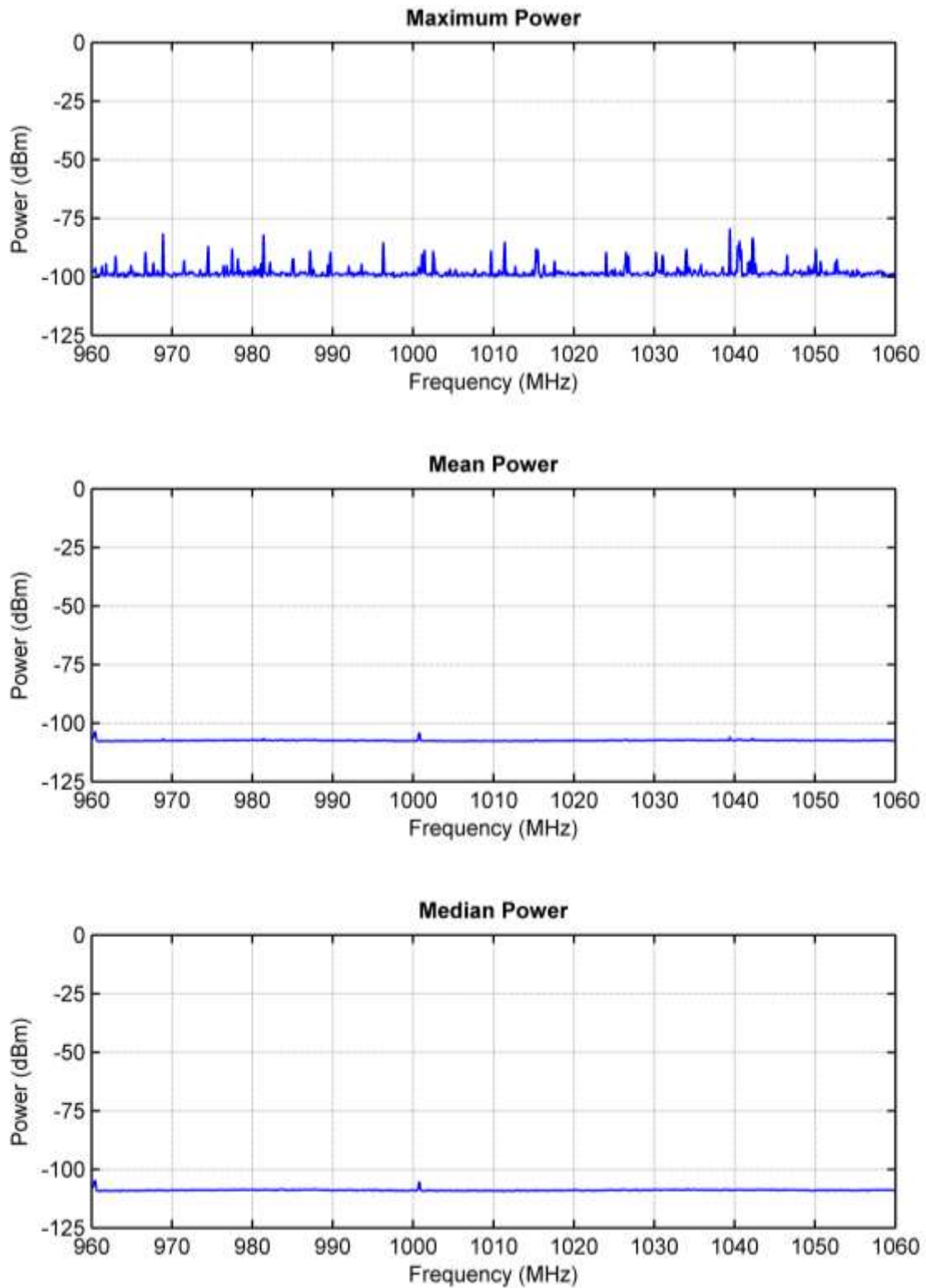


Figure A-60. Maximum, mean, and median received signal power at the Boulder business location for Event 15 (960–1060 MHz, RBW = 100 kHz, 500 sweeps, sweep time = 100 ms).

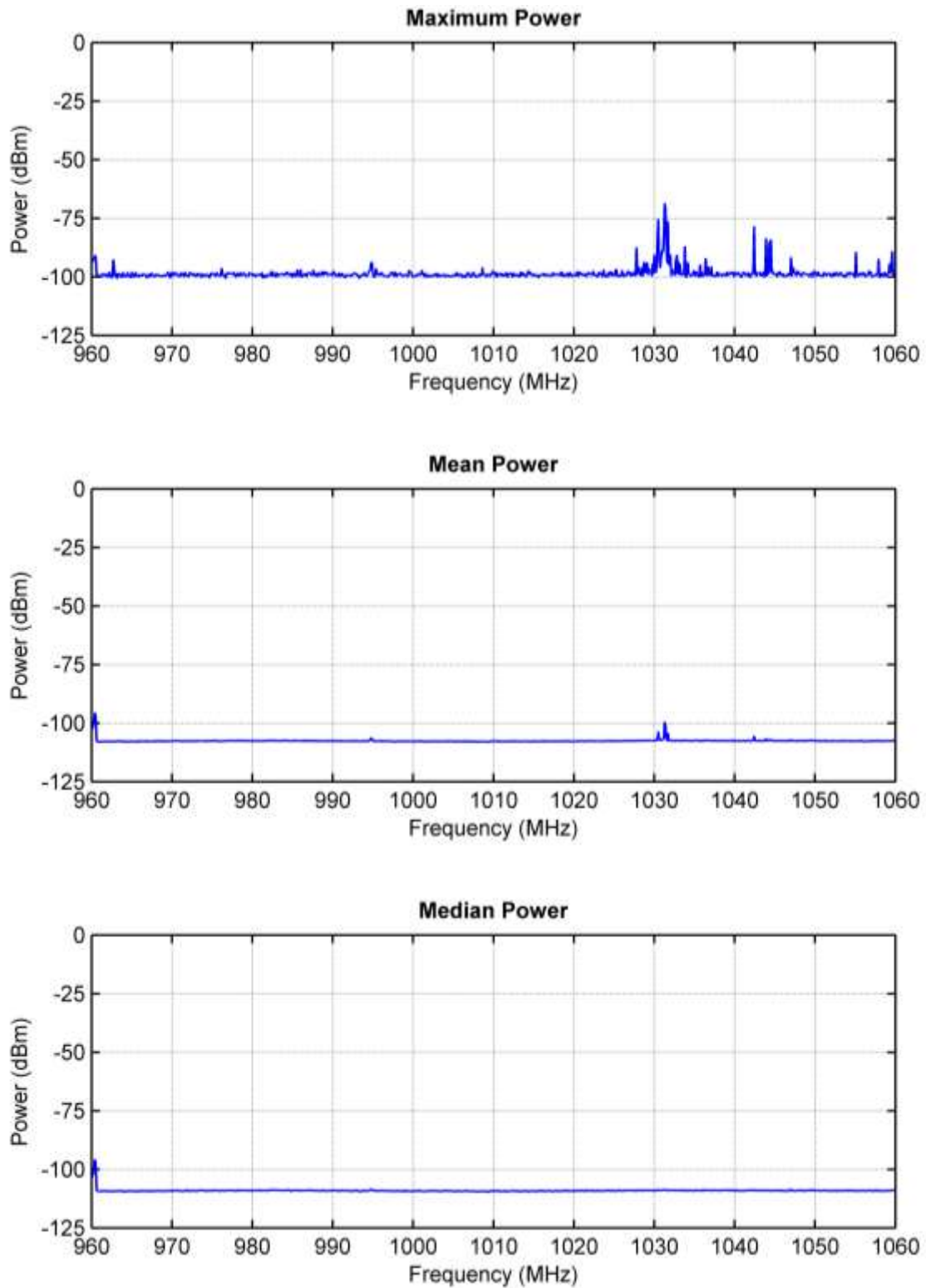


Figure A-61. Maximum, mean, and median received signal power at the Denver business location for Event 15 (960–1060 MHz, RBW = 100 kHz, 500 sweeps, sweep time = 100 ms).

A.4 References

- [A-1] F. H. Sanders and V. S. Lawrence, “Broadband spectrum survey at Denver, Colorado,” NTIA Report 95-321, Sept. 1995.
- [A-2] Agilent Technologies, “Noise figure measurement accuracy—the Y-Factor Method,” Agilent Technologies Application Note 57-2, Mar. 19, 2004.
- [A-3] Agilent Technologies, “Agilent spectrum analysis basics,” Agilent Technologies Application Note 150, Aug. 2, 2006.

BIBLIOGRAPHIC DATA SHEET

1. PUBLICATION NO. TR-11-478.	2. Government Accession No.	3. Recipient's Accession No.
4. TITLE AND SUBTITLE Wideband Man-Made Radio Noise Measurements in the VHF and Low UHF Bands		5. Publication Date July 2011
		6. Performing Organization Code ITS.M
7. AUTHOR(S) Jeffery A. Wepman and Geoffrey A. Sanders		9. Project/Task/Work Unit No. 113158011-300
		10. Contract/Grant Number.
8. PERFORMING ORGANIZATION NAME AND ADDRESS Institute for Telecommunication Sciences National Telecommunications & Information Administration U.S. Department of Commerce 325 Broadway Boulder, CO 80305		12. Type of Report and Period Covered
		11. Sponsoring Organization Name and Address National Telecommunications & Information Administration Herbert C. Hoover Building 14 th & Constitution Ave., NW Washington, DC 20230
14. SUPPLEMENTARY NOTES		
15. ABSTRACT (A 200-word or less factual summary of most significant information. If document includes a significant bibliography or literature survey, mention it here.) Man-made radio noise measurements were conducted in a 1.16-MHz bandwidth at 112.5, 221.5, and 401 MHz at two residential and two business locations in the Boulder/Denver, Colorado, area. The measurement frequencies and bandwidth were selected using the results of a spectrum survey performed over the 104–1060 MHz frequency range. The noise measurement data were collected as a complex baseband noise data record (consisting of six million in-phase (I) and quadrature (Q) samples) every 10 minutes over a 24-hour period for each frequency and location. The data were processed to provide various statistical descriptions of the noise such as amplitude probability distributions (APDs). Median values of the antenna noise figure F_{am} were determined for each measurement frequency and environment type and compared to predicted values from existing man-made radio noise models. The measured values of F_{am} , while larger than the values predicted by the International Telecommunication Union (ITU) man-made radio noise model, were still within one standard deviation of the predicted values. Further noise measurements are recommended in a greater number of locations to provide more statistically significant results.		
16. Key Words (Alphabetical order, separated by semicolons) man-made noise; man-made radio noise; impulsive noise; Gaussian noise; noise measurements; spectrum measurements; spectrum survey; antenna noise factor; external noise factor; amplitude probability distributions; International Telecommunications Union (ITU) radio noise model		
17. AVAILABILITY STATEMENT <input checked="" type="checkbox"/> UNLIMITED. <input type="checkbox"/> FOR OFFICIAL DISTRIBUTION.	18. Security Class. (This report) Unclassified	20. Number of pages 115
	19. Security Class. (This page) Unclassified	21. Price:

NTIA FORMAL PUBLICATION SERIES

NTIA MONOGRAPH (MG)

A scholarly, professionally oriented publication dealing with state-of-the-art research or an authoritative treatment of a broad area. Expected to have long-lasting value.

NTIA SPECIAL PUBLICATION (SP)

Conference proceedings, bibliographies, selected speeches, course and instructional materials, directories, and major studies mandated by Congress.

NTIA REPORT (TR)

Important contributions to existing knowledge of less breadth than a monograph, such as results of completed projects and major activities. Subsets of this series include:

NTIA RESTRICTED REPORT (RR)

Contributions that are limited in distribution because of national security classification or Departmental constraints.

NTIA CONTRACTOR REPORT (CR)

Information generated under an NTIA contract or grant, written by the contractor, and considered an important contribution to existing knowledge.

JOINT NTIA/OTHER-AGENCY REPORT (JR)

This report receives both local NTIA and other agency review. Both agencies' logos and report series numbering appear on the cover.

NTIA SOFTWARE & DATA PRODUCTS (SD)

Software such as programs, test data, and sound/video files. This series can be used to transfer technology to U.S. industry.

NTIA HANDBOOK (HB)

Information pertaining to technical procedures, reference and data guides, and formal user's manuals that are expected to be pertinent for a long time.

NTIA TECHNICAL MEMORANDUM (TM)

Technical information typically of less breadth than an NTIA Report. The series includes data, preliminary project results, and information for a specific, limited audience.

For information about NTIA publications, contact the NTIA/ITS Technical Publications Office at 325 Broadway, Boulder, CO, 80305 Tel. (303) 497-3572 or e-mail info@its.blrdoc.gov.

This report is for sale by the National Technical Information Service, 5285 Port Royal Road, Springfield, VA 22161, Tel. (800) 553-6847.

